Dynamic Simulation and Analysis of a New HVAC System in Pavilhão de Civil of IST Using *EnergyPlus*

Vasco Ascensão Marchão de Carvalho Teixeira

Thesis to obtain the Master of Science Degree in

Mechanical Engineering

Supervisors: Prof. Viriato Sérgio de Almeida Semião
Eng. Mário Miguel Franco Marques de Matos

Examination Committee

Chairperson: Prof. Edgar Caetano Fernandes
Supervisor: Prof. Viriato Sérgio de Almeida Semião
Member of the Committee: Prof. José Manuel da Silva Chaves Ribeiro Pereira

June 2019

Acknowledgments

A large number of people have contributed greatly, in diverse ways, to this work. As such, I would like to thank all off them in this section.

First and foremost, I would like to thank my supervisors, Prof. Viriato Semião and Eng. Mário de Matos. Both have contributed greatly to this work. To professor Viriato, for all the patience showed and guidance provided and to Eng. Mário, for all the availability and technical help. Their contribution to this work is invaluable.

I would also like to thank Eng. Onésimo Silva of Núcleo de Obras e Manutenção for all the kindness in providing me with the project, helping me in a great number of technical questions and also for the visits conducted to the building.

To my friends, thank you for helping me motivate myself in harder times, for serving as an anchor and for all the help given.

Finally, to my family, namely, my Mother and Grandmothers, who are the foundation to everything else. Thank you so much for believing and supporting me in all manners, each and every day.

I would like to dedicate this work to my Father, Fernando Teixeira, who, unfortunately, is not among us anymore. I hope to have made him proud and continue to do so.

Resumo

O Pavilhão de Civil do IST padece de um problema de conforto térmico preocupante e de deficiências na qualidade do ar interior. É também o edifício mais consumidor de energia no *Campus* da Alameda. Nestes sentidos, um novo projecto de AVAC foi encomendado pelo IST e deverá ser implementado por fases nos próximos anos.

Esta tese centra-se no novo sistema de AVAC projetado e usa o *Energyplus* para o implementar e analisar o seu desempenho. Para tal, um modelo *Energyplus* do edifício foi atualizado e melhorado, o novo sistema AVAC foi apresentado e analisado e uma implementação detalhada de todos os componentes no *Energyplus* foi realizada. O necessidade de um sistema de AVAC a 4 tubos foi também verificada computacionalmente. Os resultados da simulação anual foram então apresentados e discutidos.

Da simulação resultou um consumo anual de energia semelhante, com um aumento de 5% quando comparado com o modelo antigo em *Energyplus* e uma diminuição de 2% em comparação com dados reais de consumo de 2018. Foi calculado um aumento de apenas 2% do consumo de energia do sistema de AVAC quando comparado com dados de consumo real de 2018. A simulação mostrou também que é muito provável que a central de *chillers* reversíveis com recuperação esteja sobredimensionada para a carga térmica atual do edifício.

Uma melhoria notável do conforto térmico foi verificada na simulação e uma capacidade de manter os *setpoints* de temperatura interior e, ao mesmo tempo, assegurar a conformidade com a legislação relativa aos caudais de ventilação de ar novo.

Palavras-chave: Eficiência Energética, AVAC, Conforto Térmico, Pavilhão de Civil, Energyplus, Simulação Energética de Edifícios

Abstract

Pavilhão de Civil of IST has a severe thermal comfort problem and indoor air quality deficiency. It is also the highest energy consuming building in the Alameda *Campus*. As such, a new HVAC project was ordered by IST and its implementation is expected in the future years.

This thesis focus on the new projected HVAC system and uses *Energyplus* to implement it and analyze its performance. To do that, an *Energyplus* model of the building was updated and improved, the new HVAC system was presented and analyzed and a detailed implementation of all the components in *Energyplus* was performed. The need for a 4-pipe HVAC system was also computationally verified. The results of an annual simulation were then presented and analyzed.

The simulation predicted similar annual energy consumption across the building, with a 5% increase when compared to the old *Energyplus* model and a 2% decrease compared to 2018 real consumption data. The HVAC energy consumption was calculated to only increase 2% when compared to 2018 real data. The simulation has also showed that the Chiller/Heat Pump plant is likely oversized given the current thermal demand of the building.

A remarkable improvement regarding thermal comfort was verified with capability of keeping the temperature setpoints while assuring compliance with the legislated ventilation of fresh air.

Keywords: Energy Efficiency, HVAC, Thermal Comfort, Pavilhão de Civil, Energyplus, Building Energy Simulation

Contents

List of Tables

List of Figures

Nomenclature

Roman symbols

$\dot{m}$ Mass Flow Rate, $\frac{kg}{s}$.

P_{cool} Cooling Power, kW.

P_{heat} Heating Power, kW.

Q Volumetric flow rate, $\frac{m^3}{s}$.

T Temperature, $^\circ C$.

Greek symbols

ΔT Temperature Difference, $^\circ C$.

η Efficiency, [-].

Chemical Species

CO_2 Carbon Dioxide.

Acronyms

AC	Air Conditioning.
AHU	Air Handling Unit.
ASHRAE	American Society of Heating, Refrigerating and Air-Conditioning Engineers.
BEM	Building Energy Modeling.
CAPFT	Cooling Capacity Function of Temperature.
CAV	Constant Air Volume.
COP	Coefficient of Performance.
DCV	Demand Controlled Ventilation.
DOAS	Dedicated Outdoor Air System.
DX	Direct Expansion.

ECM	Electronically Commutated Motor.
EER	Energy Efficiency Ratio.
EIRFT	Energy Input Ratio Function of Temperature.
EMS	Energy Management System.
EPW	Energyplus Weather.
ESP	External Static Pressure.
EU	European Union.
FCU	Fan Coil Unit.
IAQ	Indoor Air Quality.
IDF	Input Data File.
IPMA	Instituto Português do Mar e Atmosfera.
ISP	Internal Static Pressure.
IU	Indoor Unit.
HP	Heat Pump.
HVAC	Heating, Ventilation and Air Conditioning.
HX	Heat Exchanger.
IST	Instituto Superior Técnico.
LNEG	Laboratório Nacional de Energia e Geologia.
LTI	Laboratório de Tecnologias de Informação.
nZEB	Near Zero-Energy Building.
OA	Outdoor Air.
OU	Outdoor Unit.
P&ID	Piping and Instrumentation Diagram.
PLR	Part-Load Ratio.
PMV	Predicted Mean Vote.
RECS	Regulamento de Desempenho Energético dos Edifícios de Comércio e Serviços.
SEER	Seasonal Energy Efficiency Ratio.
SHR	Sensible Heat Ratio.
TER	Total Efficiency Ratio.
TSP	Total Static Pressure.
TZ	Thermal Zone.
UTA	Unidade de Tratamento de Ar $\equiv$ AHU in English Notation.
UTAN	Unidade de Tratamento de Ar Novo $\equiv$ DOAS in English Notation.
VAV	Variable Air Volume.
VRF	Variable Refrigerant Volume.
VFD	Variable Frequency Drive.

Chapter 1

Introduction

1.1 Scope of the Work

Over the past decades, the time spent by human beings inside buildings has been rising with the ever more common office job and the growth in the world's population. This has led to increasing quality standards in indoor air quality (IAQ) and demand for better indoor comfort conditions, which has rendered highly relevant the development of more energy efficient heating, ventilation and air conditioning (HVAC) systems, of their control strategies and of other methods to improve these indoor conditions.

This has also led to marked growth in energy consumption in buildings to a point that the building sector is among the greatest primary energy consumers. In fact, according to the European Union (EU) [1], the building sector is responsible for approximately 40% of the energy consumption and 36% of the CO_2 emissions, which is a greenhouse gas, in the EU. Of these values, the HVAC portion, while difficult to assess due to the varying nature of the buildings and the different climates, is a considerable contributor that can account for over 50% of the end-use energy consumption in buildings. In fact, the energy for space cooling has been growing faster than any other end use in buildings with sales of air conditioning (AC) units having been growing steadily in the last 30 years [2], which has put a strain on the electricity grid of many countries. This demand for HVAC equipment is expected to keep growing, driven by economic and population growth [2] and also due to an ever changing climate, with average temperatures increasing and meteorological phenomenons such as heat waves ever more common.

In parallel, the global awareness of the direct contribution of the greenhouse gases emission to the global warming has been increasing and its reduction has presently achieved a status of primal importance in our time to support the future generations to come. In the buildings sector, this has been a key factor driving the energy efficiency improvements that have completely changed the legislative framework and gave birth to a complete new set of policies, targets and tools to achieve this. The International Energy Agency [2] noted that measures to make AC's more energy efficient coupled with a decarbonisation of the power generation equipment would lead to a great reduction in the CO_2 emissions scenario. Decarbonizing the building stock has, therefore, become a long time priority for the EU, and to a great extent, to the entire world.

Specifically, in Portugal, during 2014, the building sector accounted for 30% of the total final energy consumption [3], which is approximately 14 TWh [4]. At the same time, the exterior energy dependence for Portugal, while it has been improving, is still around 70%. In 2013, it was calculated as 73.7% [3]. This value is relatively high and is due to the lack of primary fossil fuel resources which leads to the necessity of importing them from other countries. However, Portugal has invested greatly in renewable energies over the last 20 years, with the massive construction of wind energy parks and the use of hydropower, which has reduced the exterior fossil fuel energy dependency. As such, the renewable electricity mix is reasonably high. Since 2010 onward, it has oscillated between 40.9% and 61.4% [5] with 2017 being the worst year since 2009, mainly due to the lack of precipitation and consequently, reduced hydropower production.

Figure 1.1 represents the share of buildings in the final energy consumption of the countries in the EU in 2012. In it, it is possible to see that the buildings sector represents a large percentage of the total final energy consumption in Europe. In the figure, it is also possible to compare the share of consumption in Portugal in relation to other EU countries. Portugal possesses one of the lowest shares across the EU, as the average in Europe is about 40%. This is, to an extent, related to the Portuguese climate that, being mediterranean and warm, requires less heating and cooling than other more northerly countries in the EU. Also noted was that the residential sector accounts for about two thirds of the share of final energy consumption in buildings.
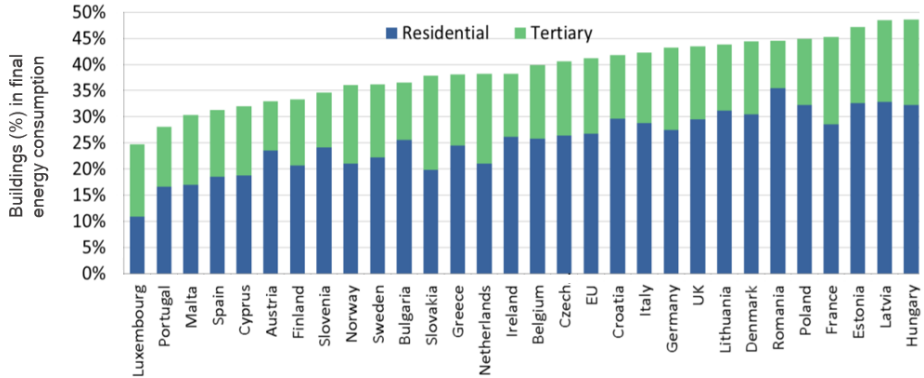
Figure 1.1: Share of buildings in final energy usage in the EU in 2012, obtained from [6]

In the context of this thesis, regarding already constructed buildings that are expected to represent over 75% of the buildings in the EU in 2050 [1], a key strategy to improve energy efficiency has been to retrofit buildings with higher efficiency equipment and/or with relatively new smart building technologies, which are being developed currently. For instance, the EU has been encouraging and in some cases demanding the building sector to adopt more innovative solutions [7] through smarter energy management in buildings and deep renovation. However, it is more difficult and costly to promote efficiency in already existing buildings and the work involved in retrofitting is usually complex as it requires diverse specialties due to highly variable conditions. Its evaluation is challenging, as a building and its environment are complex systems where every sub-system has an influence on the total efficiency performance [8]. A common way to evaluate retrofit strategies has been to employ computing power in the form of building energy modeling (BEM) software that allows for a cheap and effective way to predict conditions and

assess changes.

This thesis is developed within the scope of a planned HVAC retrofit in Pavilhão de Civil in Instituto Superior Técnico (IST), and will make use of one of these BEM software, *Energyplus*, to predict energy use and indoor comfort, as explained in the following chapters.

1.2 IST and Pavilhão de Civil

IST is the largest university of Architecture, Engineering, Science and Technology of Portugal. It is comprised of three *campi*, Alameda, Taguspark and the Tecnológico e Nuclear *Campus*, located respectively in Lisbon, Oeiras and Bobadela. Founded in 1911, it today has a large student community of approximately 11500 students and over 1200 researchers and faculty.

The building that is the focus of this thesis, Pavilhão de Civil, is the largest building in IST with an useful area of over 30,000 m^2 [9] and has consistently been the greatest energy consumer with its value accounting for approximately 16% of the total energy consumption across the *campi* in 2012. It is an education based, multipurpose building that houses the Department Of Architecture and Civil Engineering of IST, along many more functions. It was inaugurated in 1991 [9] and has four above ground floors (0, 1, 2 and 3), two partly underground floors due the terrain's moderate inclination (01 and 02) and a fully underground floor (03). It is divided in two side-by-side blocks: the east and the west block. They are laid out longitudinally on an approximately north-south direction. The building also has 3 main towers which divide the blocks, each comprised of a stairway that allows access to the diverse floors and to the roof.

The location within the Alameda *campus* as well a photograph of the building can be seen in figure 1.2. Furthermore, table 1.1 describes each floors content in an abbreviated manner.

(a)   (b)
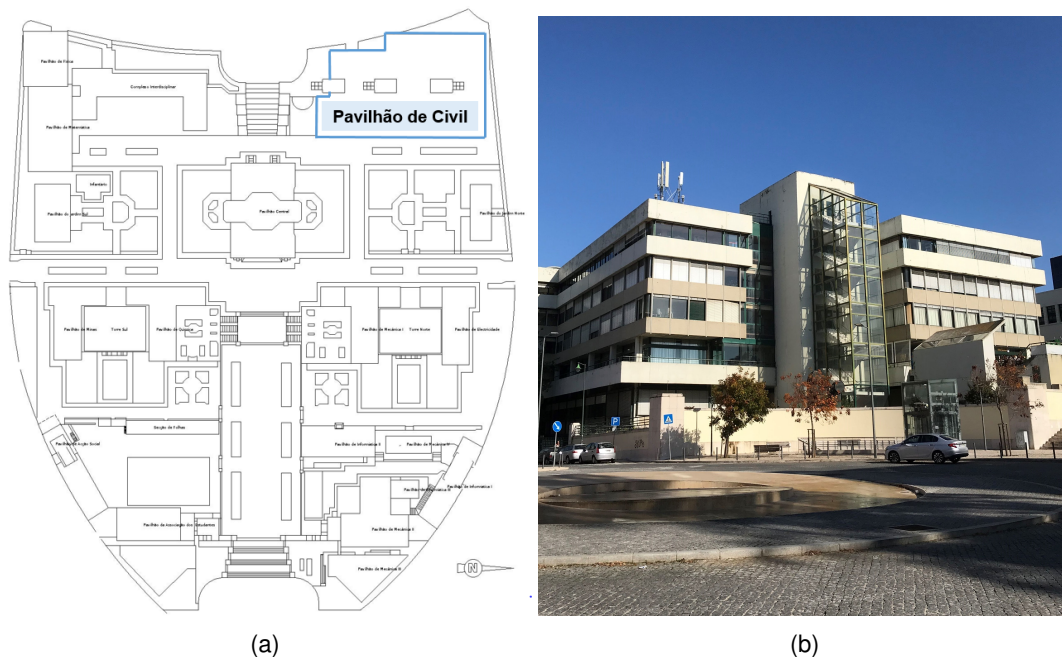
Figure 1.2: (a) - Location of Pavilhão de Civil within the Alameda *Campus*, highlighted in blue. Adapted from [10]; (b) - Photograph of Pavilhão de Civil's facade from a southwest perspective.

Table 1.1: Description of the floors of Pavilhão de Civil.

Floor	Description
03	Garage of the building; The hydraulic plant for the HVAC system is also located in this floor, as well as the electrical transformers and section switch. There is also space for general storage.
02	It houses the congress center, which connects to the above floor; some rooms for meetings adjacent to the congress center; the IST Press office; 3 offices related to the congress center management and the laboratories of Hydraulics, Geo-technical, Construction and of Structures and Strength of Materials (LERM).
01	Comprised of 6 large amphitheaters for lectures, diverse laboratories, the building's library (Biblioteca de Civil) and the main entrance to the Congress Center.
0	In the east block there is the main entrance and the lobby, the Espaço 24h with rooms dedicated for lecturing and most of them serving as study rooms which are always open to the student's community, including the Sala CGD (Aquário) and also the Bar; In the west block, there are class rooms to serve the Architecture students, the Restaurant and the Museum (Museu de Engenharia Civil).
1	Comprises mainly of classrooms (about 34 of them) as well as the computer rooms (LTI).
2 and 3	Both these floors are mainly comprised of offices and secretariats, with a few rooms for meeting purposes as well as a few laboratories.

The technical characteristics of the building, such as the type of windows and the skylight, are great contributors to the thermal comfort problem, apart from the current HVAC system. Seeing that the building was designed and constructed in the early 1990's, it is natural that the thermal insulation is not up to the standards required today and the capability to adapt to extreme climatic events, such as heat waves, is not present at all.

Regarding the windows, they are of a single-pane type with a global coefficient of heat transfer of $5.8 \frac{w}{m^2 . K}$ [11], which is relatively high and grants the building relatively poor thermal insulation. Moreover, it is characterized by a high fenestration facade ratio[1], approximately 60% of its surface [9], which provides the perimeter spaces of the above ground floors with excellent natural light during the day but also a lot of radiative thermal loads. This fact is one of the important causes for the thermal comfort problem that the building faces which has caused many worries to the users and to IST's management.

Figure 1.3: Easterly facade of Pavilhão de Civil with the recently installed exterior blinds visible in the 1st, 2nd and 3rd floor. Also visible are the different configurations for the blinds, with slat angle adjustment.

---

[1]The fenestration facade ratio, also known as the windows to wall ratio, is the ratio of window area to the total facade area of a building.

Figure 1.3 depicts the blinds in the easterly facade of the building, that were installed in most of the facade to combat the problem mentioned above and reduce sun glare. In 2016, most of the blinds have been upgraded to automated ones, which allow for manual user control at a touch of a switch or, ideally, automated control to block the direct solar radiation while optimizing natural light inside the space. This upgrade was necessary due to the elevated state of degradation of the old exterior blinds.

Additionally, the skylight occupies a great percentage of the building's roofing but it does not possess a shading system nor does it provide good enough thermal insulation. That translates into extremely elevated temperatures in the upper corridors, especially so in the 3rd floor's corridor where temperatures go up to 40 $^\circ C$ in the Summer.

Similarly to other buildings in the *campi* of IST, Pavilhão de Civil has an aging HVAC system with old and obsolete equipment whose efficiency is not up to current standards. Moreover, those equipment are also showing accelerated sign of degradation and, due to their age and consequent lack of parts or technical know-how, some are not easily serviceable anymore. Additionally, the original design of the HVAC system, that dates back to the 1980s, did not contemplate the occupancy profile that the building has nowadays, such as the occupation of the classrooms during summer months, during weekends for exam days and the study rooms of the ground floor (Espaço 24h and CGD Room) that is open 24/7. This has led to some classrooms facing indoor temperatures of up to 40 $^\circ C$ in the peak summer days, and lower than 13 $^\circ C$ conditions on peak winter days, according to the users. Moreover, according to the latest audit in the building, the HVAC system accounts for 37.6% of the building's yearly energy consumption [12]. Note that focus will be dedicated to describing the actual HVAC system in Pavilhão de Civil and its shortcomings in chapter 2.

All the factors mentioned above contribute to the deficiencies of the thermal comfort of its occupants and of the indoor air quality (IAQ), a thematic that will be further described in section 2.3, and has driven the need to renovate the HVAC system, which is the focus of this thesis.

Regarding the energy consumption within Pavilhão de Civil, figure 1.4 is presented that aims to display the end-use energy consumption in the building, according to the latest energy audit report [12] from 2015.
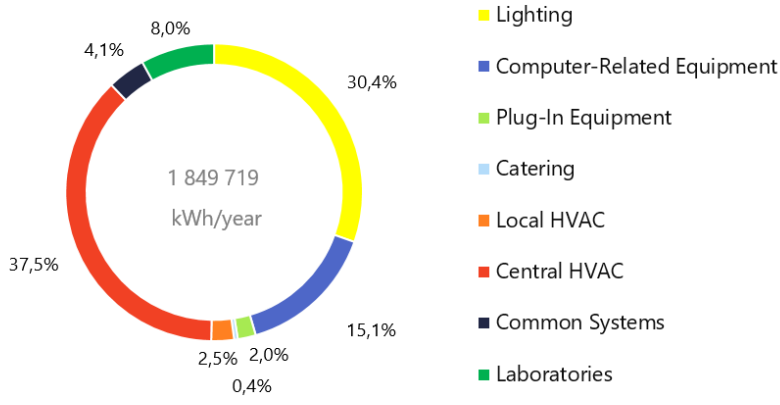
Figure 1.4: Energy consumption in Pavilhão de Civil by end-use, from 2015, obtained from [12]. Data from the laboratories include equipment which are represented in the other categories. Also, the energy consumption from the concessions (Bar and Restaurant) is not represented.

The audit shows that the main fraction of electricity consumption is the HVAC (central and local) system, at 40%, followed by the lighting equipment, at 30.4%. Moreover, a yearly electricity consumption of 1849.7 MWh was calculated, for 2015. Data from the laboratories include equipment which are represented in the other categories but were joined in that category. Moreover, the energy consumption from the concessions (Bar and Restaurant) is not represented in the figure.

1.3   Efficiency Improvement Measures in IST

In order to improve the overall energy efficiency across the three *campi*, an entity within IST was created in 2011, named *Campus Sustentável*, whose main objective is to improve energy efficiency and therefore sustainability across IST. To do that, the project's team proceeds in diverse ways [13]:

1. Through energy audits of all buildings and facilities in the Alameda Campus, which produces disaggregated data of the energy consumption as well as characterization of the energy behavior of the building's occupants. These audits are updated when significant energy efficiency measures are implemented or when considerable changes happen in the buildings.

2. Through an energy monitoring system (EnergIST), which is an online platform and database that allows real time oversight of the consumption across the *campi's* buildings, as well as historical data that can be flexibly organized in a desired time period for the intended analysis.

3. Through the use of energy simulation software, by creating energy models of all buildings in the campus using data collected in the energy audits. Those models are then used to evaluate efficiency improving measures, whether to improve the envelope (such as shading systems, windows refurbishment, green roofs, among others) or a new type of HVAC equipment or system. This work has been carried out not only by the *Campus Sustentável* team, but by master students as well for their dissertations. This thesis will use this methodology, as will be seen in 1.4.

4. Another way is to implement direct energy efficiency measures such as by replacing old and inefficient lamps in present standards (halogen, incandescent, florescent lamps, etc) for higher efficiency ones (especially LED lamps), by substituting old and inefficient electric equipment, by altering their control and scheduling, and by promoting energy sustainability awareness through campaigning, among others. One recent project, as of 2018, is related to shared mobility, in which a number of electric bicycles were distributed to members of the IST community in order to promote awareness to efficiency in transportation, as well as directly diminishing IST's dependency on typical fossil fuel based transportation.

These efforts have translated into a noticeable reduction in the electric energy consumption throughout *campus*. According to [14], a progressive reduction of the electricity consumption in IST has been achieved from 2012 onward, with a total reduction of 15.5% in the annual electricity bill in 2015 comparing with 2011, without a reduction in any of the activities of the university, which attests the positive impact that the *Campus Sustentável* project has had on the campus.

1.4 Objectives

Having established a background on energy usage in buildings, particularly on Pavilhão de Civil itself, as well as on the efforts of IST to improve energy efficiency and promote sustainability, the main objectives of this thesis are now introduced:

1. The main objective is to simulate a newly proposed HVAC system for Pavilhão de Civil based on a project that has been ordered by IST and whose access has been granted, using *Energyplus* as a tool to model all the equipment with as high a degree of fidelity as possible.

2. To evidence the need for simultaneous availability of heating and cooling in a 4-pipe configuration.

3. To analyze the new HVAC model's energy usage when compared to the currently installed HVAC plant while taking into account the thermal comfort of the occupants of the building.

4. In the process of constructing the new model, an additional objective is to update and improve the actual *Energyplus* model, especially in the internal gains descriptions of people and electrical equipment as well as improving the scheduling of these internal heat loads. In order to do that, a number of presential visits to the space have been conducted.

1.5 Thesis Outline

The chapters of this thesis are divided as follows:

Chapter 1 presents a contextualization of the issues in hand, particularly on energy efficiency and its use within buildings, on Pavilhão de Civil and on IST's efforts to improve energy efficiency and promote sustainability. This chapter also lays out the objectives of this thesis.

Chapter 2 contains the information pertaining the old and new HVAC system, with an overview of previous work done, sensor data on indoor air conditions of a specific room for diagnostics, as well as a brief description of the old HVAC system and a thorough description of the newly proposed system.

In Chapter 3, an introduction on building energy simulation and on *Energyplus* is done, the initial *Energyplus* model is introduced, the non-HVAC modifications to the original model are discussed, the computational parameters are presented, an ideal load simulation is performed and briefly discussed and the implementation of the new HVAC model in *Energyplus* is explained, divided in three logical subsections accounting for the modeling of the hydraulic plant, of the air-side equipment and of the remaining independent HVAC systems. Finally, there is also a discussion on the approximations required to build the new model.

Chapter 4 presents the simulation results of the new building model made for this thesis in regards to the operation of the HVAC plant and indoor temperature conditions across different spaces. Additionally, a comparison with the old simulation model and with real data obtained from EnergIST is performed and analyzed.

Finally, conclusions are drawn in Chapter 5, along with some suggestions for future work.

Chapter 2

HVAC Systems and Thermal Comfort in Pavilhão de Civil

2.1   Original HVAC System

The original HVAC system is a peculiar one as it employs a relatively complex and unusual set of equipment. It was custom designed in the late 1980's and most of its equipment are, as mentioned in 1.2, in the end of their life cycles. Furthermore, it is not up to the current standards regarding IAQ. A visit of the installations has been carried out in preparation for this thesis, and such visit evidenced the diverse equipment and many of the problems that the HVAC system faces.

A number of works have been dedicated to describing, analyzing and simulating the HVAC system of Pavilhão de Civil [15–18]. A brief overview of the system, based on [16], is presented below.

The chilled water and hot water plant consists of two air-cooled reversible chillers that are located in the roof of the north and central towers, however, they do not operate at the same time, as their usage is alternated with a unit serving as a backup in case of a malfunction. In the south tower's roof, there is an open type, two cell, evaporative cooling tower with constant speed axial fans. Hot and chilled water (45 and 7 $^\circ C$, respectively) is pumped from the reversible chiller in use by constant speed pumps and stored in thermal storage tanks located in floor 03, and is then distributed by constant speed pumps to the heating and cooling coils of the diverse terminal units, dedicated outdoor air systems (DOAS's) and air handling units (AHU's). The terminal units are either direct expansion (DX) heat pumps (HP's) (using R22 or retrofitted R410A) or direct AHU air. Additionally, there are also water-based fan coil units (FCU's) only for heating in the classrooms but are currently inoperative, according to the maintenance team. Regarding the AHU's, they are mostly constituted of a direct expansion cooling coil section and a water-based heating coil. The DOAS's are characterized by water-served cooling and heating coils. Additionally, both the AHU's and the DOAS's directly supply conditioned air to the spaces by means of constant speed supply fans.

In addition, there are also 2 condenser water circuits that are used to exchange heat with the DX coils of the AHU's and the DX HP's. Each of these condenser water circuits, divided by east and west

block of the building, are served by their own inertial storage tank. In turn, both inertial storage tanks exchange heat with the hot water circuit by means of a pair of plate heat exchangers (HX), P3 and P4, and with the cooling tower condenser water circuit by means of two additional plate HX's, P1 and P2. These HX's intend to keep the condenser water in the tanks in a range of $21\,^{\circ}C < \text{T} < 27\,^{\circ}C$, which is favorable for best efficiency in the DX coils.

Finally, there are also two variable refrigerant flow (VRF) systems and single split air-conditioners for the LTI and the CGD study room.

This system is summarized in figure 2.1.
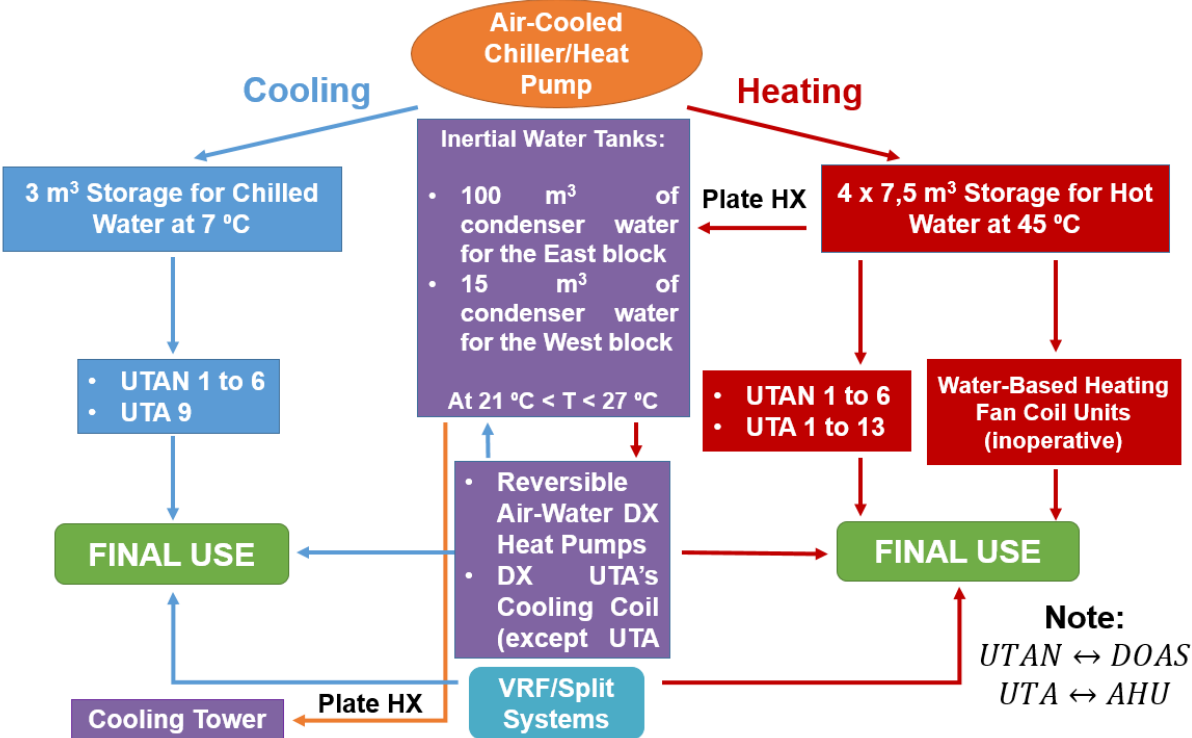
Figure 2.1: Simplified diagram of the current HVAC system, adapted from the master thesis of Vilhena [15]. Red refers to heating and blue to cooling. The purple relates to the condenser water circuits, which are used both in the heating and cooling season.

Important to note is that all the water pumping is done with constant speed pumps that switch on and off according to the demand. Moreover, the air-side is a constant air volume system (CAV) in which the supply temperature is adjusted according to the current load - an increase in load induces a lower (higher) supply air temperature for cooling (heating). Therefore, the supply fans for the diverse AHU's and DOAS's are of a constant speed nature. Furthermore, no air-side heat recovery is employed, only mixing of recirculated air from the spaces with outdoor air (OA) in the AHU's, as well as no air economizer for free-cooling operation. Additionally, the plate HX's are a source of inefficiency for the system because, besides the fact that there are not perfectly efficient HX's, they have never been opened and cleaned.

2.2 Previous Energy Modeling in Pavilhão de Civil - A Review

As mentioned above, in section 2.1, a great deal of attention has been dedicated to the energy usage of Pavilhão de Civil, regarding both the envelope and the HVAC system. This has been achieved mostly through building dynamic simulation software, such as *TRACE 700* and especially *Energyplus*, however, some experimental data collection has also been performed. Presented in this section are some results that are relevant to this thesis, as well as the main conclusions of the work done.

In 2012, Faustino [19] studied, with the use of *Energyplus*, the influence of the windows glazing systems on the performance of buildings and established a case study on an easterly oriented office of the Department of Civil Engineering. His main conclusions were that the single-pane glass of the offices window is not ideal for the thermal comfort, which was aggravated by the substantial window-to-wall ratio (66%), hence, as expected, the cooling needs are vastly superior to the heating needs and that a shading system with a highly reflective external blind, which at the time were not functional yet, could account for annual savings of 37.6% in the cooling season when compared to not having any blinds at all.

In 2013, Patrício [16] made a comprehensive energy audit which allowed for an integral disaggregation of the electricity consumption in Pavilhão de Civil for the first time. This audit has subsequently been updated by the *Campus Sustentável* team, using the tools developed in that thesis. A number of efficiency-improving measures were studied and recommended based on an simple payback economic analysis. Besides recommendations based on altering scheduling of equipment and lighting equipment, modifications to the HVAC system were proposed, such as to suppress the condenser water circuits, including the cooling tower and the plate heat exchangers, by a 2-pipe system with conversion of the inertial tanks to chilled water storage units. The removal of the HX's would allow for an efficiency gain due to the lost energy in the water-to-water exchanger being eliminated. Also suggested was to use 2-pipe FCU's as terminal units, replacing the DX heat pumps, which would allow for a reduction in energy consumption due to the suppression of the compressors of the DX heat pumps. Furthermore, the AHU's with DX cooling coil would be substituted by a water based cooling coil, again, allowing for reduction in compressors operating energy. Finally, it was suggested that the hydraulic pumps should either be substituted by more efficient ones, or be retrofitted with a variable frequency drive (VFD) to allow for better energy performance during part-load conditions.

In addition to the previous work, Vilhena [15], in 2013, also constructed an energy model of Pavilhão de Civil using *TRACE 700* and performed a dynamic simulation to study the implementation of energy efficiency improvement measures. Having calibrated and validated the model with experimental data, these improvement measures were focused on the lighting, by downgrading the actual lighting system and substituting by higher efficiency lamps yielding a 7.1 % reduction in annual electricity consumption; and the envelope of the building, by applying an outer smoked solar protection film to glazed elements of the 2nd and 3rd floors' facades, yielding a 3.3 and 4.4 % reduction in annual electricity consumption.

In 2015, Marçal [17], similarly to Vilhena [15], produced an energy model of Pavilhão de Civil to perform a dynamic simulation, this time using *Energyplus*, which is a more complete tool to model a

complex HVAC system, when compared to *TRACE 700*. Aside from all the input needed in the software, a calibration of the system was possible due to some experimental measurements campaigns performed, particularly on the water volumetric flow rate of the cooling and condenser circuits, temperature of the water in some locations within the circuit and finally, electricity consumption and schedule of some equipment. One interesting finding that explains some of the malfunctioning of the system is that the cooling tower circuit was functioning with a 46% smaller flow rate comparing to the design flow rate. Furthermore, the flow rates passing in the plate heat exchangers P1 and P2 were found to be substantially lower than the design flow rates (14% for P1 and 68% for P2). It is acceptable to assume that the plate heat exchangers are functioning at a point far from the design conditions, which translates to a lower efficiency heat exchange which is probably aggravated by the lack of cleaning of the HX's resulting from fouling on the surfaces. This corroborates with what was said by the maintenance team when the presential visit was conducted. Marçal[17] was able to validate the model after calibration. The total electricity consumption of the building was calculated by the model to be, on average, about 16% off when compared to the real consumption, while the HVAC alone managed to be, on average, within 6% of the real yearly consumption, which validated the model. A thermal comfort analysis was also conducted and it was concluded that the HVAC system is not sized correctly in order to offer thermal comfort to all occupants, especially so on the classrooms.

In 2016, Santos [18] used Marçal's [17] model to diagnose the performance of the HVAC system of Pavilhão de Civil, using *Energyplus* and also suggested some improvements and evaluated their impact. Five thermal zones (TZ's) were studied, at differing solar exposition during a week on the cooling season and heating season: two TZ's of classrooms, two TZ's of offices and the TZ of the LTI. He concluded that in the easterly faced classrooms, thermal comfort is not achieved throughout the year; on the westerly faced classrooms, thermal comfort can be achieved to a comfortable degree during the winter (heating) season, while during the summer (cooling) season it was not possible to achieve thermal comfort. Concerning the offices, it was concluded that thermal comfort was achieved during the summer season for both orientations, in contrast to what happens during the winter season where the temperatures achieved within the offices were well below the comfort zone. With the VRF multi-split system, the LTI was able to maintain comfortable conditions throughout the periods considered.

In 2017, Almeida [20] studied the effects of the newly installed automatized blinds on the thermal comfort within the building and on the HVAC's energy consumption. An algorithm to optimally adjust the slats angles was designed based on the thermal comfort model (Predicted Mean Vote - PMV) calculated by *Energyplus*. An overall improvement was noted, especially on the cooling season. Using the results from the algorithm developed, it was reported a noticeable reduction in the number of hot hours in a number of TZ's. For instance, in TZ 114 (2nd floor, south faced offices), during June, the number of neutral sensation hours went from 37% to 81% during occupancy periods, which demonstrated the usefulness of the blinds to improve thermal comfort during the cooling season. During winter months, the blinds could not solve the coolness felt in some spaces, being reported that in TZ 160 (easterly faced, 3rd floor offices), during April, most of the hours were in a cool or even cold category, with zero hours of neutral sensation. It was concluded that, despite the improvements from the blinds in the thermal

comfort and HVAC electric consumption, " there is still a long way to go regarding comfort conditions" as there are still situations with indoor air temperatures of over 30 ºC. This was justified on an HVAC system that is "poorly designed" and "incapable of removing the heat loads in too many moments". Almeida, therefore, advised that, for future work, the HVAC system be reviewed and improved.

In 2017 as well, Garção [21] studied refurbishment measures on the envelope of the building using dynamic simulation with *Energyplus* with the goal of approaching it to a nZEB. To do that, a number of retrofitting strategies were studied such as the influence of the windows, having studied different single-pane and double-pane windows, of the shading devices with overhangs and external blinds and of the skylight, by applying a shading device or a tinted foil and the construction of a cover. The most cost-effective singular solution found was the application of a spectrally-selective tinted coating to the windows of the skylight. Several combinations of measures were deemed to be beneficial for reduction of the building thermal loads and for the occupants thermal comfort. The combination strategy that accounted for the highest saving allowed a reduction of 15.8 % of the annual electricity consumption. However, these combinations were reported to be unprofitable with a Net Present Value (NPV) analysis.

2.3 Thermal Comfort Within the Building

Thermal comfort is, according to Fanger [22], "that condition of mind which expresses satisfaction with the thermal environment", and can be expressed by a number of thermal comfort models, the most widely being Fanger's PMV-PPD Model (PMV = Predicted Mean Vote, PPD = Predicted Percent Dissatisfied), as introduced in [23]. The PMV index can be used to predict the mean response of a large group of people through a thermal sensation scale, ranging for -3 to 3, that can be seen in table E.1 of Appendix E, and the predicted percent of people dissatisfied (PPD) can then be estimated using PMV.

(a)   (b)
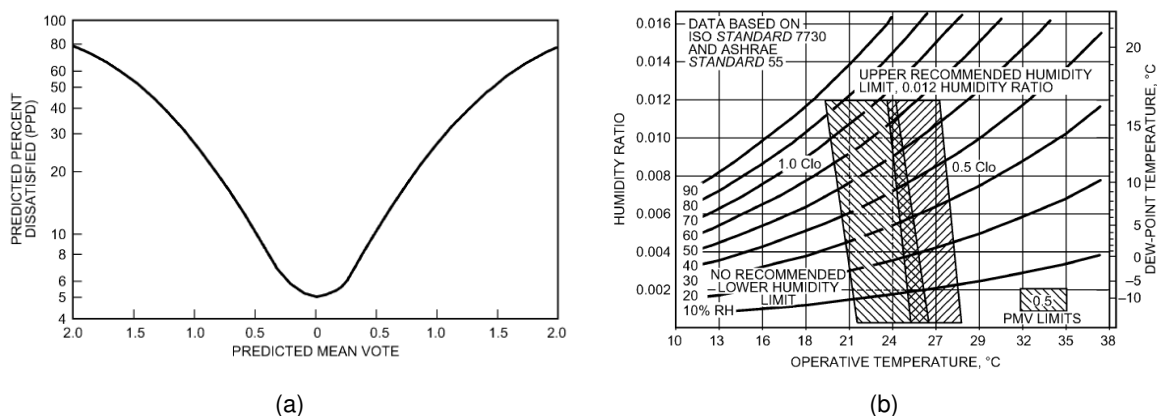
Figure 2.2: (a) - PPD as a function of PMV [24]; (b) - ASHRAE's Summer and Winter Comfort Zones [24]. The Winter's comfort zone is on the left and it characterized by a lower operative temperature due to higher clothing insulation (1 clo $= 0.155\frac{m^2.K}{W}$) while the summer zone is on the right with a 0.5 clo $= 0.078\frac{m^2.K}{W}$ clothing insulation. This is valid for primarily sedentary activity.

In figure 2.2a one can see the relationship between the PMV and the PPD. Furthermore, using

ASHRAE-defined thermal comfort zones, *Standard* 2013-55, shown in figure 2.2b, one can observe the ranges of temperatures and humidity ratios that enable thermal comfort.

The thermal comfort within Pavilhão de Civil has been a highly debated subject that has originated diverse efforts to diagnose, quantify and especially improve, an example of which are the works referenced above in section 2.2. The consensus is that the thermal comfort in the building is not up to the standards required for a public building, especially a teaching facility. This is exacerbated in a typical classroom from the ground or the 1st floor or in the circulating areas of the 3rd floor with elevated indoor air temperatures. One can easily experiment this by being present in a room with a high degree of occupancy, such as during a class or an exam. The HVAC system is, therefore, commonly not able to remove the heat loads from the spaces. Moreover, the air is not renovated at an advisable rate. In a room served by the central HVAC system, in general, the flow rate of fresh air does not guarantee enough air renovations for an adequate indoor air quality in the periods of high occupancy. It is, therefore, absolutely necessary to review and improve the HVAC system and the ventilation system within the building. These are conclusions that can be drawn from simply being present in the building.

Apart from the diagnosis that was conducted by Correia Guedes *et al.* [11] and Santos [18], among others, there is a classroom, V1.10, that has also been a subject of several studies [25, 26] regarding the management of the blinds with the illumination and the HVAC system, trying to optimize the communications of those systems to maximize the thermal comfort and minimize electricity usage. This room is characterized by a capacity of 50 people during normal classes and 25 people during exams, possessing 54.24 m^2 of useful area and is a perimeter room located on the east block of the building. It therefore has morning exposure to direct sun radiation but possesses a shading system that is able to block most of such radiation. This room is served by the UTAN 2 that supplies fresh OA as well as by a FCU with a water-air heating coil that has been inoperative for a long time, according to the maintenance team. There is no room thermostat available to control the supply air rates, rather it is controlled centrally by the HVAC management team. An image of the room is shown in figure 2.3, where it is possible to observe the aforementioned shading system (blinds) that were installed in 2016.

Figure 2.3: V1.10 with blinds visible and the location of the sensors highlighted.

In order to evaluate the thermal properties of the room and to derive and validate computational models, a number of sensors have been installed by *IN+*[1] : 1) a temperature and humidity sensor, 2) a CO_2 sensor, 3) a VOCs (Volatile Organic Compounds) sensor and 4), a suspended particles sensor. Access to these sensors historical data was granted by *IN+*. Only the data from sensor 1) and 2) will be presented because the analysis of the temperature and CO_2 was deemed enough in the context of this section. The data can be used to showcase the lack of air quality present in this room, the usage of which is similar to many other classrooms in the ground and the 1st floor. The sensor's location is showcased in figure 2.3 and the models and properties of the sensors are presented in the Appendix F, table F.1.

Presented below in figure 2.4 are 2 plots of temperature and CO_2 levels registered by the sensors installed in V1.10 for two selected days.
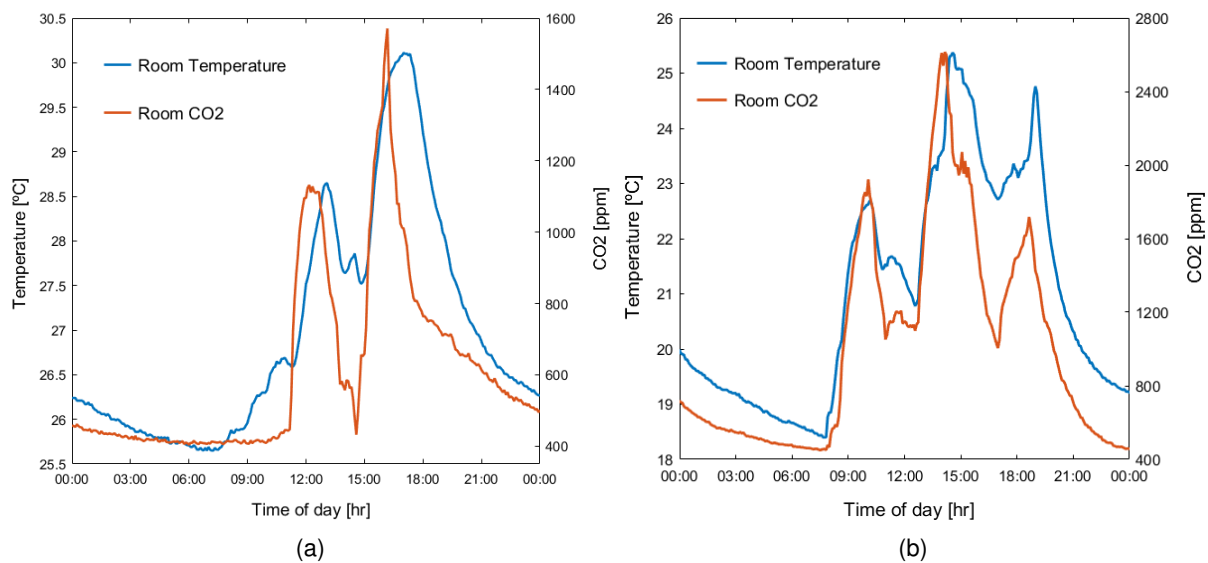
Figure 2.4: Room sensor data of temperature and CO_2 concentration: (a) - data from 29th of May of 2018 (Tuesday); (b) - data from 13th of November of 2018 (Tuesday).

The first, from 29th of May of 2018, was a class day having had occupation from 09:00 to 18:00, with null occupancy between 13:00 and 14:30, as per the available online schedule. The data is consistent with this occupancy profile: firstly, the temperature increases in the morning, until 11:00 due to the sun radiation heat gains and then, a rapid increase from 11:00 on due to the internal thermal gains originated from the occupants as well as the increase in OA temperature. This is also visible from the rapidly increasing CO_2 concentration, having risen from about 400 ppm to 1150 ppm. Then, one can observe the great dip in CO_2 levels during the null occupancy with probable air infiltration from the windows also renovating it. The temperature also shows a reduction in this period of about $1\,^\circ C$. From 15:00 up until approximately 16:30, a great number of people are present in the room which can be inferred by the rapid increase of both the CO_2 concentration and the temperature, the latter reaching a daily maximum of about 30.1 $^\circ C$. The temperature of the room during occupancy times is always in the

---

range of 26 to 30.1 $^\circ C$, with most part of the day above 27 $^\circ C$. For reference, the OA temperatures of that day were between 14 and 19 $^\circ C$ [2]. A similar profile can be observed in the second figure, from 13th of November of 2018. The room's schedule is from 08:30 to 18:30, with a break from 11:30 to 12:30. Temperatures during occupancy times range between 20 and 25 $^\circ C$ while CO_2 concentration reaches higher levels, with a maximum of about 2500 ppm. Taking into account the OA temperatures during this day (minimum was 11 $^\circ C$ and maximum was 17 $^\circ C$) [3], the clothing insulation tends to be stronger and more oriented towards winter conditions. Since the temperature is remarkably above the typical 20 $^\circ C$ interior temperature setpoint, it is highly likely that the occupants had to remove some layer of clothes to achieve a more tolerable thermal comfort.

Regarding the CO_2, while it is not considered a toxic air contaminant, its measurement can be an important tool when diagnosing IAQ. It is widely used for demand-controlled ventilation (DCV) as changes in its concentration mirrors changes in space population, and therefore, ventilation rates can be adjusted dynamically. For high concentration levels, it can induce some symptoms on occupants. For reference, normal outdoor levels are about 330-370 ppm [24]. Values of over 1000 ppm lead to increased drowsiness and therefore, lower productivity and concentration. Values of over 2500 ppm may cause "adverse health effects" [27]. In general, ventilation rates try to keep CO_2 concentrations below 1000 ppm [27]. Several studies have been conducted on the influence of the CO_2 levels on IAQ, well-being and productivity. For example, Allen *et al.* [28] evaluated the impacts of a CO_2-heavy indoor atmosphere on a high-order cognitive function. In this study, regarding CO_2's concentration impact on performance, it was noted that a higher concentration of CO_2 led to lower cognitive performance. When compared to a healthy atmosphere of about 550 ppm, it was reported that a moderate CO_2 concentration (945 ppm) led to 15% lower cognitive function scores and that, for a higher CO_2 concentration of about 1400 ppm, those scores were 50% lower. When analyzing the levels on both graphics of figure 2.4, one can see that they surpass 1000 ppm frequently - for figure 2.4a, the levels are more modest and, despite surpassing 1000 ppm on multiple hours, over half of the occupied hours are below that level; for figure 2.4b, all of the occupied hours are above 1000 ppm, with a maximum of about 2500 ppm. However, regarding the second day presented, it was noted that the valid CO_2 sensor range is only up to 2000 ppm, therefore, the instances that surpass these value are considered invalid. This does not relieve the fact that the room atmosphere is indeed CO_2-heavy.

Quantitatively speaking, the data from both days are consistent with the thermal discomfort reported and corroborated by ASHRAE's Thermal Comfort Zones in figure 2.2b during the peak occupation. The HVAC system in this room and in other similar rooms is, therefore, unable to remove the sensible thermal loads to a comfortable indoor temperature state as well as to assure enough air renovation, especially during high occupancy periods. Air renovation is sometimes achieved by natural ventilation from the windows air infiltration whose opening is controlled by the occupants, as well as by the doors grilles that remove a portion of the room air to the corridor.

---

[2]Temperature data from the closest weather station available was obtained from `https://www.wunderground.com/history/daily/pt/lisboa/ILISBOAL20/date/2018-05-29` on 22 November 2018.

[3]Temperature data from the closest weather station available was obtained from `https://www.wunderground.com/history/daily/pt/lisboa/ILISBOAL20/date/2018-11-13` on 22 November 2018.

2.4 Proposed Retrofit for the HVAC System

A frequently cited measure and future work from previous master theses and technical reports concerning the energy consumption and thermal comfort is to substitute the obsolete HVAC system for a new, more up-to-date and more suited to the usage profile. Steps have been taken to study this issue and this thesis arises within this context.

The *Núcleo de Obras* of IST is an entity responsible for commissioning and supervising construction projects throughout *campus*. In 2017, their team commissioned the development of a project to design a retrofit to the HVAC system of Pavilhão de Civil. This project, "Projecto de Reabilitação dos Sistemas de AVAC do Pavilhão de Civil", from now on referenced as EACE [29], was concluded in 2018 by EACE [4] (Engenheiros Associados, Consultores em Engenharia, Lda.) which is a company that provides projects commissioning as well as consultancy services on diverse fields of engineering, including HVAC.

Access to the final execution project was kindly granted by *Núcleo de Obras* for the making of this dissertation and the following sections will describe the main philosophy of the design alongside the main components.

2.4.1 Design Conditions

In a HVAC project, the climatic design information is used for sizing of the different components. As usual, for this project, EACE defined 2 design days - one for the cooling and one for the heating seasons. Therefore, the summer design day will allow for sizing of the cooling equipment while the winter design day will allow for sizing of the heating equipment. These days were considered as those exhibiting the peak load climatic conditions and the HVAC system was then sized to satisfy the corresponding thermal loads. The outdoor dry-bulb design temperature was chosen for an annual percentile of 1% for the cooling season and 99% for the heating season. These percentiles represent the value that is exceeded on average by the indicated percentage based on the total number of hours in a year, 8760 [24]. Therefore, on average, the summer design temperature is exceeded 87.6 hours per year, while for the cold season, the temperature falls below the defined value, on average, for 1% of the yearly hours, 87.6 hours. Also defined were the design internal air conditions. Those values were considered to be the temperature setpoint that will allow thermal comfort to the occupants, namely the room temperature that the terminal units will try to achieve and maintain through the thermostat and the control mechanism. The latent load will not be directly controlled. These values are presented in table 2.1.

Table 2.1: Climatic design conditions in Lisboa as defined by EACE for the new project.

	Variable	Summer	Winter
Exterior	Dry-Bulb Temperature [$^\circ C$]	33.3	3.2
	Relative Humidity [%]	50	80
Interior	Dry-Bulb Temperature [$^\circ C$]	24	20
	Relative Humidity [%]	Uncontrolled Directly	

---

[4]EACE's webpage can consulted on `http://www.eace.pt/`.

2.4.2 Hydraulic Plant

The new HVAC system will force the deactivation and replacement of the vast majority of the actual system[5]. A more standard chilled/hot water system will be employed. It will be a 4-pipe system, meaning that there will be 2 pairs of water pipes, for supply and return, of chilled and hot water. This will allow for simultaneous availability of heating and cooling that will be specially employed in the Autumn and Spring seasons. During these months, in the morning, it is expected that heat will be needed in some days to heat the spaces to a comfortable temperature, especially so in the interior rooms with no sun exposure or in the westerly and northerly faced rooms, while cooling may be required simultaneously in the spaces that receive morning sun radiation. This is not exclusive to the morning hours, it is just an example of the usefulness of the 4-pipe system. This subject will be further explored computationally in section 3.5 of the next chapter.
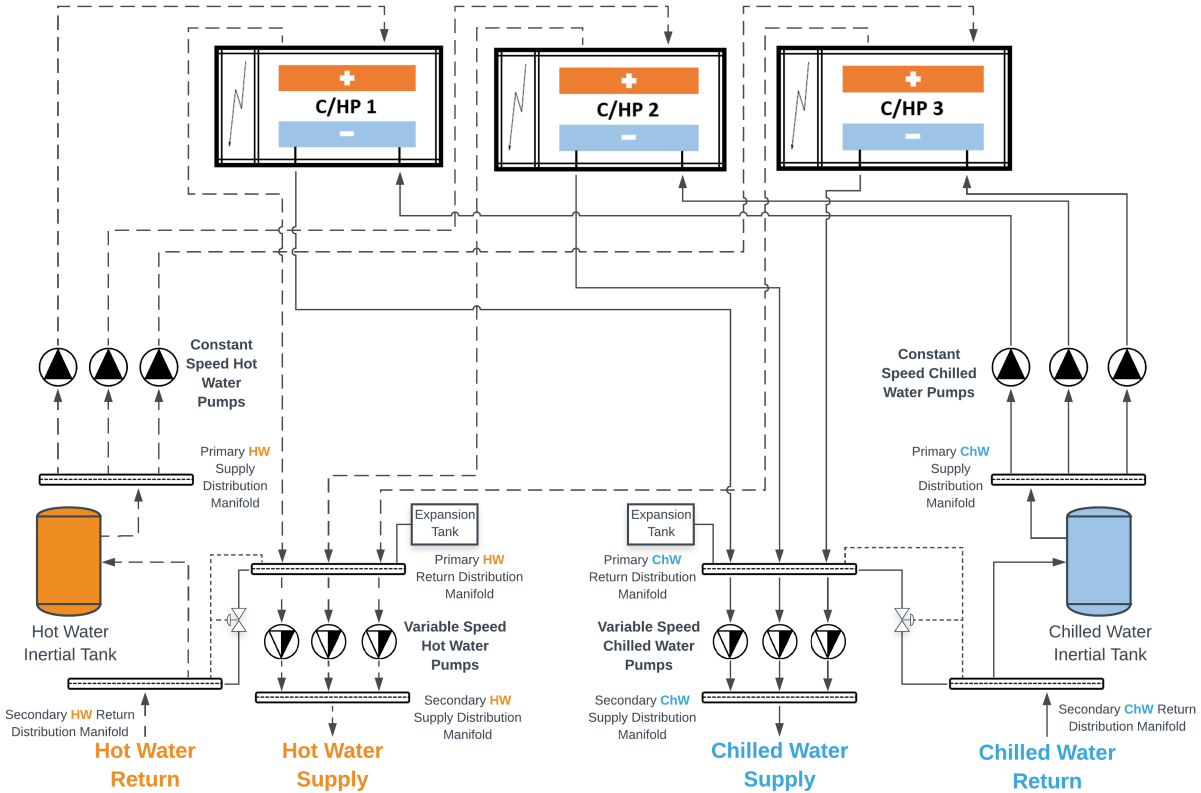
Figure 2.5: Simplified version of the P&ID for the new proposed HVAC system for the production and distribution, as designed by EACE.

To present the hydraulic plant, firstly, a piping and instrumentation diagram (P&ID) is displayed with the main equipment of production and distribution projected, in figure 2.5. In it, simplifications were introduced such as the suppression of most balancing and emergency valves, of the backup pumps in the primary and secondary circuit that allow for system redundancy and of the diverse sensors employed for the control mechanism. Therefore, only what was deemed essential to the understanding of the plant was presented in the diagram.

The hydraulic plant design can be decoupled in a primary production circuit and a secondary distribu-

---

[5]The only exception is the allocation of two of the hot water storage tanks to serve as inertial tanks for the primary water circuit.

tion circuit. The primary water circuit refers to the flow that leaves the inertial tanks, is pumped through the primary supply distribution manifolds by a set of 3 constant speed pumps, is cooled/heated in the chillers/HP's and arrives to the primary return distribution manifolds. A secondary water circuit can be identified by the flow that is pumped by another set of 3 variable speed pumps through the secondary supply distribution manifolds, flows through the AHU's, DOAS's and FCU's and returns to the secondary return distribution manifolds. Therefore, the primary water circuit is of a constant flow rate nature while the secondary water circuit has variable flow capability in order to adapt the operation to the demand. This configuration requires careful design of the primary and secondary pumps to ensure minimum flow under part-load operation throughout the system as well as to ensure that the secondary flow rate does not exceed the primary flow, to avoid low ΔT syndrome [30]. The balancing of this is assured by the connection between the secondary return and the primary return manifolds, from now on referred to as the common pipe that is the notation used by *Energyplus*.

Additionally, inertial tanks were also designed in the return of the secondary circuits to introduce a buffer to the circuits in order to minimize compressor start-ups from the chillers.

A common feature in hydronic HVAC systems is to be efficient for a certain design load but when that load is reduced, the system's efficiency is worsened. For instance, the use of constant flow pumps does not allow for much adjustability in the water side. Moreover, older equipment did not allow for the precise control that modern technology allows, such as digital compressor control. This capability to be especially efficient at part-loads is important but it obviously depends on the usage profile of the building. In the case of Pavilhão de Civil, it was deemed that most occupancy hours will be at part-load conditions, therefore, a key objective of this HVAC retrofit is to achieve maximum efficiency under part-load conditions.

Additional information on the components of the plant will be given in the following subsections.

4-Pipe Reversible Chiller with Heat Recovery

Regarding the Chillers/Heat Pumps, EACE's project calls for 3 equal units to be installed in the roof of the towers of the building, where the 2 actual reversible chillers and cooling tower are currently installed. One unit is projected to serve as a backup unit to assure a good safety factor and continuous operation. One unit per tower is the solution adapted regarding the location. The units will be of a vapor-compression, 4-pipe, air-cooled type, with variable speed axial fans to cool/heat the condenser/evaporator refrigeration fluid (depending on the operating mode) and with condensing energy recovery capability. They will have three operating modes:

1. Chiller mode, which is production of chilled water only, working as a typical vapor-compression air-cooled chiller;

2. Heat pump mode, which is production of hot water only, working as a typical air-source heat pump;

3. Heat recovery mode that allows for simultaneous production of chilled and hot water, the latter obtained through condenser energy recovery. It has the ability to reject condenser heat to the hot water circuit. Typically, the unit would be controlling the supply chilled water temperature and, as a

by-product of the cooling cycle, it would be able to produce tempered/hot water [31] that can serve for space heating/re-heating coils, domestic hot water or other application that uses hot water. A possible setpoint on the hot water recovery loop may also be employed, which will dictate which circuits are active and their mode [31]. This capability is achieved by a complex system design and control that is relatively new technology with a scarcity of public information regarding the operation at this mode.

It will, therefore, eliminate the need for separate equipment of heating and cooling, as these units will be capable of both, allowing for a certain system simplification when compared to a more traditional Boiler plus Chiller 4-pipe setup, although a complex and state-of-the-art chiller and building management control system will be required to assure a dynamic optimization of the working point. Moreover, the efficiency of a typical DX HP unit is much higher when compared to a typical natural gas boiler, with COP's of over 3 while an efficient boiler will typically have a thermal efficiency of 0.8-0.9. This drives energy saving and less CO_2 emissions as an added benefit of the increasingly renewable mix of electric energy production.

Each unit will have 2 independent refrigeration circuits using R410A, with the objective of assuring good part-load performance and good reliability in case of a broken component. Moreover, each unit will have 6 hermetic scroll compressors with VFD capability. Therefore, each refrigeration circuit will use 3 scroll compressors. The compressors speed will be adjusted to modulate refrigeration fluid flow rate and pressure rise and, therefore, the leaving water temperature according to the current load, which is a technology that was not standard in the recent past. Moreover, sequential compressor activation will be performed based on rising demand. Both these factors will contribute to the efficiency at part-load by adapting to the load required, reducing the number of compressor start-ups as well as contributing to a higher useful life and lower repair times and costs due to the modular nature [32].

The proposed unit will have variable speed fans which will improve the part load performance of the chiller/HP units. This is due to the fact that fan power is proportional to the cube of fan speed and, therefore, a reduction of energy consumption can be achieved by slowing the fan at relatively low ambient temperatures (while operating as a chiller only), or at relatively high ambient temperatures (while operating as a heat pump), that is to say, during part-load operation. During energy recovery operation, the control of the unit shuts the fans off when maximum recovery is needed (100% cooling + 100% heating) to ensure that all the energy available from the condensing fluid is used to heat the water and modulate the speed of the fans when partial heat recovery is desired.

Regarding the power, these units will be large-sized and typical of applications for the service and industry sectors.

The main technical specifications are presented in table 2.2, as well as the design functioning temperatures.

Table 2.2: EACE's chiller/HP technical specifications for each unit.

Chiller/HP	Parameter	Value
Cooling Only	P_{cool}[1] $[kW]$	544
	Q_{design} $[\frac{m^3}{h}]$	93.7
	EER [1]	≥ 2.9
	SEER	≥ 4.1
Heating Only	P_{heat}[2] kW	512
	Q_{design} $[\frac{m^3}{h}]$	88.2
	COP [2]	≥ 2.8
Operating Temperatures[3]	Chilled Water Temperature, Supply/Return $[^\circ C]$	7/12
	Hot Water Temperature, Supply/Return $[^\circ C]$	45/40

[1] Cooling Power and EER were calculated at 35 $^\circ C$ Outdoor Dry Bulb Temperature and 50% Humidity Ratio at the cooling operating temperatures shown.

[2] Heating Power and COP were calculated at 4 $^\circ C$ Outdoor Dry Bulb Temperature and 90% Humidity Ratio at the heating operating temperatures shown. Typically, these units have higher heating than cooling capacities. It is unclear whether this was considered when sizing.

[3] These operating temperatures refer to the standard design *Eurovent* conditions, with a ΔT of 5 $^\circ C$

Regarding the technical specifications, some remarks are important. Firstly, the EER and COP are, theoretically, the same concept, which is the ratio of useful power output [W] to the electric power input [W]; the difference is that they refer to cooling and heating, respectively. The value intervals for these parameters were specified in the project to assure the selection of an efficient machine. Secondly, the design ΔT is $5^\circ C$, but it will effectively be lower when the load on the system decreases. Thirdly, an additional parameter is widely used to describe the efficiency of these types of chillers with condensing heat recovery, the TER (Total Efficiency Ratio), as defined by *Mitsubishi Electric*[TM] or GLE (Global Efficiency), as defined by *Clivet*[TM]. Both represent the same value but use a different notation (most manufacturers use different notations) and are used to describe the efficiency of the units when in cooling with condenser heat recovery. It is calculated by:

$$\text{TER} = \text{GLE} = \frac{\text{Cooling + Heating Power in Recovery Mode [W]}}{\text{Electric Power Input in Recovery Mode [W]}} \quad (2.1)$$

Typical values are 7 to 8, which is equal to saying that per unit of electric input power, 7 to 8 units of cooling plus heating power are achieved. In the project, however, this parameter was not specified.

As a title of example, figure 2.6, obtained from a *Mitsubishi Electric*[TM] catalog [33], shows the expected operation of a 4-pipe air-cooled unit, for a typical year, with the TER shown and, while it is merely illustrative, it demonstrates the benefit of having heat recovery available, especially so in March-April and October-November, when the TER has it highest value due to evenness of the heating and

cooling loads. This clearly depends on the weather data but Lisbon's average weather does possess the same tendencies shown in the figure.
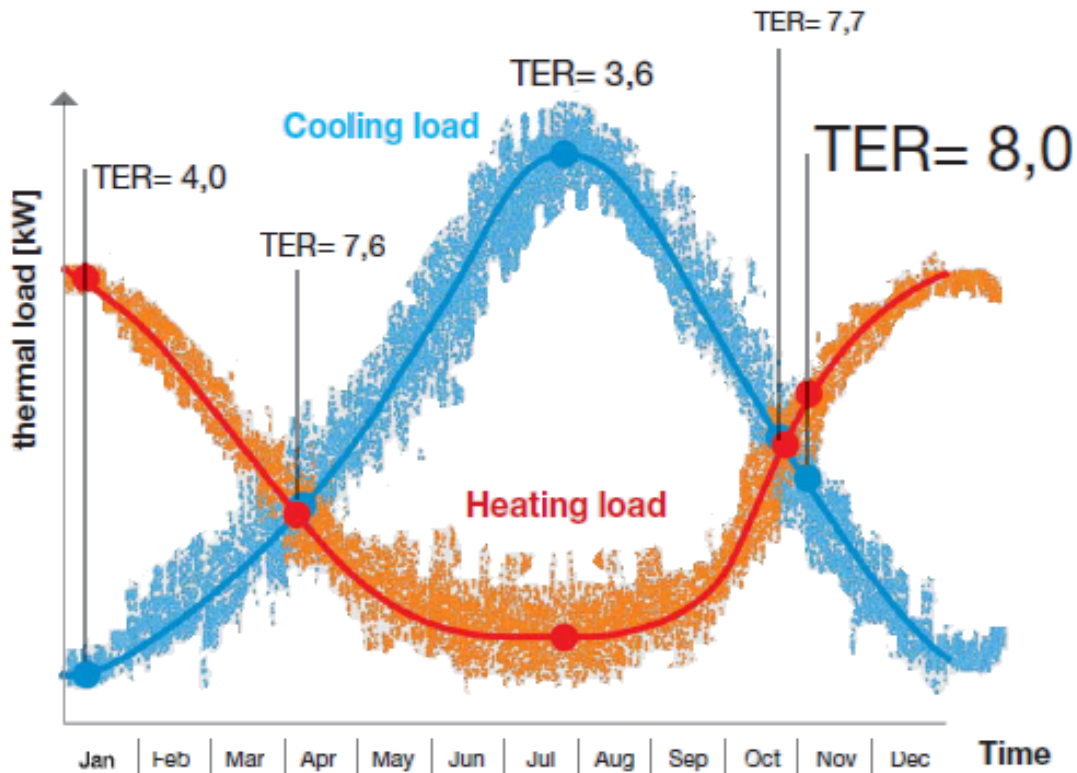
Figure 2.6: Annual cooling and heating loads for an unknown location with TER shown for a 4-pipe air-cooled unit, obtained from [33].

The thermal loads of Pavilhão de Civil are expected to have a similar profile, with the exception of August, when most of activity in the building is stopped for holidays. This matter will be further explored in section 3.5.

Additionally, there is also another important parameter that is defined by *Eurovent*[6]. Regarding chillers and heat pumps, it certifies the performance ratings according to the EN 14511-1:2018 norm[7]. A parameter that is certified is the ESEER, namely European Seasonal Energy Efficiency Ratio. Chillers usually operate at full load during a very small portion of time during a year and that is what will happen in Pavilhão de Civil. Therefore, to describe the part load performance in a more realistic manner, taking into account weather data, building load characteristic and operational hours, the ESEER was developed by *Eurovent* and it is used to describe the seasonal energy efficiency for the entire cooling season. EACE [29] projected the units to possess SEER $\geq$ 4.1. The ESEER is typically higher than the EER because the latter is calculated at full load while the former takes into account performance at part-load as well, it showcases the higher efficiency at part-load in these type of units. Its calculation parameters are shown in table 2.3.

---

[6]*Eurovent* is Europe's association for HVAC, process cooling and food cold chain technologies industry, and provides technical and regulatory services and equipment certification.
[7]"Eurovent EN 14511-1:2018 - "Air conditioners, liquid chilling packages and heat pumps for space heating and cooling and process chillers, with electrically driven compressors. Terms and definitions".

Table 2.3: ESEER, parameters and calculation, according to *Eurovent*.

ESEER = A × EER(100%) + B × EER(75%) + C × EER(50%) + D × EER(25%)		
Part Load Ratio (%)	**Air Temperature [$^\circ C$]**	**Weighting Parameters**
100	35	A = 0.03
75	30	B = 0.33
50	25	C = 0.41
25	20	D = 0.23

Distribution Pumps

As mentioned before, EACE projected for two types of pumps - constant flow in the primary circuit and variable flow in the secondary circuit - see figure 2.5. Both will be of a centrifugal kind and close-coupled to the electric motor (impeller directly mounted on the motor shaft). Regarding the selection of the pumps, it is expected that for the constant speed pumps, its efficiency is maximum for the design operating point. The variable speed one will have to be sized taking into account the power required at the different operating conditions as well how long they will operated at those conditions.

Concerning the technical parameters of the pumps, technical specifications were projected for the design flow rate, the design head, as well as the rated power. It was mentioned, however, that these values will still need to be checked for the final head of the installation to ensure that the available head can overcome the piping pressures losses and the losses in the equipment as well as for the actual Chiller/HP model that will be selected, as these units are limited in the flow rate that they can take. Therefore, these values are not presented here.

Staging and Control Logic

The staging and control logic of the plant is relevant for understanding the mechanisms that allow a good overall efficiency of the plant and the efficient part-load performance. These strategies, such as the control of the chillers/HP's through the return water temperature, the parallel staging of the chillers/HP's and the hydraulic pumps and also the use of inertial tanks are explained in Appendix B. In it, figure B.1 showcases the benefit of controlling these units with the return water temperature, instead of the supply temperature, which is more usual.

2.4.3 Centralized DOAS, AHU and Fan Coil Units

In this section, the air-side equipment will be described, namely the diverse DOAS's, AHU's and the terminal units.

As mentioned above and in other previous works, the building has a problem regarding the IAQ. As such, EACE's priority, besides the thermal comfort of the occupants, has always been to assure a satisfactory IAQ that also complies with the current legislative obligations. Therefore, it was decided to extensively use DOAS coupled with energy recovery modules to precondition the outside air to a neutral indoor state.

Regarding the ventilation rates for each space, EACE took into account the current legislation, the Portaria n.º 353-A/2013 that arose from the RECS, to assure compliance with the legislation. The prescriptive method of calculation was used to dictate the minimum OA flow rates that guarantee dilution of the pollutants. For the spaces with occupancy, the values of minimum fresh air per occupant were used with a correction factor taking into account a ventilation efficiency ϵ_V of 0.8. The calculation of the OA flow rate for each space was then possible and table 2.4 shows the ventilation rates for each type of space and per person, alongside the calculation corrected for the ventilation efficiency.

Table 2.4: Ventilation rates per type of space according to Portaria n.º 353-A/2013 and corrected values considered by EACE with the ventilation efficiency ϵ_V set at 0.8.

Types of Space	Q_{AN} **- Minimum OA Flow Rate [$\frac{m^3}{h.person}$]**	$Q_{ANf} = \frac{Q_{AN}}{\epsilon_v}$ **- Corrected OA Flow Rate [$\frac{m^3}{h.person}$]**
Waiting Rooms, Conference Rooms, Libraries	20	25
Offices, Secretariats, Class Rooms, Museums	24	30
Laboratories, Drawing Rooms and Workshops	35	43.75

Additionally, the supply air temperature for heating and cooling will be constant seeing that it will be a variable air volume (VAV) system, as discussed in section "Ventilation", presented below. These temperatures were not selected for the project perhaps due to the need to select the diverse equipment models beforehand and optimize the working points. Despite this, for this thesis, cooling and heating supply air temperatures have had to be assumed for the simulation model, based on typical values for these systems. Table 2.5 presents the values chosen.

Table 2.5: Assumed supply air temperatures for the diverse terminal equipment, for cooling and heating.

Type of Equipment	Heat Mode	Supply Air Temperature [$^\circ C$]	ΔT[1][$^\circ C$]
FCU's and AHU's	Cooling	14	8
	Heating	29	9
VRF Indoor Units	Cooling	12	12
	Heating	40	20

[1] The ΔT is the absolute difference between the supply air and the interior setpoint temperatures.

Typically, DX systems, such as VRF units, allow for higher/lower temperatures of air for heating/cooling when compared to hot and chilled water systems, as such, their ΔT is higher.

DOAS

The DOAS's decouples the conditioning of the OA from the conditioning of the internal loads [34]. In this project, its function will be to precondition OA to a neutral indoor state[8], namely, to match the indoor

---

[8]Note that some DOAS systems cool the OA below the indoor temperature conditions, however, EACE projected the DOAS's for a neutral state air conditioning.

temperature setpoint presented in 2.1. To do that, sensible energy is added or removed, depending if heating or cooling is required, through the water coils, latent energy is added or removed in the recovery wheel heat exchanger and on the cooling coils, and the air is filtered. Furthermore, the conditioned OA is then delivered either directly to each occupied space through diffusers and grilles, to small terminal units located in the space, or to a central AHU that is serving the spaces.

There will be 3 types of DOAS in this project. The first and second are water-based and the only difference between them is that one will have exhaust energy recovery capability while the other will not. The third type will be a direct expansion (DX) DOAS. Figure 2.7 depicts the layout of the water-based DOAS with air-to-air energy recovery, which will be the most common type.
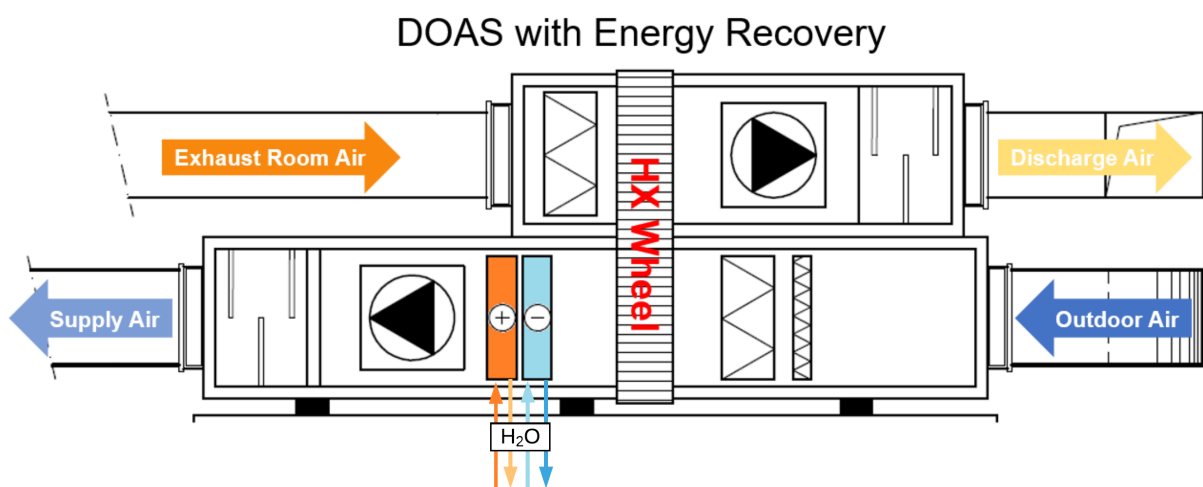
Figure 2.7: Layout of the most common DOAS type, with supply and exhaust fans, heating and cooling coils, air filters and air-to-air wheel energy recovery. Image adapted from [29].

There will be a total of 7 DOAS like the one presented in the above figure 2.7. One unit will be the UTAN 2 that will be located in the 02 floor and will precondition the OA and supply it to a number of locations: to the inlet of UTA 10, 11, 12 and 13; directly to the space of a number of rooms and laboratories located in the northerly facade of the 01 floor that will have 4-pipe FCU's as the terminal equipment and directly to the inlet of some FCU's of some congress center rooms located in the 01 floor. The other 6 DOAS of this type are: UTAN - EN, ES, E, ON, OS and E. These will be located in the roof cover and their name is based on the geographical location of the zones they will serve. For instance, UTAN - EN will serve the floors 1, 2 and 3 of northeastern zone of the building. They will serve the terminal equipment of these zones, which will be 4-pipe FCU's. That will be done in two ways: 1) by supplying air directly to the space which will then be recirculated through the fan coils and 2) by supplying the air directly to the inlet of the FCU's. In the 1st floor, all of the air supply will be done directly into the inlet of the FCU's. Both in the 2nd and 3rd floor, the supply will be to the room through supply grilles. This is due to the fact that, in the classrooms, the thermal loads are higher than in the offices from the upper floors due to former being a bigger space with larger occupancy. Therefore, the FCU's selected for the classrooms are larger when compared to the units for the offices in the upper floors.

A different type of DOAS without air-to-air energy recovery will be employed, UTAN 1. It will supply neutral pre-conditioned OA to the intake of UTA B, 2, 3, 5, 6 and 7, and also to the spaces of the westerly offices of the 02 floor. These spaces will possess 4-pipe FCU's for terminal air treatment.

Finally, the third type, the DX DOAS, will be used to serve the spaces that will have independent HVAC systems, namely, VRF systems. The main difference is that these units will have direct expansion coils with an integrated vapor compression refrigeration cycle. The refrigerant fluid will be R410A and the compressor of the scroll type. Moreover, they will be air-cooled. These will also have possess energy recovery capability through a rotary air-to-air enthalpy wheel, equivalent to the one shown on 2.7. They will deliver ventilation air while the VRF's indoor units will handle the zone's heating and cooling loads. The preconditioned OA will be supplied to the inlet of the VRF's indoor units. More details on the diverse DX DOAS and the spaces that will be served by them will be given below, in section 2.4.4.

Additionally, they will be able to function as an air economizer and utilize OA when in favorable conditions that will bypass the water coils and stop the rotation of the enthalpy wheel, thus saving energy with the shutdown of the wheel motor and lower demand from the supply pumps and the chillers/HP's. It will, therefore, be able to provide free-cooling or free-heating, although free-cooling will be much more frequent. For instance, it will be useful in the cooler days when indoor cooling is required. A set of conditions for the air properties will need to be programmed into the DOAS control unit. These conditions were not mentioned in the project and were not studied in the context of this thesis.

AHU's

The AHU's (UTA's) will not suffer a radical change in the new project as their number will be the same as well as the zones that each serve. Table 2.6 synthesizes the AHU's and the space that each serves.

Table 2.6: AHU's proposed by EACE for Pavilhão de Civil.

Served by DOAS	AHU	Zones Served
Yes, UTAN 1	UTA - B	Library and librarian's offices
Yes, UTAN 1	UTA - 2	VA1
Yes, UTAN 1	UTA - 3	VA2
Yes, UTAN 1	UTA - 5	VA3
Yes, UTAN 1	UTA - 6	VA4
Yes, UTAN 1	UTA - 7	VA5
No	UTA - 8[1]	VA6
No	UTA - 9[2]	Congress Center
Yes, UTAN 2	UTA - 10	Video Conference Room 01.25 and Circulation Zone 01.26
Yes, UTAN 2	UTA- 11	Conference Room 02.03
Yes, UTAN 2	UTA- 12	Conference Room 02.05
Yes, UTAN 2	UTA- 13	Conference Room 02.04

[1] UTA - 8 will directly receive untreated OA due to space constraints.

[2] The UTA - 9 will employ an enthalpy wheel in its intake section. It will be the only AHU with this configuration.

The UTA - 9 will maintain its current design philosophy but with revised power and better efficiency achieved by employing variable speed ventilation and air-side heat recovery.

Unlike the current AHU's that have a DX cooling coil connected to the condenser water loop (with the exception of UTA - 9), the new AHU's will solely have water coils, both for heating and cooling. Most of them will receive the preconditioned neutral fresh air from the DOAS's and treat it to the final supply air conditions. Therefore, the coils will be smaller because the DOAS's will take part of the load. They will also have a mixing box to mix the recirculated air from the spaces with the preconditioned OA. A draw-through (located after the heating coils) variable speed supply fan will move the air directly to the conditioned zones.

Fan Coil Units

The main terminal equipment selected for the retrofit were 4-pipe fan coil units (FCU's). They provide cooling or heating through the use of 2 finned-tube water coils (one for heating and one for cooling). They function by making air flow across the water coils and heating/cooling it thorough forced convection. In this case, EACE selected variable speed inverter motor fans for the fan coils, which are typically located before the coils in a blow-through configuration. Several configurations are possible for the fan coils. EACE projected 2 configurations, both of which will be ceiling mounted:

1. Ceiling wall mounted with room air circulation - these units recirculate the room air and treat it to handle the room sensible loads. The OA will be introduced in the spaces by the diverse DOAS in a neutral thermal state, as explained in the DOAS section above. These will be employed in the smaller load spaces, specially, but not exclusively, the offices of the 2nd and 3rd floors.

2. Ceiling concealed, which will use the already available space in the false ceilings. These directly receive DOAS air in their inlet duct, mix it with recirculated air from the room and treat it sensibly to supply it to the space. This configuration will be used in higher load requirement spaces, namely, the class rooms of the 1st floor, the architecture class rooms of the ground floor and some bigger rooms in the 2nd floor, namely 4.47 and 4.41 which are meeting and gathering rooms.

The load will be adjusted by a combination of two strategies. The first consists of varying the speed of the supply fan. The second will be via the modulation of the water flow rate through the heat exchanger coils by means of flow-modulating valves. Moreover, an indoor room thermostat will be present in each space to allow communication with the modulating valves and the fan motor speed controller and grant local control to the thermal conditions of each space. These will allow for energy savings when the rooms are vacant through manual handling of the indoor controller or, possibly, in an automatic way based on the scheduled occupancy of the room.

Regarding the sizing of each FCU, it was designed for the nominal cooling and heating based on the medium speed flow rate, out of three-speed fan control. This allows for an overhead for peak loads by introducing a safety factor. Quieter operation is also an added benefit. It was decided not to present each equipment here due to the sheer complexity of variations of the sizes of the FCU's and corresponding spaces.

Ventilation

A typical fan employs an electric motor to rotate an impeller to move air. The impeller adds work to the air, which translates in added static and kinetic energy, which therefore increases the total pressure of the flow passing through it [34]. EACE [29] conceived a VAV system, which means that the air flow rate is adjusted according to the load. This is widely considered to be the prime energy efficient choice for air distribution [35], despite a large amount of possible configurations and control techniques. Traditionally, a VAV system utilizes an air damper located in the outlet of a variable speed fan, with an actuator that can be opened or closed to modulate the flow, similarly to a butterfly valve. Likewise, in this project, fans with VFD control will be employed to achieve the variable flow rate and variable pressure rise, in communication with the dampers through a PID control loop using static pressure sensors data downstream of the dampers. This communication/control strategy is essential to assure good energy performance for the fans. There are several methods to control the fan volume flow rate but it is widely accepted that high efficiency VFD fans allow for the least fan power requirements while also having soft start capability [36] because they allow the control of the pressure rise such that, at low flow rate fractions, the fan pressure rise falls as well. Different VAV control techniques and their typical consumption are shown in table 2.7 [34]. It can be concluded that with an efficient VFD-controlled fan, substantial ventilation energy savings can be achieved. In this particular case, a 65% reduction in annual energy consumption for the fan is achieved when comparing the use of a fan with the outlet damper air volume control to a VFD air volume drive to modulate the flow. The other methods are traditional and are now considered obsolete.

Table 2.7: Comparison of fan energy consumption for a VAV system with 4 different volume control techniques [34].

Control Technique	Outlet Damper	Inlet Guide Vane	Eddy Current Coupling	VFD Drive
% Input Power[1]	68	46	46	21
Annual kWh[1]	335000	244000	158000	118000

[1] For a NEMA Premium 75 kW motor producing 60% flow during 5000h, driving a fan system that requires 75 kW at unrestricted flow.

Therefore, this configuration, despite having a higher first cost, will allow for energy savings throughout the equipment life when compared to CAV systems, especially taking into account the variability in occupation that leads to frequent part-load periods. This is due to advancements in motor technology and damper/fan communication that have allowed for higher efficiencies and lower consumption at part load through more complex control systems with the usage of pressure sensors or air velocity sensors in the air ducts and control algorithms that optimize the fan's working point and the damper's position [37]. It is also due to the inherent affinity laws (which also hold for pumps), which partly state that fan power is proportional to the cube of velocity, to the cube of the rotational speed and, therefore, to the cube of the flow rate, in a constant diameter system. It should be noted though, that these relationships do not account for duct frictional losses, such as ducts entrances/exits, elbows and bends, turning vanes,

balancing valves, etc. These inevitable losses extract some of the savings that theoretically would be possible without considering them.

For the DOAS's, both the water-served coils units and the DX coils units will have variable speed centrifugal supply and return fans, which will be highly efficient plug fans. In addition, the AHU's will also have supply plug fans. These type of fans use backward inclined blades in a single inlet configuration, an inherently more efficient design than forward inclined fans which is one reason why they are so widely used. Speed control with VFD's will be possible with the usage of electronically comutated motors (ECM's), which are highly efficient DC brushless motors, with up to 96% efficiency [34], that are controlled by an external electronic circuit board that typically modulates the voltage to accommodate the fan pressure rise, and therefore, speed to the load. Total fan efficiency of over 70% is achievable with this configuration, although depending on the fan size (typically, smaller fan sizes lower the systems total efficiency). Exhaust fans will also be employed in the spaces that are directly served by AHU air to renovate the air while also controlling the building's inner pressure to avoid an excessive built up of pressure that would lead to significant air balancing problems. Regarding the FCU's fans, they will be centrifugal variable speed with ECM's as well that will allow for continuous speed variation.

Air to Air Energy Recovery

A widely used method to achieve higher efficiency across the HVAC system while maintaining adequate IAQ is to employ air-to-air energy recovery. This energy would be transformed as a byproduct of the HVAC system and would typically be released to the outside air, but in recent years, building energy codes and standards have been trending towards requiring energy recovery capabilities to reduce the electricity consumption and increase sustainability, particularly for large service buildings. EACE designed this system to widely employ energy recovery.

Exhaust room air energy recovery will be employed in the DOAS's units and in the AHU's, in a comfort-to-comfort application, where the enthalpy of the supply air is lowered in the warm season and is raised during cold weather by transferring energy between the supply and exhaust air streams [34]. The AHU's will employ room air to temper the incoming DOAS air that will allow for a portion of the sensible and latent load that is carried in the exhaust stream to be transferred to the incoming stream. This will allow for a certain room air recirculation. A typical outdoor air fraction is 0.3 although it varies according to the occupancy and room temperature with a concern to maintain acceptable ventilation rates. This method is not a novelty as it is already used in the current AHU's.

More relevant is the usage of enthalpy wheels, which are in its essence, a rotary air-to-air heat exchanger with an electric motor to power the rotation. Both the water-based and the DX DOAS's will be equipped with them. They will have sensible and latent heat transfer capability. A minimum efficiency for sensible heat recovery of 75% was called for, which is a relatively high efficiency unit comparing to the standard. The efficiency for the latent recovery was not specified. The velocity of rotation of the wheel will be adjusted to guarantee a maximum working efficiency point. In economizer mode, the rotation of the wheel will stop automatically to allow for free-cooling/heating.

2.4.4 Independent Air Conditioning Systems

This section is related to the HVAC systems that are not connected to the central plant and therefore, allow for independent use, both at the ventilation and terminal air treatment level. This type of systems were deemed necessary by EACE due to some spaces that have a different schedule than most of the other spaces. These independent HVAC systems will be direct expansion variable refrigerant flow (VRF) systems, more precisely, heat pump VRF's. They will be capable of cooling or heating with the particularity of, for each outdoor unit (OU), the correspondent indoor units (IU) will only be able to cool or heat at a particular time. They will have scroll compressors with speed modulation (VFD's) to adapt the cooling/heating power to the current load. These characteristics allows for excellent part-load performance, which is essential taking into account the varying load in these spaces. Additionally, this technology allows for great modularity as a number of OU's can be combined with the IU's freely, with diverse capacities available on both.

The units serving the rooms of Espaço 24h and the CGD Room will function 24/7 during the year, weekends included. They will only be closed for the summer holidays during August. This is due to the fact that these rooms are always open to the student community. In fact, Espaço 24h rooms are in dire need of this update as their thermal environment usually does not allow for thermal comfort to the users and are not up to an acceptable standard regarding IAQ. This arose from the initial projected use for these rooms, which was not 24/7 usage but simply normal classrooms[9]. Each room will have their local controller to select the desired functioning mode, temperature and fan speed, among other functions. The indoor unit's fan will have 3 speeds for local adjustment. Table 2.8 summarizes the spaces that will employ these VRF's, whether they will be served by a DOAS, and the number of outdoor and indoor units.

Table 2.8: Independent HVAC systems for Pavilhão de Civil and their location.

Served by DX DOAS	VRF	Zones Served
Yes, UTAN - B	1 OU, 5 IU's	Bar
Yes, UTAN - R	1 OU, 6 IU's	Restaurant
Yes, UTAN - E1	1 OU, 2 IU's per room	6 Rooms of the 24h Space
Yes, UTAN - E2	1 OU, 2 IU's per room	5 Rooms of the 24h Space, Reception and Forum Civil's Room
Yes, UTAN - LTI	1 OU, 10 IU's	LTI's rooms
No	1 OU, 4 IU's	CGD (Aquário)

Note: *OU - Outdoor Unit; IU - Indoor Unit*

To assure the needed ventilation rates, as well as to reduce the terminal equipment power, a DOAS into VRF solution will be used. DX DOAS's will be employed to pre-treat the OA to neutral indoor conditions with the usage of DX coils and energy recovery. This OA will be supplied directly to the inlet of the indoor units to be terminally treated according to the room needs. A portion of the room air will be recirculated back into the indoor unit and there will also be exhaust air grilles in each room that will

---

[9]Note that some spaces of Espaço 24h serve as classrooms during the normal class hours but also serve as study rooms for the remaining periods.

supply the enthalpy wheel of the DX DOAS to permit energy recovery. This approach will be employed for all of the VRF systems except the CGD room, which is already served by a multi-split VRF unit and will employ a fresh air fan to introduce OA in the VRF IU's inlet and an exhaust fan to remove used air from the space and therefore assure acceptable IAQ. Seeing that both the DOAS's and VRF's will use variable speed fans, careful air-side balancing and communication between units will be necessary. This configuration is similar to that employed for most of the FCU's. Figure 2.8 showcases the connections for the VRF and DOAS systems.
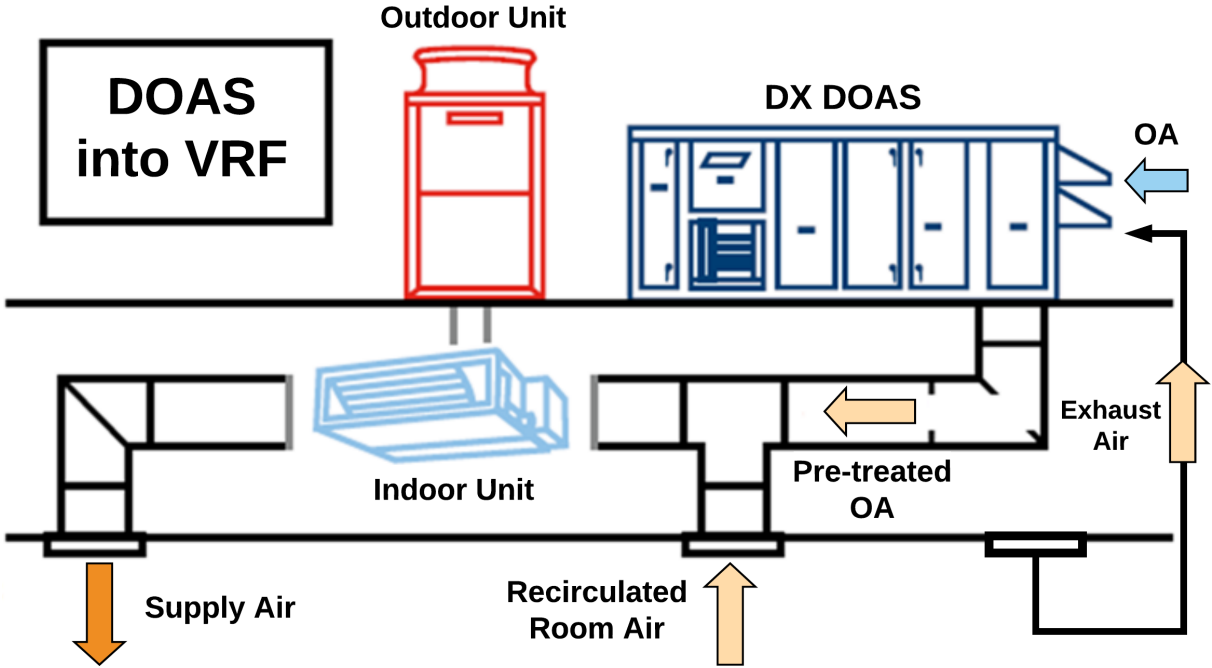
Figure 2.8: Layout of a DOAS with energy recovery into a VRF system, adapted from [38].

Chapter 3

Energyplus Modeling and Primary Outcomes

Having introduced the designed solution conceived by EACE in chapter 2, it is now timely to introduce the numerical *Energyplus* implementation. Therefore, in this chapter, besides an introduction on dynamic energy building simulation and on the *Energyplus* software, the old model is introduced, the non-HVAC related updates that were added are addressed, a secondary ideal load simulation to assess the 4-pipe necessity is presented and the main model's implementation is explained, alongside the needed simplifications introduced in it. Also, some primary outcomes of the previous modeling are analyzed.

3.1 *Energyplus* Software

Energyplus is a free, widely employed, open-source software focused on building energy modeling (BEM). It started development in 1996 combining two BEM programs, DOE-2 and BLAST. It has been in development since by a number of entities, funded by the U.S. Department of Energy Building Technologies Office and developed by the National Renewable Energy Laboratory (NREL) alongside with other academic institutions and private firms. It is essentially a simulation engine with a rudimentary user interface, based on comma-separated, ASCII text files that include the user's input and output requests [39]. It is a solver-based engine since the governing equations under simulation are implicit and the engine itself includes the numerical solvers (that solve or iterate and approximate the equations in time). It includes diverse modules that contain a set of equations for simulation of building physics for air, moisture and heat transfer, allowing for multi-zone simulation with heat and mass balances, which allows for a prediction of temperature and comfort as well as to energy usage and efficiency. A fundamental assumption of the heat balance model is that each thermal zone is modeled as well stirred with uniform temperature throughout, which is not completely realistic but necessary, otherwise, CFD would have to be employed. In order to better understand the structure of the software, figure 3.1a showcases the overall program structure, which is fundamentally made of 3 basic components: a heat and mass balance module, a simulation manager and a building systems simulation module. Figure 3.1c showcases

the simulation manager structure, while figure 3.1b shows the building systems simulation manager.
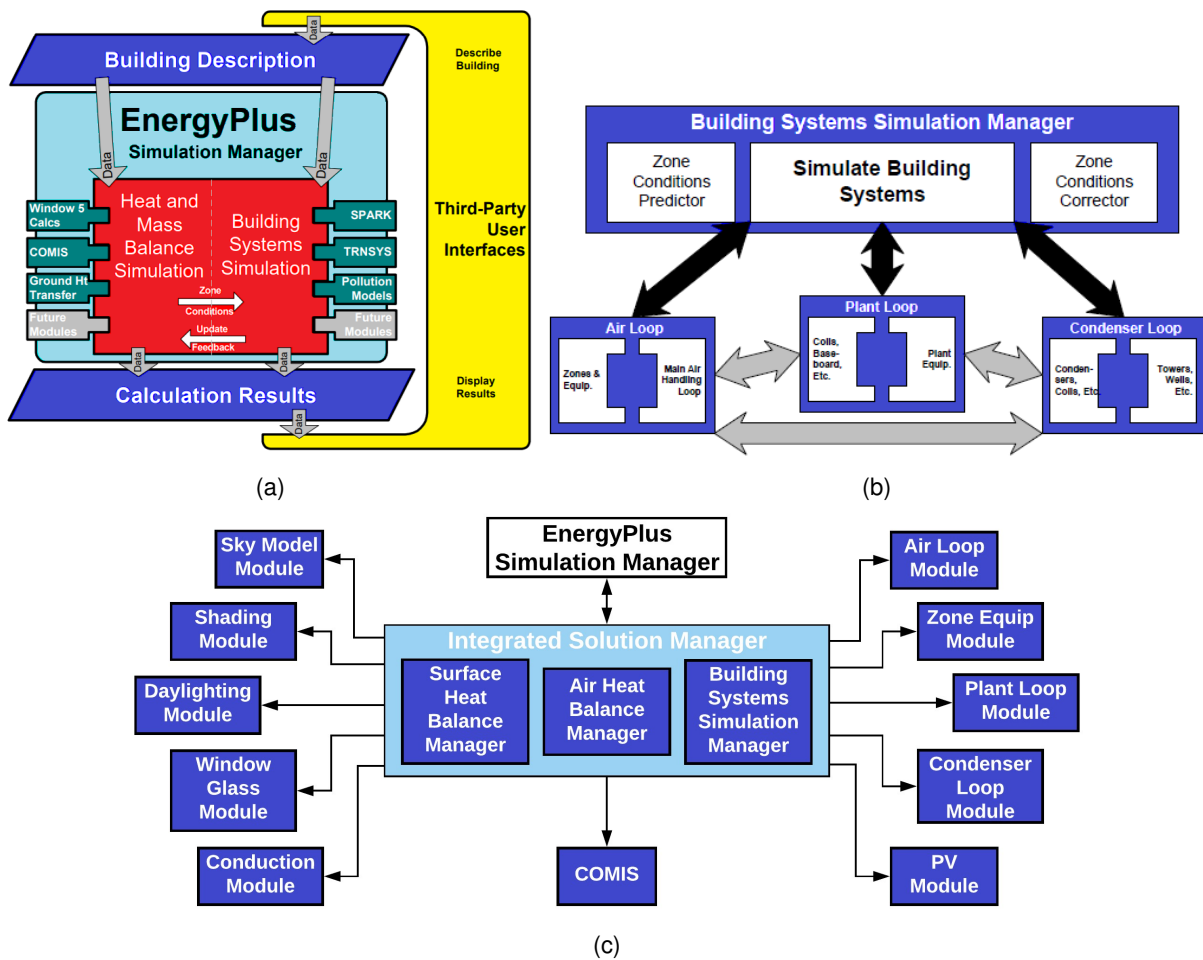
Figure 3.1: Overview of *Energyplus*'s structure and the communication between the modules, adapted from [39]. (a) - Overall structure, where the 3 basic components can be seen; (b) - Building simulation manager and communication between different sub-components; (c) - Integrated simulation manager and its sub-components. Note that additional modules have been added to the program, as these figures are not up to date.

3.2 Original Model of Pavilhão de Civil

The model developed in the context of this dissertation was based on a previously created one that was provided by *Campus Sustentável*. The initial model, with the construction of the geometry and the HVAC, was done by an outsourced company that was employed by IST to model all of the Alameda *campus* buildings, in *DesignBuilder*$^{\text{TM}}$ software. The intention was to use dynamic energy building simulation to study energy efficiency measures. This model showed limitations on the HVAC modeling and subsequently, a number of theses have been done focusing their study on energy simulation of Pavilhão de Civil using *Energyplus*. The initial *Energyplus* model, that was converted from the *DesignBuilder*$^{\text{TM}}$ model, implemented the current HVAC system in a detailed manner, calibrated it and implemented the internal gains and schedules. It was carried out by Marçal [17] in 2015, with the internal gains (lighting, electronic equipment and occupancy) and schedules entirely based on the 2013 energy audit performed

by the *Campus Sustentável* team. Following this, the *Campus Sustentável* team improved the model by updating the schedules and internal gains description based on an updated 2015 energy audit, by adding some missing fenestration elements (some interior windows) and by including a simplified implementation of the shading system that was being installed by then. Subsequently, other thesis were developed during that time that used the initial Marçal's model, without the improvements that had been introduced. This was the case of Santos's [18] thesis in 2016. Subsequent dissertations by Almeida [20] and Garção [21] that also used the model were concluded in 2017.

Having had access to all these models except that of Garção [21], it was decided to use the *Campus Sustentável* improved Marçal's model as the base model. This was done due to a couple of reasons:

1. Unfortunately, Almeida [20] used the older Marçal's model without the added geometry improvements but did an excellent work modeling and analyzing the newly installed shading system (electronically controlled venetian blinds). Moreover, the method Almeida employed to control the angles of the slats was based on the calculated PMV, an *Energyplus* output. Seeing that all of the HVAC system is being replaced, it did not seem reasonable to use this method because, firstly, new PMV values will be obtained with different HVAC equipment. Secondly, the method to input the slat angles calculated by the algorithm in the software is way too time consuming to be practical. However, the shading system was considered and modified in this thesis model, based on Almeida's work. This is further explained below in section 3.3.

2. Santos [18] focused on diagnosing the thermal comfort and Garção [21] studied improvements to the building envelope. For the most part, no improvements were added to the model to describe the real building in both cases, only hypothetical improvement measures. It should be noted, however, that Garção found some geometrical errors and improved the model, but his simulation used an ideal load analysis, which simplified the description of the HVAC systems in the model to an ideal one.

Figure 3.2 showcases the 3D building model of Pavilhão de Civil.
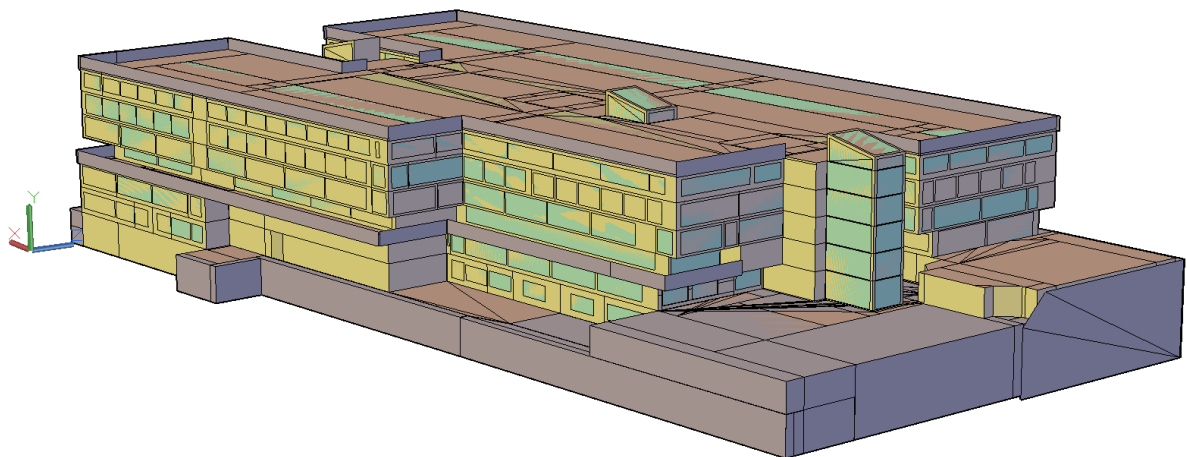
Figure 3.2: Image of the 3D Pavilhão de Civil model from a southwest perspective.

33

The initial thermal zoning was done in *DesignBuilder*^{TM} and remained unchanged since. There are a total of 186 thermal zones[1]. Seeing that it was extremely time consuming to change these zoning owing to the rudimentary graphical user interface of *Energyplus*, it was decided to maintain the original layout. Minor problems arose due to this when defining the HVAC system. These will be addressed below, in section 3.6.2.1. The thermal zones defined can be consulted in Appendix A.

3.2.1 Weather File

In order to run the simulation, a .EPW weather file is mandatory. This file will serve as a boundary condition and an input in the software for it to obtain the yearly climatic data necessary to perform the simulation, such as dry-bulb temperature, dew-point, relative humidity, direct and diffuse solar radiation, among others. The file used was obtained from LNEG and presents data in an hourly format; however, *Energyplus* interpolates these values according to the simulation timestep. The location corresponds to Lisbon and is adjusted to 109 meters, which is the altitude of the building relative to sea level. The data was gathered for the Portuguese Building Certification (SCE in Portuguese notation) update of 2013, and is based on IPMA's 1971-2000 climatology data with 2015-2060 climate change predictions from the RCP4.5 and RCP8.5 emission scenarios [2]. Previous models used this weather file. This future-centered weather file is a benefit on the analysis as it accounts for weather changes in the coming decades while basing itself on past data.

3.3 Non-HVAC Modifications to the Original Model

The initial models obtained were in an older *Energyplus* software version, v8.1 and v8.3. The model used was initially in the v8.3 version. After running some simulations to gain experience with the model and the software itself and to compare with the results of the theses of Marçal [17] and Santos [18] (which matched to a satisfactory degree), the model was updated to v8.8. This was not only due to general updates and bug fixes, but as well due to some recently added features that were necessary to more accurately describe EACE's HVAC system. The main non-HVAC modifications introduced in the *Energyplus* model will be addressed below.

3.3.1 Shading

With the installation of a new shading system, as mentioned in section 1.2, and after Almeida's work in his thesis not being present in the model adopted, it was decided to transpose some of the shading system implementation from Almeida's model to the new model. *Campus Sustentável* added shading

---

[1]A thermal zone is a volume within the simulation model which includes a space or, more commonly, a set of spaces within a building that possess similar internal gains, solar orientation and HVAC equipment and are thermally controlled in a equivalent manner as such, for modeling reasons, they possess the same thermal characteristics at a particular timestep of the simulation. For *Energyplus*, each thermal zone must be served by the same HVAC equipment

[2]The RCP (Representative Concentration Pathway) is a greenhouse gas concentration projection used by the IPCC (Intergovernmental Panel on Climate Change). RCP4.5 assumes peak greenhouse emissions in the 2040's and then decline and projects a global warming of 0.9 to 2 $^\circ C$, while RCP8.5 predicts that emissions continue to increase throughout the 21st century and projects a global 2.6 to 4.8 $^\circ C$ temperature increase.

to the spaces but used a more simplified description of the blinds and of the radiative properties of the glass when compared to those of Almeida. Concerning the blinds, Almeida obtained manufacturer data for the material of the blinds model [20] (Model - "Daylight TLT" from *Warema-Cruzfer*[TM]) and input these data in the *WindowProperty:Blind* object. Regarding the windows glass, he used a spectral data set to describe the windows glasses transmittances and front and back reflectances for varying wavelengths, using the *MaterialProperty:GlazingSpectralData* object while the previous implementation simply used spectrally averaged data. Both these improvements were added to the model. Moreover, some errors were detected in implementation of the blinds in the *Campus Sustentável* model that were fixed, such as exterior blinds that were input as interior and the Museum's interior blinds, which are for the vast majority of the time down, were controlled according to the solar radiation focusing on their windows.

The *WindowProperty:ShadingControl* object was used to select the control method and it was decided to simplify the control when compared to Almeida's implementation by using automatic control of the type "OnIfHighSolarOnWindow". This will activate the blinds at a preselected slat angle when a selected setpoint of global horizontal irradiance (direct normal plus diffuse horizontal irradiance) is surpassed. This value was set at 400 $\frac{W}{m^2}$, which is slightly below that of an intermediate value between the yearly average midday (12h) of 854.6 (direct normal) added to 101.7 (diffuse horizontal), which is $956.3\frac{W}{m^2}$ in clear sky solar conditions, calculated from the ASHRAE weather data of Lisbon's airport, weather station WMO:085360 [40]. This value is present in the weather file. In practice, for a sunny day, the blinds will be active if the sun is facing the shading system window. Regarding the angle of attack of the slats, a constant $45°$ angle was selected as it is a compromise value between letting solar light in while blocking some of the incoming solar radiation. The capability of adjusting the angle dynamically was not implemented. The shading system does influence the final results and therefore is an important factor when analyzing them. Despite this, seeing that this dissertation is focused on the HVAC modeling, this implementation was a compromise.

3.3.2 Internal Gains

Some time was dedicated to improving the internal gains modeling. For energy modeling purposes, these internal gains were defined by the following 3 *Energyplus* objects: *People*, *Lights* and *ElectricEquipment*. The latter object accounts for computing equipment, plug-in equipment, catering equipment and the lifts of the building. These were initially input by Marçal based on the energy audit [12]. It was possible to improve the utilization profile for these 3 different sources of internal gains to improve the accuracy of the model. To achieve that, a number of presential visits were performed during the making of this dissertation. Those were accomplished with the intention of aiding the *Campus Sustentável* team on the update of the energy audit (last updated in 2015), but ended up serving as a basis to update the internal gains section of the simulation model. The offices and secretariats from the 2nd and 3rd floor were not visited, therefore, most of the modifications were on the remaining 4 occupied floors (02, 01, 0 and 1).

People

Regarding the occupation modeling, some slight inaccuracies were found when analyzing the model. In order to synthesize the modifications done, table 3.1 is presented below. These occupation values refer to the design conditions and will be controlled in time by the schedules that were input into the software.

Table 3.1: Modifications on the number of people in the model for some spaces and thermal zones (TZ).

Space	TZ	Old Occup	New Occup	Comment
–	19	6	0	New HVAC Equip Technical Space
02.10, 02.11, 02.12	46	6	2	IST Press Offices
01.36, 01.37, 01.38, 01.39	59	3	55	Library + Librarian Offices
V0.10, V0.11, V0.12, V0.13	57	152	104	Based on Gestão de Espaços
VA2	63	52	65	Based on presential visit
01.07, 01.08	71	1	6	Labs, presential visit
Bar	78	4	60	Based on presential visit
CGD (Aquário)	81	0	90	Based on presential visit
V0.05 (Silence Room)	83	4	40	Based on presential visit
V0.01, V0.02, V0.03, V0.04	84	150	170	3 24h rooms and prayer room
Restaurant	91	2	100	Based on presential visit
V1.27, V1.27, V1.29, V1.30	98	150	120	Based on presential visit
Main LTI Space	103	0	84	Based on presential visit
V1.20.3	105	0	35	Computer room in LTI
V1.20.1	172	0	30	Computer room in LTI
4.41	127	0	6	Meeting Room for DECivil
4.06, 4.06.1	136	0	4	PhD Students Room

Additionally, within the *People* object, the fraction of radiant energy emitted by the occupancy was manually changed from 0.3 to 0.5 in all occupied spaces. This was based on information presented in ASHRAE Handbook - Fundamentals [24] for sedentary work in an intermediate to low air velocity. This value will be multiplied by the total sensible heat emitted by the people, which will account for long wavelength radiation gain, while the rest is assumed to be convective heat gain. The latent heat gains are computed outside this calculation and are not included in the radiant and convective gains. A brief test was done in an *Energyplus* example file to understand the influence of this parameter in the people's heat gains. For a 183 m^2 space with 20 people, the annual sensible heating rate from the people was calculated to be only 0.2% higher for the 0.5 case. This change is therefore regarded as inconsequential but more accurate nonetheless.

Lighting and Electric Equipment

Lighting is often a major space cooling load source but calculating it is not straightforward because the load from lighting can be considerably different to the heat equivalent of input power [24]. In the building, an effort has been underway to gradually substitute the common space lamps, such as corridors and lobbies, to higher efficient ones. Despite that, the internal gains for lighting were not changed in a significant manner due to the copious amount of lights that the building has. However, corridor lights from TZ 93 were added since they were missing. The lighting level added, in Watts, was based on the

presential visit.

Regarding the amount of energy from the lights that goes into the space and effectively adds sensible heat gain, it was possible to improve the definition that was in the model. *Energyplus* defines the heat gains from lights through 3 user-input parameters: fraction radiant, fraction visible and return air fraction. A 4th parameter, fraction convected to the zone air, is calculated by the program as the remaining portion to account for 100%. It was verified that, for the vast majority of the lights defined in the models, the fraction radiant was equal to 1, meaning that all of the lighting energy is transferred into the space through radiation. This is not realistic and therefore, it was decided to find a more accurate compromise for these parameters. Taking into account the *Energyplus* Input Output Reference manual [41], one can consult a table with approximate values for these lighting parameters for different luminaire configurations, based on ASHRAE's 1282-RP - " Lighting Heat Gain Distribution in Buildings ". Despite the tendency being to continue installing higher efficiency lighting, including LED's, the most common lighting fixtures in Pavilhão de Civil are recessed luminaires with non-ducted parabolic louvers and ballasts housing fluorescent lamps (mostly tubular). In these, most of the heat gain goes into the space and not into the return air ducts. Therefore, for the spaces that are conditioned by the HVAC system, it was decided to use 0.05 for the return air fraction, taking into account the lamps that are close to the return air ducts and transfer heat through conduction from the luminaires to the fake ceilings and therefore, to the return air ducts, despite these being thermally insulated. For the remaining parameters, the values were based on [41], mentioned above: fraction radiant at 0.2, and fraction visible at 0.2, meaning that most of the lighting heat will be convected to the space, at 0.55. This is an approximation because not all of the lamps of the building are of this type. However, in the whole building, the percentage of tubular fluorescent lamps (T8 and T5) is approximately 86% and on the 2nd and 3rd floors, which were not visited thoroughly, is about 92 %, according to the 2015 energy audit excel spreadsheet [12]. This confirms that this is a good approximation of the lighting heat gains.

The definition of the electric equipment is important to the accuracy of the model, especially so when a large number of equipment is used in a single space, introducing, therefore, a considerable sensible heating load. This was also not a subject of huge changes, although some small improvements were introduced. In the 2nd and 3rd floors, most offices had some space heaters modeled, assumed to mainly be fan or radiant heaters, that were used to heat the space locally. This was due to the incapability of the current HVAC system to heat these spaces to a comfortable state during the heating season. These were eliminated as it was assumed that the new HVAC system, using FCU's, will be able to maintain the space temperature at a comfortable level. Moreover, the computers heat gains from laptops were added to the CGD (TZ 82) and Espaço 24h (TZ's 41, 83 and 84) rooms, where laptop usage is extremely common for study purposes. From [24], the peak heat gain for a typical laptop is 46W with 75% convective heat and 25% radiative heat. These were input separately from all other objects, as summarized in table 3.2.

Also lacking in the model was the description of the internal gains through electric equipment (other than lights) in both the bar and restaurant. The reason is that, when the last energy audit was done, these spaces were left out as they are externally explored by different companies and are, therefore, regarded as concessions. However, taking into account that these spaces will have new HVAC installed (VRF

Table 3.2: Added laptop heat gains to different thermal zones. The number of laptops refer to design levels and were based on direct observation in the spaces.

Space (TZ)	Number of Laptops	Peak Design Level [kW]
Silence Room (83)	25	1.15
4 Espaço 24h Rooms (84)	$4 \times 25 = 100$	4.60
4 Espaço 24h Rooms (41)	$4 \times 25 = 100$	4.60
CGD Room (81)	80	3.68

systems) that will be modeled, it was important to approximate the model internal gains description to the real case. It was considered unpractical and beyond the scope of the present dissertation to survey each equipment used in these 2 spaces as well as to schedule each of the equipment. Therefore, a gross estimate was performed taking into account the values for kitchen appliances from ASHRAE's Fundamentals Handbook [24], during idling and during cooking, and taking into account the equipment present in each space. For the bar, TZ 78[3], a 10.8 kW peak heat gain was estimated, while for the restaurant, TZ 91[4], 4.5 kW. A 0.2 latent fraction was assumed, while the rest is sensible heat. Of that sensible load, a 0.2 radiative fraction was assumed.

Regarding other spaces, the existing modeling of the electric equipment's gains was deemed accurate enough.

Schedules

Furthermore, a number of schedules for the occupation have been updated. That was accomplished by changing the hourly multiplier, from 0 to 1, for an entire day. There are 5 different types of days, as defined in the audit [12]: working days during the academic year, working days during the holiday season, Saturdays during both the academic year and during the holiday season, Sundays and holidays during both as well, and the reduced activity period (2 weeks in August). Most of the updates were on the more frequent type of days, the first one, as most of the rooms are closed on the other types of days. An exception is the spaces from Espaço 24h. These updates were based on presential visits, online rooms timetables and experience gained during the time as a student of IST and therefore, as a frequent occupant of Pavilhão de Civil.

The spaces that will be served by the new VRF's were lacking in the occupation scheduling: the occupation of the all rooms of LTI was matched with the real schedule during the academic year (8h-23h during weekdays and 9h30-15h30 on Saturdays), the CGD Room (Aquário) was adjusted to allow for all-day occupation during the week and during the weekends as well, the bar schedule[5] was adjusted to better match the real occupation, the restaurant occupation was also changed according to the real timetable[6], and in the TZ's from Espaço 24h (83, 84, 41), occupation was added during Saturdays and Sundays as well. Moreover, the library schedule was adjusted to match the real timetable (9h-18h during weekdays), the schedules from the architecture rooms of TZ 57 were tweaked as well to

---

[3]The kitchen of the bar (TZ 79) will not have its electric equipment modeled, only the public space.
[4]Similarly to the bar, only the public space of the restaurant will be modeled.
[5]The bar schedule is from 9h to 20h for week days.
[6]The restaurant only serves lunch, during the week from 12h to 15h.

allow for occupancy during the after-classes period and the schedules for the amphitheaters VA1, VA2, VA3, VA4, VA5 and VA6 were tweaked to better match the expected occupancy according to the online timetables. Furthermore, for all of the 1st floor classrooms (ZT's 94, 96, 98, 100, 101, 102 106, 107, 108, 109 and 110), the occupation schedules were matched to the real timetable for the academic year (1st semester of 2018) that can be consulted online. Additionally, the spaces referenced in table 3.1 that had null occupation had their normal occupation schedule adjusted as well. Finally, during July, occupation was removed from the classroom spaces that are the VA amphitheaters in the 01 floor, the architecture classrooms of TZ 57 and the classrooms from the 1st floor. All these measures allow for a more accurate yearly input of the building occupation.

The computer gains schedules were also subject to changes. For all the LTI's rooms, the computer (desktops) usage schedule was tweaked according to the real schedule. Additionally, for the zones where the laptops were added, shown in table 3.2, schedules had to be created for the entire year. These were created taking into account the yearly occupation of these spaces as well as the hourly occupation, which was based on observation and previous experience as a user.

Additionally, having added the heat loads from the Bar and the Restaurant, it was necessary to input new schedules for the hourly parameterization of the electric equipment in these spaces for all types of days. These were done on the basis of the scheduled people occupation as well as on the assumption that early morning is a typically higher equipment usage rate period in the bar, while in the restaurant's case, this is during late-morning and lunch hours.

Other Remarks

Despite this section being focused on the non-HVAC related modifications, an additional modification was conducted taking into account the 4-pipe system projected, with the capability of simultaneous heating and cooling, which was the timing of changeover for the indoor temperature setpoints, which can be seen in the following table 3.3:

Table 3.3: Interior temperature setpoint changeover dates.

Period	Interior Setpoint [$^\circ C$]
01/01 to 20/04	20
21/04 to 20/10	24
21/10 to 31/12	20

For instance, for a particular winter morning, cooling may be required to meet the 20 $^\circ C$ setpoint in a perimeter, sun exposed room, while in another room (probably an interior room or a westerly or northerly faced room), heating will be called for to achieve the setpoint. The criterion for the selection of the dates was 1 month after both the start of Spring (21/04) and the start of Autumn (21/10) in the Portuguese calendar. This was chosen taking into account that lately, the Summers have been quite extended and that in April cold weather is still frequent. These dates were selected to input in both the new main model and in the ideal loads one, but obviously, the final dates for the changeovers are open to debate and are up to the technical management team of the building to decide. In fact, in the majority

of the conditioned spaces, the indoor setpoint will be able to be controlled directly by the occupants in the room thermostat. However, this is highly dynamic and not possible to implement in the model.

3.4   Computational Parameters for the *Energyplus* Simulations

Energyplus offers a vast amount of possibilities regarding the numerical simulation parameters, such as the choice of algorithms for heat transfer, for shadowing calculation inside and outside, while also allowing to define the convergence tolerances, the simulation timestep, among others parameters. While it is not feasible to go over each of the possibilities, this section intends to summarize the most important and generic simulation parameters. These were used across all simulations, whether they are the ideal load simulation or the main model with the detailed HVAC implementation. The implementation of Marçal [17] suggested some parameters while Almeida [20] added to it by changing the shadowing algorithm. These were taken into account with additional input from [42] that analyzed the influence of these parameters in the simulations runtime. One of the main parameters is the timestep of the simulation. The timestep chosen was 10 minutes that is a compromise between accuracy and runtime[7]. The main parameters are shown in the following table 3.4.

Table 3.4: Computational parameters on *Energyplus* for the simulations.

Energyplus Parameter	Choice used	Comment
Number of Timesteps per Hour	6	A compromise between accuracy and reasonable run times
Maximum HVAC Iterations	40	-
Warmup Loads Convergence Limit	0,04 (4%)	-
Minimum Plant Iterations	4	Increased from 2 to improve plant calculation stability
Maximum Plant Iterations	12	Default is 8
Temperature Convergence Limit	$0,2\,^{\circ}C$	-
Minimum System HVAC Timestep	5 Minutes	Increases run-time compared to 10 min but adds stability
Heat Balance Algorithm	ConductionTransferFunction (CTF)	-
Solar Distribution	FullExterior	-
SurfaceConvectionAlgorithm:Inside	AdaptiveConvectionAlgorithm	-
SurfaceConvectionAlgorithm:Outside	AdaptiveConvectionAlgorithm	-
ZoneAirHeatBalanceAlgorithm	ThirdOrderBackwardDifference	-
ShadowingCalculation Method	TimestepFrequency	Improves the shadowing calculation accuracy despite increasing run time

---

[7] *Energyplus* allows for a timestep of up to 1 minute, however, the norm for larger buildings and annual simulations is 10 or 15 minutes.

3.5 Ideal Loads Simulation with *Energyplus*

An ideal load simulation using *Energyplus* is one that allows the rapid assessment of the thermal loads within a space/building without the need to model a full HVAC system, with the usage of the *Zone-HVAC:IdealLoadsAirSystem* object. This zone component can be considered an ideal HVAC unit that mixes room exhaust air with OA and adds or removes heat and possibly moisture at 100% efficiency to produce a supply air stream in the desired conditions. It is also a VAV system, as it varies the supply air flow rate dynamically. In order to assess the simultaneity of heating and cooling load needs across the whole year and, therefore, determine the need for a 4-pipe system in Pavilhão de Civil, an ideal load simulation was performed. *Campus Sustentável* supplied an ideal load *Energyplus* model that was employed to evaluate changes in the building envelope. It was updated to v8.6 and had all of modifications and improvements added to it in the internal gains, shading and scheduling department, as described in the above section 3.3. The ideal load object was changed to better suit the new project's energy recovery capability and supply temperatures set. Therefore, for the zones that will be served by the HVAC system, the following characteristics in the ideal load object were defined: 1) unlimited cooling and heating capacities; 2) unlimited air flow rate; 3) maximum supply temperatures for the terminal units as described in table 2.5, taking into account which spaces uses FCU's or direct AHU air and which spaces are served by VRF terminal units; 4) heating and cooling availability changed according to the real schedule of the space; 5) no dehumidification control; 6) OA requirements per occupant in each thermal zone, as defined in table 2.4, and finally 7), energy recovery capability through a rotary wheel with 0.75 sensible and 0.7 latent heat recovery efficiency in the spaces for which OA will be pre-treated in an energy recovery equipped DOAS. Additionally, schedules for the updated indoor temperature setpoint values and changeover dates were constructed, based on the information on table 3.3 and were fit to the spaces using the *ThermostatSetpoint:DualSetpoint* and *ZoneControl:Thermostat* object while taking into account the occupation schedule of each space. It is important to note that the value of the thermal loads output for each space in this simulation does not accurately represent the real values as this is an ideal, 100% efficiency (COP = 1) system. In fact, it will output a higher energy consumption that reality owing to not simulating a vapor-compression cycle that has an efficiency larger than 1. More important are the loads trends and whether it calls for heating or cooling at a particular time.

Firstly, the graph presented in figure 3.3, intends to evidence the yearly distribution of the heating and cooling loads for all conditioned spaces, through the usage of the "DistrictCooling" and "DistrictHeating" output variables. These are, for an ideal load simulation, the total (sensible plus latent) energy spent to cool or heat the incoming supply air stream to the desired temperature and humidity ratio. They can be regarded as the ideal "cooling coil" or "heating coil" load [41]. The energy supplied by exhaust air heat recovery is not accounted for in this parameter. It is possible to observe that, for some part of the year, mostly during March/April and October/November there is a simultaneity of cooling and heating loads, as expected. This drives the logic for the future installation of a 4-pipe system, as projected by EACE [29]. Additionally, the changeover date of the interior setpoint at 04/21 can easily be seen. Up until that date, from approximately the 2nd week of March, the cooling loads dominate in order to cool the

air up to the 20 $^\circ C$ setpoint whereas after that date, for some time, heating is still needed and actually dominates in order to heat the air to the 24 $^\circ C$ setpoint. That is not as easily seen for the other date, 21/10. Furthermore, one can confirm that the cooling loads dominates the energy needs in the building, as expected. In fact, the peak cooling demand is approximately 80% higher than the peak heating load, for these setpoints. Two additional remarks that should be noted: 1) the peaks and valleys correspond to the weekends, during which, only the VRF systems (for the Espaço 24h and CGD room) are available; 2) during the first 2 weeks of August, all off the HVAC systems are deactivated for holidays, therefore the big gap of null energy consumption.
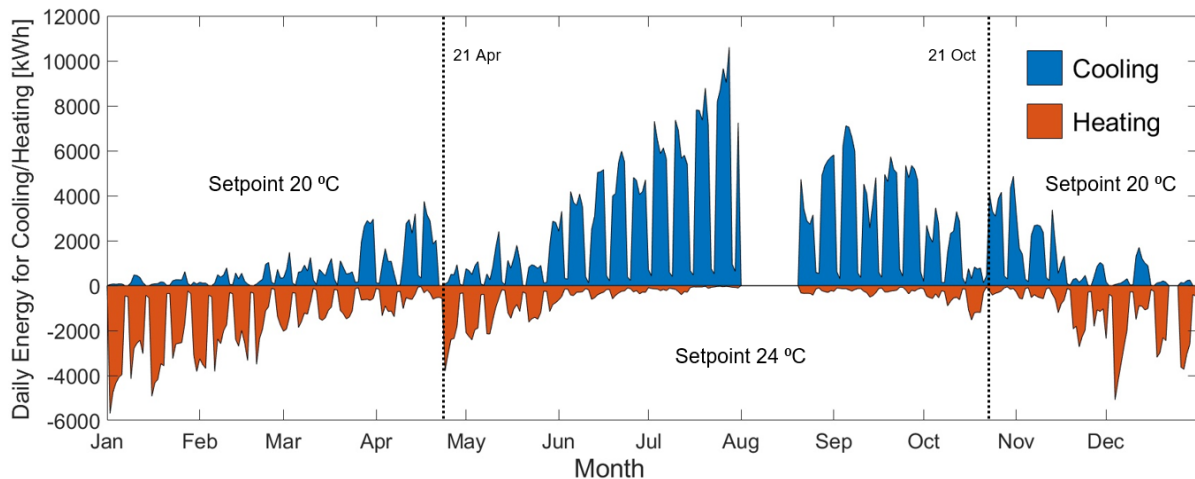
Figure 3.3: Annual graph of the daily energy usage to cool or heat Pavilhão de Civil in an ideal load simulation with the changeover date of the interior setpoint temperature and its value visible. Note that a negative value represents heating.

Secondly, two direct comparisons between two spaces over a single day are presented as an example of the diversification of the cooling and heating loads. Despite the fact that the times of the year mentioned above have a higher probability of simultaneous needs, a winter day in late February was chosen as a comparison, the 20th, and a Autumn day in November, the 6th.

Regarding the spaces, for the February day, two perimeter classrooms in the 1st floor were selected, TZ 109 that has an easterly orientation and will have sun radiation during the morning and 102, which is in the northern tip of the building with easterly-faced windows and has highly residual sun exposure due to self-shading from the building, only during very early morning. While TZ 109 is comprised of 3 classrooms and a PC room, TZ 102 is only comprised on 2 classrooms. Moreover, in the occupation schedule, TZ 109 has later afternoon occupation, until 20:00, while TZ 102 has no occupation after 17:00. The HVAC equipment is available from 8:00 until 20:00, during which the temperature setpoint will be met. The design occupation per room in each TZ is similar, 38 per room in 102 and 35 per room in 109.

For the November day, TZ's 114 and 123 were compared. Both are comprised of offices in the 2nd floor but, while TZ 114 is south-oriented perimeter zone with blinds and 5 offices for total zone occupation of 5 people, TZ 123 is an interior zone with no sun exposure and 15 offices for total zone occupation of 15 people. Both have equal occupation profile though.

The results are presented below in figure 3.4 and figure 3.5:
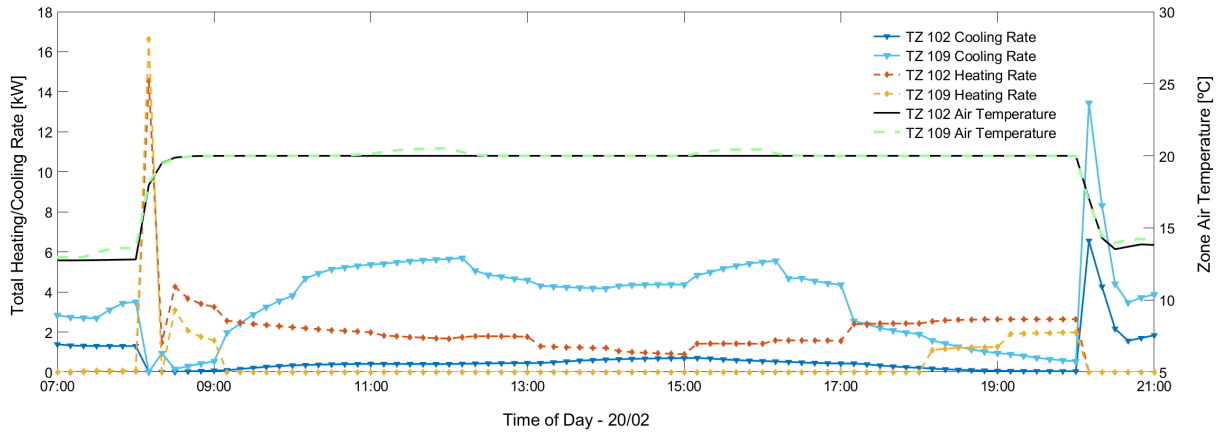
Figure 3.4: Comparison between the heating and cooling thermal rates for TZ's 102 and 109 on the 20th of February in an ideal load simulation.
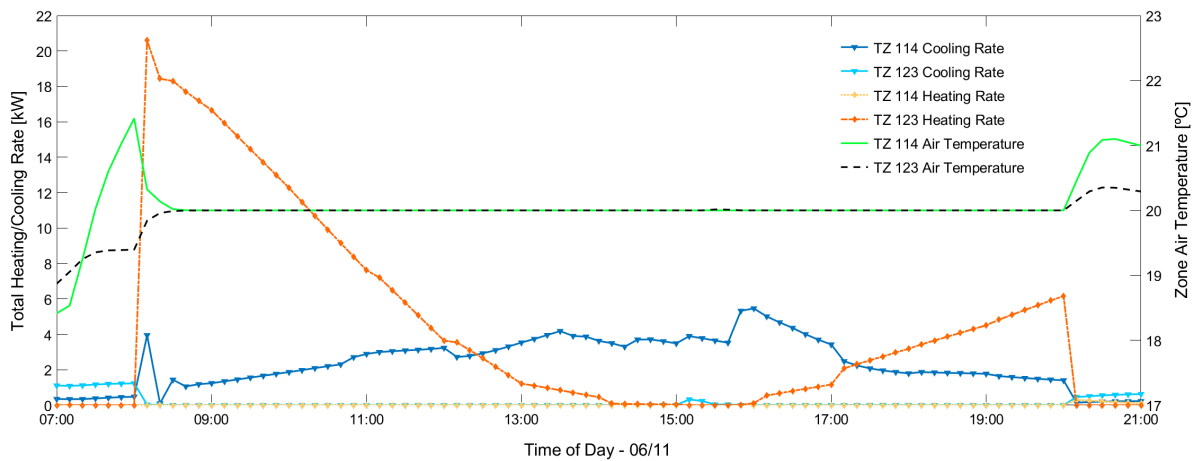
Figure 3.5: Comparison between the heating and cooling thermal rates for TZ's 114 and 123 on the 6th of November in an ideal load simulation.

For figure 3.4, at 8:00, there is a sudden heating demand to heat the room from the lower night temperature to the $20\,^{\circ}C$ setpoint, in both spaces. In TZ 109, this heating demand lasts until 9:00, from then on, there is a cooling demand across the day to achieve the setpoint. Contrarily, in TZ 102, heating is required during all day in order to maintain the setpoint, with the morning heating spike still present. The blinds in both TZ's, in this particular day, do not activate due to the overcast day in the weather file, in with diffuse radiation being predominant and the irradiance setpoint is, therefore, not met. The absolute values of the loads (the loads from TZ 109 are at least twice of those of TZ 102) are related to the actual size of the TZ's. This daily profile is fairly common between these 2 spaces, specially during winter days, in January/February and November/December. During the remaining part of the year, the norm is for both spaces to call for cooling during most of the day, with the morning heating spike still present in the colder Autumn and Spring days.

Regarding figure 3.5, the profile is similar to 102 and 109 TZ's behavior as for most part of the day,

43

there is a distinct load. However, it differs as during the morning, with the HVAC activation at 8:00, the interior TZ 123 denotes a big spike in heating while the TZ 114 calls for cooling as the air temperature at that time is above the setpoint. Moreover, an afternoon period in TZ 123 between approximately 14:00 and 16:00 is noticeable, as it requires almost no heating and cooling input to maintain the desired setpoint. That seems to correspond to an almost equilibrium state between the heat input from the internal gains and the conditioned ideal air and the heat's dissipation through the envelope. Regarding the blinds, TZ 114 does make use of them in most shading surfaces throughout the day, from 8:00 to 15:30. These contribute in attenuating the cooling loads.

Overall, this ideal load simulation allows to confirm and show that the cooling needs are indeed, vastly superior to the heating needs. Moreover, two examples were given of two distinct TZ's that show opposing cooling/heating needs during a single day. As such, it was evidenced that there is, in fact, a need for a 4-pipe system in Pavilhão de Civil to meet the temperature setpoints to a satisfying degree throughout the year.

Having introduced this simulation, the next section will focus on the modeling of the new projected HVAC system in *Energyplus*.

3.6   Modeling of the New HVAC System

In this section, the *Energyplus* implementation of the HVAC system retrofit, as designed by EACE [29], is summarized. The subsections are separated into 3 subsections: the hydraulic plant modeling in subsection 3.6.1, the air-side equipment modeling in subsection 3.6.2 and the independent VRF systems in subsection 3.6.3. In each subsection, the main approximations of the model are discussed.

3.6.1   Modeling of the Hydraulic Plant

The implementation of the hydraulic plant proved to be a challenge taking into account the models that are available in the *Energyplus* software and the configuration of the real plant, as shown in the previous chapter in figure 2.5.

Chillers/Heat Pumps

Having been given some guidelines for the type of chiller/HP intended, such as the cooling and heating capacities, the flow rates and the efficiencies, a unit was selected that matched the premises and was, therefore, used to model the performance curves with precision. The unit selected is from *Clivet*[TM] and the *SPINChiller*[3] *WSAN-XSC3 MF 200.4 4T SC* was the model chosen. It was selected not only because it matched the vast majority of the requirements but also, and fundamentally, because of the information that was available in the technical bulletin [32], specially the part-load performance, which is not that common to be present in other manufacturer's technical bulletins. In Appendix C, this data is presented. The cooling capacity for this unit is 545 kW while the heating capacity is 627 kW, therefore, regarding the projected capacities by EACE [29], the heating side is oversized, however, the cooling

side is practically equal to the project capacity. The heating capacity oversizing is acceptable, however, because these units perform better at lower part-load ratios. For instance, for cooling only, the optimal performance takes place in the 30-40% part load range. Moreover, this unit has 2 refrigeration circuits so the implementation of each unit was divided in 2, accounting for the 2 circuits.

The implementation was separated in 3 parts: cooling only mode, recovery operation for simultaneous heating and cooling and heating only mode. For all of them, performance curves from the data presented in Appendix C were constructed.

The *Chiller:Electric:EIR* model was used for both the cooling only mode and the cooling with recovery. It is an empirical model that uses 3 polynomial equations for performance at part-load conditions. The capacities were divided in two to account for each circuit, so, for a single unit, two *Chiller:Electric:EIR* objects were used. This will allow for a more accurate description of the performance at part-load, which, as said before, will be key. These curves are represented in figures 3.6a, 3.6b and 3.6c and can be used for a single circuit or for both at the same time as the outputs are normalized and are described as:

1. **CAPFT** - Cooling capacity function of temperature - $CAPFT = C_1 + C_2 \times LChWT + C_3 \times LChWT^2 + C_4 \times OADBT + C_5 \times OADBT^2 + C_6 \times LChWT \times OADBT$. This biquadratic curve parameterizes the variation of the cooling capacity as a function of the water temperature leaving the chiller (LChWT) and the dry-bulb temperature of the entering condenser fluid (OADBT), which is the OA seeing that the units are air-cooled. If the unit were water-cooled, this would be the temperature of the water entering the condenser, from the cooling tower outlet. This curve has a value of 1 at reference conditions, $7° C$ LChWT and $35° C$ OADBT. Data from figure C.2 in the Appendix was used and the "HVACCurveFitTool" available in *Energyplus* was used to calculate the coefficients. The curve used for the chiller, for cooling only operation, is presented in the following figure 3.6a. The recovery curve is very similar to the cooling only curve, therefore it is not presented. This curve is important to tell the simulation how the unit capacity changes at different leaving water temperatures and ambient conditions. The maximum capacity for the most frequent water and OA conditions that are expected is approximately 20% over the rated capacity. Moreover, data outside the 25 to 40 $° C$ OA temperature range was extrapolated when deriving all of curves' equation, including the following.

2. **EIRFT** - Electric input ratio function of temperature. Similarly to the biquadratic CAPFT curve, this EIRFT curve parameterizes the energy input ratio (EIR) at full-load as a function of leaving water and entering OA dry-bulb temperatures. The EIR is the inverse of the EER. For reference EIR values, the curve has a value of 1, which is at EIR = 1/3.17 for cooling only or 1/3.39 for recovery operation, however, these cannot be directly compared because, in the implementation, the cooling only operation does not take into account the energy from the condenser fans while the recovery operation does. However, a higher EIR is translated into a lower COP and therefore, a less efficient working point. Data from figure C.2 in the Appendix was used and the "HVACCurveFitTool" was again used. This curve, presented in figure 3.6b, is important to tell the simulation how the unit efficiency changes at different leaving water temperatures and ambient conditions. The lower the

45

outdoor temperature, the higher the efficiency and the higher the leaving water temperature, the higher the efficiency is as well. The recovery operation is implemented to be more efficient than the cooling only for the most part, which can be seen through observation of the dashed recovery lines in the figure, which are below the solid cooling only lines.

3. **EIRFPLR** - Electric input ratio function of part load ratio (PLR) - $EIRFPLR = C_1 + C_2 \times PLR + C_3 \times PLR^2$. This quadratic curve parameterizes the EIR as a function of the PLR. Again, for reference conditions, at PLR = 1, it is equal to 1. This curve is, therefore, fundamental to describe the efficiency at lower loads. Data from figure C.5 in the Appendix was used and the curve can be seen in figure 3.6c. It is possible to see, apart from the normalized EIR values for the curve, 6 working points with their EER's that were obtained from figure C.5 for the cooling only case and generated from table C.1 for the recovery case, both present in the Appendix. It is visible that the chiller is most efficient in the 30 to 40% range.

(a)

(b)

(c)
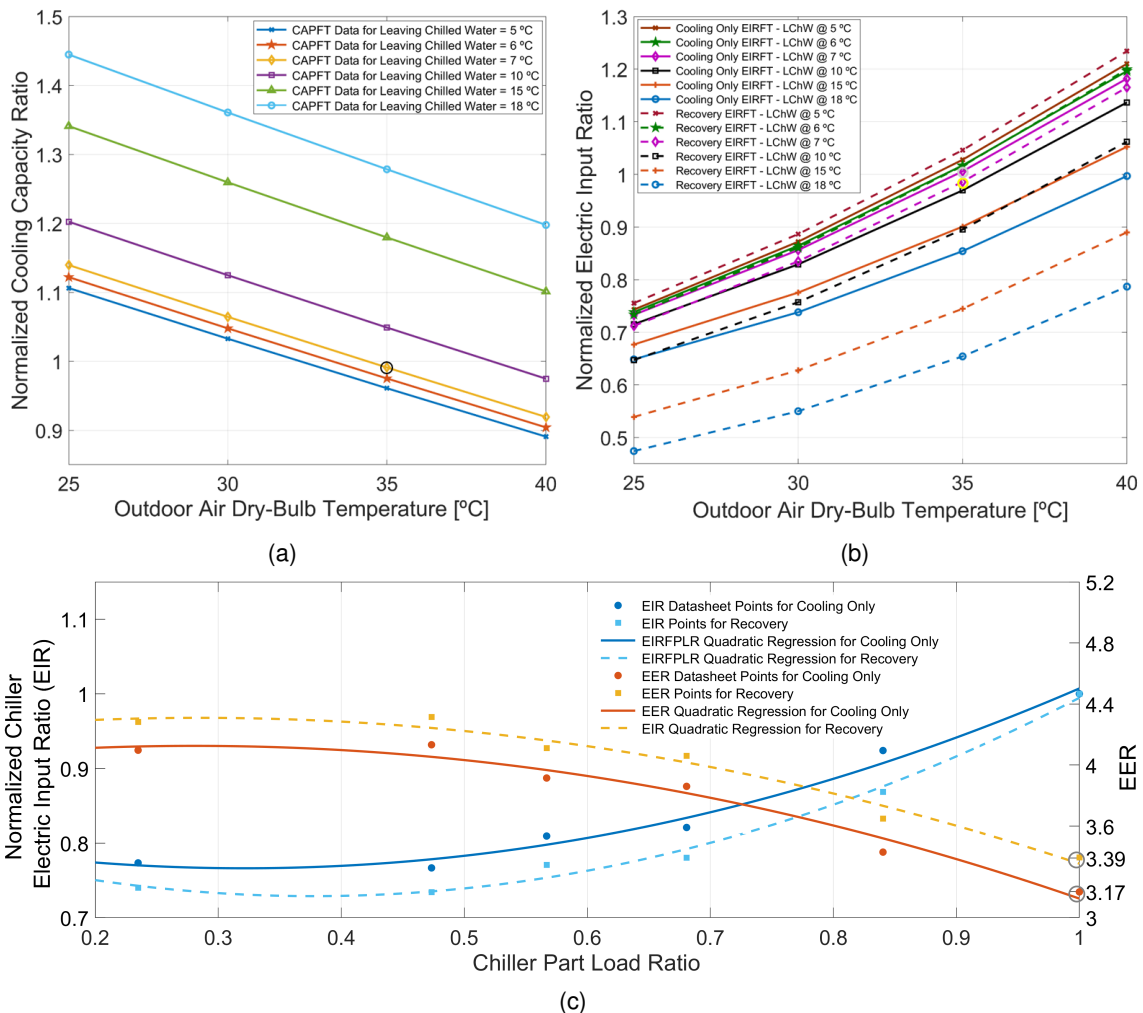
Figure 3.6: Operating *Chiller:Electric:EIR* performance curves. (a) - CAPFT curve for cooling only operation; (b) - EIRFT curve for cooling only and recovery operation; (c) - EIRFPLR regression curves for cooling only and recovery operation alongside the working EER's at 6 different part load ratios and their regression curves. Nominal working points highlighted in each figure with a circle.

Additionally, the condenser fan power ratio, which is the ratio of the condenser fan power to the reference

chiller cooling capacity, was entered in the cooling only implementation due to the incoherence in the data that was available, with figure C.2 detailing compressor input power and figure C.5 detailing the total power input, including the condenser fans. As such, the condenser fan power was modeled separately from the compressor power and not included in the curves described above for the cooling only case.

The *Chiller:Electric:EIR* model allows for condenser heat recovery, but, unfortunately, only through the use of a water condenser loop with a cooling tower, due to the inherent model. This is not accurate to the real project as the units will be air-cooled. Therefore, in order to achieve cooling and heat recovery, a condenser loop with a cooling tower was constructed to comply with the requirement of the model. The *CoolingTower:VariableSpeed* model was used and is based on empirical algorithms and has a variable speed fan built in that allows for more adaptability when compared to the single speed one. This was the main reason for choosing this model. The "YorkCalc" algorithm was employed with the air and water loop flow rates autosized. A variable speed pump bank of 3 was also used in the inlet branch of the tower. For the chiller's curves, the OADBT will, in this case, refer to the entering condenser water temperature. Therefore, the *SetpointManager:FollowOutdoorAirTemperature* object was used to control the tower's leaving water temperature so that it is equal to the OA dry bulb temperature to serve as input to the curves and allow for a good output, as these curves were constructed for an air-cooled unit. In the object of the chiller, an important parameter to define the recovery operation is the fraction of total rejected heat that can be recovered at full load, which was set to 1 according to the data from the technical bulletin. A diagram of the unit in recovery operation is shown in figure 3.7. The cooling tower loop and the condenser's fans were represented to show the computational implementation and the projected reality, respectively.
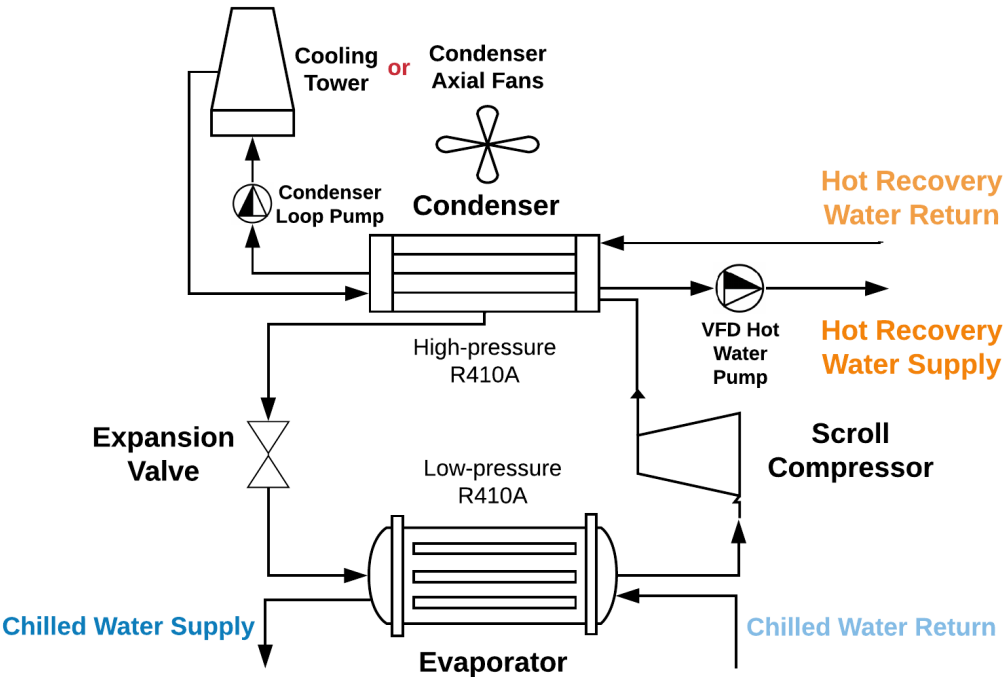
Figure 3.7: Simplified diagram of the unit with heat recovery operation. Note that the cooling tower is implemented in the model but, in reality, the unit's condenser will be air-cooled.

The curves for recovery operation were subjected to some assumptions due to the available datasheet

data, displayed in figure C.5, in which the performance for 100% cooling plus 100% heating is displayed for several hot and chilled leaving water temperatures. The compressor input power is also shown, allowing for an efficiency calculation at these points. The ambient conditions for which these points are calculated are not shown. Therefore, it was assumed that these points equate to a 35 $^\circ C$ OA temperature as this is the typical rating point for cooling. Moreover, seeing that 100% recovery capability is presented, it was assumed that the condenser fan is turned off to allow for all the condenser fluid latent heat release to be used for the recovery hot water. Therefore, all the input power is to the compressor. To interpolate the data for different OA conditions, the cooling only data from figure C.2 was used as a bridge between the recovery data from figure C.4 at 7 $^\circ C$ leaving chilled water temperature and 45 $^\circ C$ leaving hot water temperature [8]. The calculation can be seen in the Appendix, in table C.1. For the construction of the EIRFPLR curve for recovery, again, no data was found. Therefore, similarly to the other recovery curves, an interpolation of the cooling capacity and the compressor power input was done between the part-load data for cooling only, in figure C.5, and the full load recovery data at the 7/45 chilled/hot leaving water temperatures with the assumption that, at part-load, the condenser fan energy is negligible. This assumption may not be the most accurate one as it is expected a certain fan operation during part-load recovery conditions, however, not having available data, the best solution found was to neglect that fan power.

For heating only operation, again, *Energyplus* does not have a model that simulates this unit easily. Therefore, it was decided to use the *WaterHeater:HeatPump:PumpedCondenser* object which is a compound object that models an air-source HP for water heating. In this model, water is pumped out of a tank, through a DX heating coil (the condenser) and is returned to the tank. This tank is modeled with a *WaterHeater:Mixed* object which simulates a well-mixed, single-node water tank, the DX Coil and vapor-compression system is modeled with the *Coil:WaterHeating:AirtoWaterHeatPump:VariableSpeed* object, the evaporator's fan is modeled with the *Fan:SystemModel* and all these are united in the compound object *WaterHeater:HeatPump:PumpedCondenser* object. This objects allow for the air source to be OA, which is the case. The configuration will be further detailed below.

It is important, however, to detail the coil implementation that is, in its essence, the HP. The variable speed unit was selected to better describe the part-load ratio. This object requires the number of speeds, the rated heating capacity, the rated evaporator inlet air dry-bulb temperature and the rated evaporator inlet air wet-bulb temperature. Moreover, the rated condenser inlet water temperature is defined, alongside the evaporator air flow rate and the condenser water flow rate. The rated data for the performance curve used was for a temperature of 30 $^\circ C$ of the water entering the condenser, assuming a ΔT of 5 $^\circ C$ so that the leaving water temperature is 35$^\circ C$, at 7/6 $^\circ C$ outdoor dry-bulb/wet-bulb temperatures. For these conditions, the rated heating capacity is 650 kW with a COP of 4.58, including the evaporator fans that are rated at 16 kW. Six speeds were input taking into account the data available being divided in six steps, as seen in figure C.6, with the 6th speed being the nominal one. For all speeds, performance curves were constructed and introduced as described in the following list:

1. **CAPFT** - Water heating capacity function of temperature. This biquadratic curve is equal to the

---

[8]The 7/45 temperatures were selected as they will be the intended working temperatures for the units

CAPFT used in the cooling only implementation explained above with the exception that one of the independent variables refers to the entering condenser water temperature, instead of the leaving water temperature in the previous case. The "HVACCurveFitTool" with data from figure C.2 was used and a correction to the heating capacity was employed according to figure C.3 to account for operation during defrosting at low outdoor dry bulb temperature ($\leq 2°$). The curve generated was used for all speeds and it is shown in figure 3.8a. The fit is not perfect which can be seen in point at the rated conditions, which is approximately 0.96 and should be 1. This is due to the data available and the type of curve.

2. **COPFT** - COP function of temperature - This biquadratic curve is similar to the EIRFT curve with the difference that the output parameterizes the COP directly and not the EIR. It was decided to use it for all speeds. The curve used is shown below in figure 3.8b. Similarly to the CAPFT curve, the fit is not perfect but is considered acceptable for the purpose of the present thesis.

3. Four additional performance curves related to the heating performance and COP as function of hot water flow rate and evaporator air flow rate fractions were simplified for all speeds by introducing them as constant. This is assumed based on example files provided by *Energyplus* and also due to not having any related information in the technical bulletin.
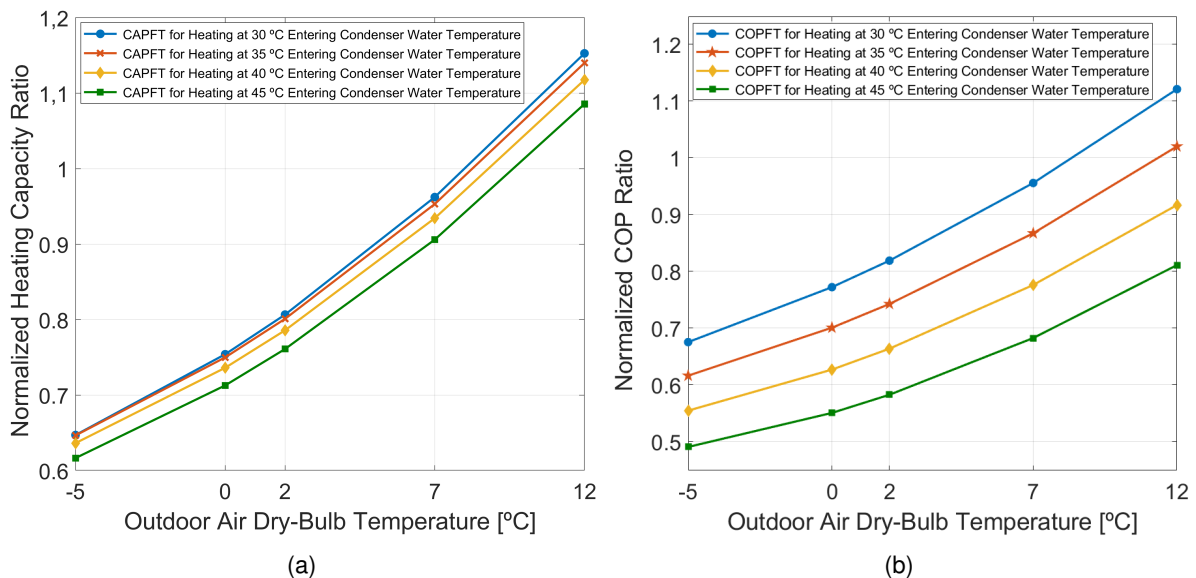
Figure 3.8: Heat pump performance curves introduced in the model; (a) - CAPFT curve; (b): COPFT curve.

The *Fan:SystemModel* object was used to model the evaporator's fans which allows for variable speed control, in which the rated power and nominal air flow rate were entered and the power fraction to air flow fraction was controlled through the same equation as the other fans (this will be mentioned below), as seen in figure G.1 in the Appendix. The rated power per unit is 16 kW (8 kW per circuit), according to *Clivet's*$^{\text{TM}}$ datasheet, and the nominal air flow rate entered was 61 $\frac{m^3}{s}$ (30.5 $\frac{m^3}{s}$ per circuit), which is the norm for this unit's size.

Additionally, the *WaterHeater:Mixed* implementation was done with the buffer tank's size in mind, as such, the volume of each tank entered was $1.25m^3 = \frac{7.5}{6}$. The tank was controlled according to a temperature setpoint such that, when the temperature is $44.7\,^\circ C$, the tank calls for heat from the DX coil until $45\,^\circ C$ water temperature is achieved. Such control was the best solution found to control this compound object. This means that, for the heating only implementation, it will not be possible to modulate the supply water temperature as it would be in reality, the water will be always near $45\,^\circ C$. This was a necessity given the nature of this compound object in *Energyplus*.

Hydraulic Loop

Energyplus allows for the introduction of water loops through the *PlantLoop* object which is composed of a supply side and a demand side that must adhere to certain rules regarding the format. On the supply side, typically, the equipment that generates the heating/cooling water is located, such as the chillers. On the demand-side, typically, the building load (the water coils) is located. On the inlet or supply branch of these half-loops, the pumps are typically located. The projected hydraulic loop demanded a rather complex set of loops. These were created separately for the hot water and the chilled water.

Regarding the chilled water, a single *PlantLoop* was enough and it is visible in figure 3.9.

Acronym	Meaning	Energyplus Object
CSPB	Constant Speed Pump Bank	HeaderedPumps:ConstantSpeed
VSPB	Variable Speed Pump Bank	HeaderedPumps:VariableSpeed
C/HP	Chiller/Heat Pump	Evaporator Side of Chiller:Electric:EIR
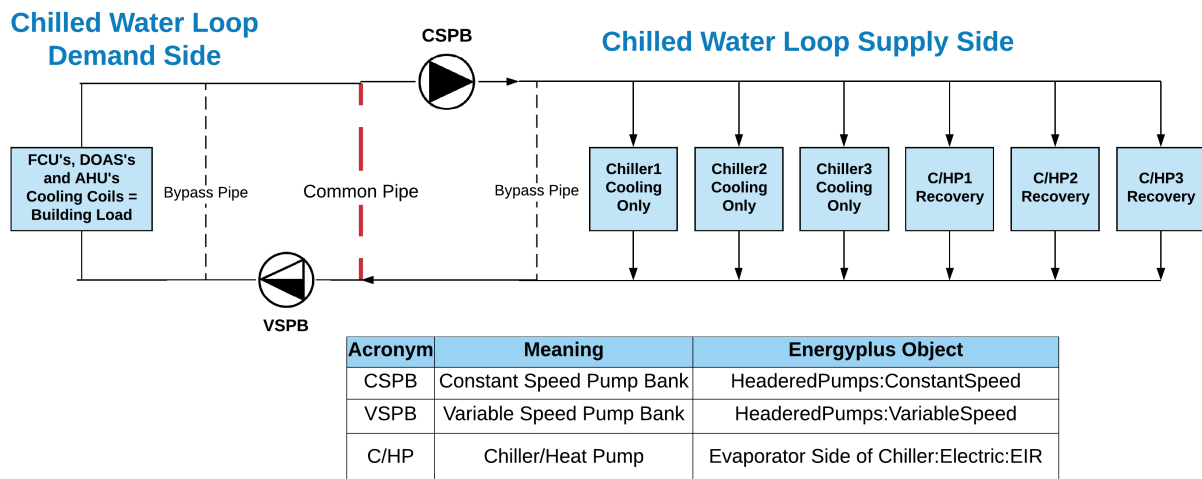
Figure 3.9: Simplified diagram of chilled water loop as implemented in *Energyplus*. For each chiller represented, 2 objects were constructed to account for each circuit but are not represented in this figure for simplicity.

In the supply side, in the inlet branch, the primary constant speed pump bank is located. These pumps will serve as the driving force for the water passing through the evaporators of the chillers. Then, in parallel, the chillers were added: 6 objects accounting for each circuit of 3 units for cooling only operation and 6 for 3 recovery operation units. In the demand side inlet branch, the secondary circuit variable speed pump bank is located. These pumps will drive a varying flow rate of chilled water to the several coils present in the building. These coils are present in parallel and are all *Coil:Cooling:Water* objects that are present in the DOAS's, AHU's and FCU's across the building. For both the supply side and the demand side, it is mandatory to add a bypass pipe that will serve as as buffer for the fluid that is not needed in the coils, effectively, to make sure that only the calculated necessary flow passes through

them.

Regarding the heating *PlantLoop*, presented in figure 3.10, it was a bit more complex to simulate owing to the limitations of *Energyplus*. In it, two *PlantLoops* were constructed, the primary loop and a secondary loop, which were required to satisfy the *Chiller:Electric:EIR* needs in recovery operation. The secondary loop calls for the chiller condenser to be located on the demand side and in the supply side, water tanks must be present. This secondary loop was constructed with 6 parallel chiller condenser objects and 6 parallel source side *WaterHeater:Mixed* objects, accounting for the 3 units. These *WaterHeater:Mixed* objects have 4 possible connections: 2 on the use side and 2 on the source side. The source side nodes are located on the secondary loop, which is where the hot water is generated, and the pair of use nodes are located in the primary loop supply side. The primary loop supply side, besides the use side of the recovery operation, also has the compound 6 *WaterHeater:HeatPump:PumpedCondenser* objects.The demand side is similar to the cooling loop, it is composed of the variable speed pump bank and the *Coil:Heating:Water* objects of the diverse equipment.

Acronym	Meaning	Energyplus Object
WH	Water Heater	WaterHeater:Mixed
WHHP	Water Heater Heat Pump	WaterHeater:HeatPump:PumpedCondenser
CSPB	Constant Speed Pump Bank	HeaderedPumps:ConstantSpeed
VSPB	Variable Speed Pump Bank	HeaderedPumps:VariableSpeed
CC	Chiller's Condenser	Heat Recovery Side of Chiller:Electric:EIR
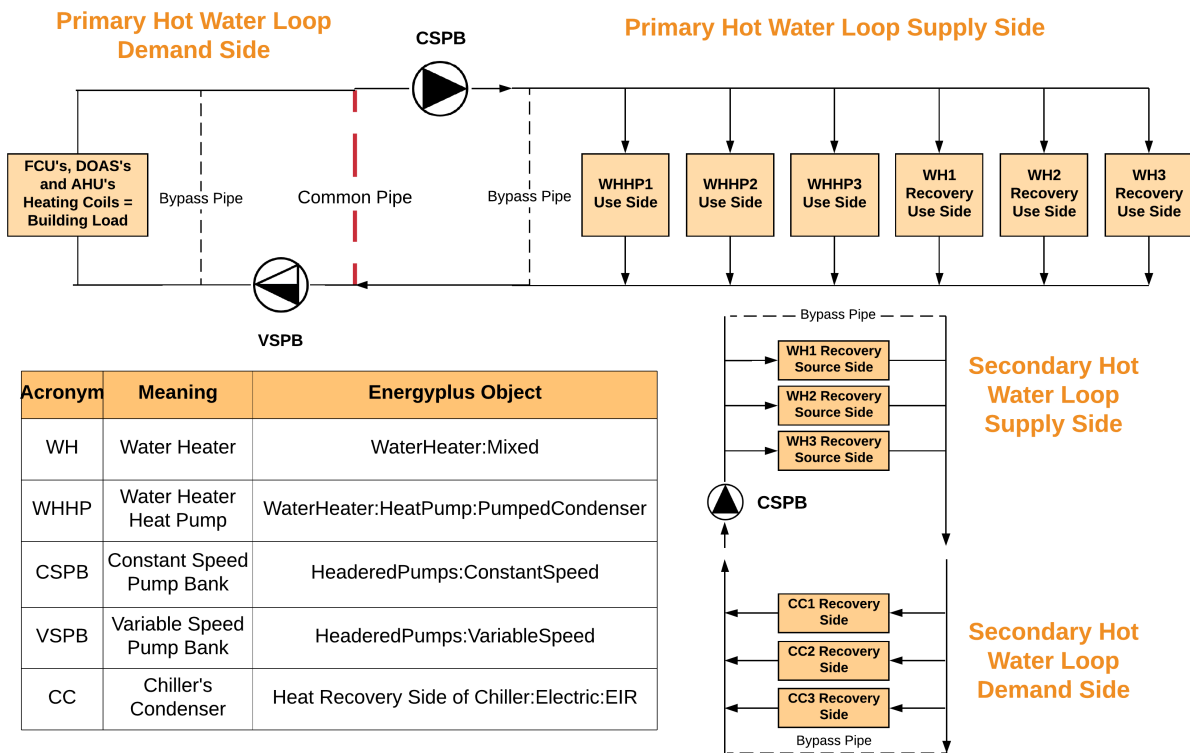
Figure 3.10: Simplified diagram of the primary and secondary hot water loops as implemented in *Energyplus*. For each heat pump and water heater represented, 2 objects were constructed to account for each circuit but are not represented in this figure for simplicity.

In both cases, as these loops are separated in a constant flow primary side and a variable flow secondary side, each with their own pump bank, it was necessary to add a pipe to allow for flow continuity, as shown in figure 2.5. This was added with the "CommonPipe" option selected in the *PlantLoop* object, which is present to satisfy the secondary demand side flow request and therefore achieve flow continuity. This object has a consequence of providing differing water temperatures between the return of the demand side and the inlet of supply side, with the common pipe taking some of the flow, the amount of which is dictated by the demand side request.

Hydraulic Pumps

The implementation of the pumps was facilitated with the objects *HeaderedPumps:VariableSpeed* and *HeaderedPumps:ConstantSpeed* that simulate a pump bank with an arrangement in parallel of the pumps. For the constant speed pumps on the primary side, 6 were selected for each bank, and each was coupled with a single circuit seeing that each unit was divided in 2 to account for a single vapor-compression circuit. This does not correspond directly to reality, however, it is not expected to account for added consumption as each pump design power was divided in half. For the variable speed side, 3 pumps were selected since it was not necessary to couple each circuit with a single pump. Furthermore, for the variable speed units, flow fraction curves were introduced through the use of a 3rd degree polynomial curve in which the input power fraction is a function of the water flow rate fraction. At rated water values, this curve is equal to 1 and the minimum flow fraction was set to 0.2 and it can be seen in figure G.1 in the Appendix. The data for the curve was obtained from [43]. Additionally, the efficiency of the motor was selected to be 95%, which is relatively common for present electric motor technology. The control type was selected as intermittent that allows for pump shutdown during no-load situations. A continuous control type, which is the other option, would fit the projected reality better but was found to be accumulating too much heat in the water loop when the equipment was turned off, which led to errors in the simulation. The electric power input can is calculated according to the following equation:

$$P_{input} = \frac{Q_{rated}\Delta P}{\eta_{pump}}$$

(3.1)

The flow rate was set by the chillers selected and according to the technical bulletin, and the power input and the design pump head (ΔP) was sized to achieve a total pump efficiency (η_{pump}) of approximately 70%.

Control and Equipment Sequencing

The control of the plant proved to be a challenge taking into account the models used for heating and recovery operation. As mentioned above, for each unit in the 3 operating modes, the capacity was split in half to account for the 2 independent refrigeration circuits. Therefore, it was necessary to sequence the activation of the circuits. Initially, each unit was activated to its optimal part load ratio (approximately 0.33) and the last unit would modulate between the minimum and maximum part load to meet the current demand. However, a bug was found in the implementation that led to lower than expected EER's at part loads that should be higher than the rated EER, in the cooling only and cooling with heat recovery case, where the *Chiller:Electric:EIR* object was employed. This matter will be further explained in chapter 4. Therefore, the control was changed to sequentially activate to full load (at full PLR) and the last unit needed will modulate its PLR to satisfy the load demand. This control logic allows for overall chiller operation at higher EER's in the simulation. It also simulates having one backup unit, which is realistic, since, as it will be seen in Chapter 4, only 2 units (4 circuits) activate for a yearly simulation.

The return water temperature control to a constant setpoint was achieved through the use of the *SetpointManager:ReturnTemperature:ChilledWater* and *HotWater*, in which the constant return temper-

ature of 12 and 40 $^\circ C$, respectively, was entered and the supply temperature to be adjusted between 7 and 10 $^\circ C$ for cooling and 42 to 45 $^\circ C$ for heating. This control works satisfactorily for the cooling only and for the cooling with recovery operation. However, the heating only operation could not be controlled in such way, as mentioned above, and for recovery heating this also does not function as well as on the recovery cooling side, despite working better than during heating only operation. This will be visible in the subsection 4.1.1.

Referring to the recovery hot water temperature control, a leaving temperature setpoint was input in the outlet water nodes of the recovery chillers condensers and the *SetpointManager:Scheduled* was used to introduce a 45 $^\circ C$ setpoint for these nodes. Setting these setpoints and associating them with the nodes in the *Chiller:Electric:EIR* object changes the condenser model used in the simulation, that allows for a higher temperature heat recovery. This however, also introduces a limitation to the simulation as the intended idea is to modulate the hot water temperature according to the current load in order to maintain the return water temperature constant. Such will be more difficult taking into account these setpoints, however, they were introduced to activate this higher temperature condenser model in the simulation and as such, was the best solution found in useful time.

Additionally, the *Controller:WaterCoil* object needed to be defined and suited for the heating or cooling coil. This object allows for water flow rate control to meet the specified leaving air setpoint.

The *SetpointManager:FollowOutdoorAirTemperature* object, regarding the condenser loop temperature control, was used to control the leaving water temperature of the cooling tower to follow the OA dry-bulb temperature, as mentioned above.

The daily and yearly availabilities of the plant components were introduced in the model through schedules and the *PlantEquipmentOperationSchemes* object and are described in table 3.5.

Table 3.5: Daily and yearly availability for the hydraulic components.

Type of Availability	System On Days	System	On Time Interval	On Time of Year
Daily	Weekdays	All Systems	07:30 - 20:00[1]	-
Yearly	-	Heating Only	-	01/12 to 22/02
		Recovery		23/02 to 31/05 and 16/09 to 30/11
		Cooling Only		01/06 to 15/09

[1] Note that this availability is due to the projected occupation of the spaces and is similar to the current HVAC system schedule.

Having used the objects described above for the 3 different operating modes, it is obvious that the system will only effectively be 4-pipe, that is, with simultaneous cooling and heating available, during the part of the year that condenser heat recovery is active. In order to decide these schedules, the weather file was analyzed regarding the dry-bulb temperature and the results were filtered to show the most colder and hotter days. Regarding heating only, they were filtered to only show temperatures below 13 $^\circ C$ between 11h00 and 19h00[9]. For January and December, 102 and 46 instances were found, respectively. For February, 68 instances in total but 67 instances until the 22nd. For March, April

[9]This time range was only selected as a filtering parameter to decide the heating availability, it is not related to the daily schedule of the HVAC plant.

and November, only 4, 6 and 5 instances were found, respectively. It was, therefore, decided to be available from the 1st of December until the 22nd of February. Regarding the cooling only operation, a similar analysis was conducted for outside air temperatures of over 25 $^\circ C$ during the same time-frame as before and the best dates were selected, from the 1st of June to the 15th of September. During the remainder of the year, the chiller is operated with heat recovery as well.

3.6.1.1 Hydraulic Plant Approximations

A number of approximations had to be introduced taking into account the complexity and sheer size of Pavilhão de Civil and its proposed HVAC system and also the limitations of the software itself. Therefore, a compromise had to be achieved and in this section, a list and analysis of the most relevant approximations is presented.

Regarding the implementation of the chillers/HP's, the limits of the OA conditions for the performance curves are not ideal, leading to extrapolation. For cooling only operation, the lowest OA temperature for which data was available is 25 $^\circ C$ and for lower temperatures than that, the performance curve will extrapolate, loosing accuracy. The same takes place at recovery operation, in which lower OA temperatures are expected due to the mid-season scheduling of recovery operation. This fact will, therefore, slightly degrade the energy consumption of the chillers at certain atmospheric conditions. Moreover, having decided to implement separately each compressor, the flow rate to each unit had to be halved in order to guarantee the desired total water flow rate.

The workaround for the recovery operation was the best possible given the constraints of the software but not ideal, with the necessity to introduce a condenser loop with a cooling tower and with the energy consumption associated with these (the pumps and the fan of the cooling tower) having to be subtracted manually post-simulation. Moreover, the construction of the curves for recovery operation were not ideal due to the data available in the technical bulletin, as discussed above. Additionally, the recovery operation is simulated as, according to [44], a passive benefit to the cooling demand and despite being possible to control the condenser leaving hot water temperature, it is not possible to control the recovery heating rate. Therefore, it is expected that, at certain times when heating is more required than cooling, there will not be enough chillers working to satisfy these heating demands. Consequently, the recovery operation chiller is expected to have lower accuracy when comparing to the cooling only or heating only operations.

The *WaterHeater:Mixed* objects for heating only and recovery represent elements that will not be employed in the project in this manner and its necessary use adds variability and complexity to the model, in parameters such as the tank volumes and the setpoint cut-in and cut-out temperatures. However, they were sized based on the dimensions of the projected buffer tanks that can be seen in figure 2.5 and it is intended that they act as a buffer to minimize compressor start-ups. The values selected were deemed as likely but it was not clear what the optimum values would be in this particular case. Despite that, the heat transfer effectiveness in both the source and use sides were set as 1 to simulate perfect heat transfer between these. For cooling only, no water storage objects were introduced. In a nutshell, the storage tanks projected in the return of the secondary circuit were not modeled in the way they were

conceived.

The issue with the availability schedule in the simulation is that the system is only effectively a 4-pipe system for about 6 months. This was done because it was verified that during the peak heating loads in the winter months, the recovery operation was not enough to satisfy the heating demands, which led to uncomfortable thermal conditions. Therefore, it was decided to implement the heating only HP. What is likely to happen is that during the time when only heating is available, some cooling loads can not be met which will lead to overheated conditions in some spaces. The same can happen during the time when only cooling is available, despite being quite less likely. This was the compromise found taking into account the limitation of the plant objects within *Energyplus*.

An added approximation that is common with BEM's is to disregard piping and duct heat transfer with the usage of the *Pipe:Adiabatic* object, especially through conduction, as convection is usually highly controlled with surface isolation, and also piping pressure losses. Although it is possible to simulate pressure losses, it still is not possible with a common pipe simulation.

3.6.2 Modeling of the Air Side

Having completed both *PlantLoop's* supply and demand side, it is time to model the air circuits through the usage of *AirLoops*. These, along with the zone equipment, form the forced air heating and cooling system. The *AirLoops* divide the airflow components in those representing the primary air system and those representing zone equipment. Similarly to the *PlantLoop*, it also has a central supply side that may include supply and return fans, heating and cooling coils, economizers, energy recovery, among others, and zone equipment in the demand side, with objects such as air terminals, fan coils, window units, and so on.

DOAS - Water-based and DX

The diverse water-based DOAS's use 100% fresh air and were modeled simply by assembling together a set of objects. Firstly, both the *HeatExchanger:AirToAir:SensibleAndLatent*, that models the enthalpy wheels, and the *OutdoorAir:Mixer* were assembled together with the usage of an *AirLoopH-VAC:OutdoorAirSystem* object, that is a subsystem of the main *AirLoop* and treated as a single component. The *OutdoorAir:Mixer* is necessary to control the OA flow rate. Despite return air mixing not occurring, a *Controller:OutdoorAir* is used to control the air flow rate of the air loop. In this object, a schedule was created to impose full fraction of OA at all times.

From then, the already-created water coils are coupled to the diverse DOAS's air loops with the correspondent nodes, the cooling coils first and then the heating coils. For the DX DOAS units, both *Coil:Cooling:DX:VariableSpeed* and *Coil:Heating:DX:VariableSpeed* objects were used to simulate the the reversible vapor-compression cycle. These objects already include the compressor, which is modeled as a 10 speed compressor whose performance data was based on an example file from the software and whose rated air flow rates and gross rated heating and cooling capacities were adjusted according to the project as well as the operating EER's and COP's at the 10 different speeds. Regarding these,

seeing as this unit will essentially be a VRF outdoor unit, they were adjusted for each speed according to the EIRFPLR curves from one of the VRF units. The coil object also includes the condenser/evaporator fan of the refrigeration cycle, seeing that it is an air-cooled unit and whose consumption is included in the EER and the COP. The performance curves for information at the different outdoor conditions were employed from an *Energyplus* example file. The *CoilSystem:Cooling:DX* and *Coil:System:Heating:DX* were used to assemble these two components and some added controls. Then, two *Fan:VariableVolume* objects were created to simulate the supply and return fan. The details of their implementation will be approached below, in the ventilation section. The layout and therefore implementation of these DX DOAS air loops is identical to the water-based DOAS's with only the difference in the nature of the coils.

Regarding the sensible and latent effectiveness of the enthalpy wheels, *Energyplus* only allows for input at 100% and 75% flow for cooling and for heating. Other values are assumed to be within this range. The values chosen are presented below in table 3.6. Those were based on the minimum efficiency called for in the project and on other example files with exhaust air energy recovery.

Table 3.6: Effectiveness of the enthalpy wheels as input in *Energyplus*.

Type of Load	Air Flow Fraction [%]	Rotary Wheel Effectiveness η_{HX} [-][1]
Sensible	100	0.75
	75	0.8
Latent	100	0.7
	75	0.75

[1] The effectiveness of the HX for the sensible load is calculated by $\eta_{HX} = \frac{T_{supply}-T_{OA}}{T_{extract}-T_{OA}}$

Air Handling Units

The implementation of the AHU's was done in a very similar way to the DOAS's implementation. Each AHU accounts for an *AirLoop* in which the OA system is defined. The OA system is, for the majority of AHU's, simply an *OutdoorAir:Mixer* object whose control is achieved with the *Controller:OutdoorAir* object. The exception is UTA - 9 which will employ an enthalpy wheel located in the OA system of its *AirLoop*. Similarly to the water-based DOAS's, the cooling and heating water coils were defined as well as the variable speed supply fans, for the supply and the return.

Fan Coil Units

The 4-pipe FCU's in *Energyplus* are modeled through 4 objects - a supply fan, the cooling and heating coils and an OA mixer. These are assembled together in the *ZoneHVAC:FourPipeFanCoil* parent object. In this object, a number of parameters were selected to best represent the real system. For the capacity control method, the "VariableFanVariableFlow" option was selected to allow for modulation of the water flow through the coils and the fans flow rate. The maximum supply air flow rates and the water flow rates through the coils were autosized according to the desired ventilation rate from the DOAS, for the air flow rate case and the supply water temperature and ΔT desired, for the water flow rate case.

Moreover, a distinction had to be done between the ceiling conceived and the ceiling wall mounted

units, as explained in section 2.4.3. For the concealed units that receive neutral DOAS air in the inlet, the *AirTerminal:SingleDuct:Mixer* object was used to set up the mixing box. In it, the primary DOAS air inlet node was defined alongside the secondary zone return air node to be put in the inlet side of the FCU. For the wall mounted units, a normal *AirTerminal:SingleDuct:VAV:NoReheat* object was employed to supply DOAS air directly to the spaces and additionally, an *OutdoorAir:Mixer* object had to be created to associate the inlet and return air nodes with each other. The condition imposed for the OA air in this object was to set its maximum flow rate to 0 in the parent object, forcing all of the treated air in these FCU's to be room recirculated air.

Ventilation

The implementation of the ventilation can be separated in two parts: 1) the actual implementation of the fans in the software and 2), the control of the OA flow rate within each thermal zone.

Regarding the fans, the *Fan:VariableVolume* object was widely employed because it allows for variation of the volume according to the heating and cooling demands, which is essential in a VAV system. This object allows for the sizing of the total efficiency of the fan, the efficiency of the motor, the maximum flow rate, the pressure rise and the fan power as a function of the flow fraction through a performance curve. Despite all of these objects being important, particular attention was given to the pressure rise and to the fan performance curve. The pressure rise, defined in Pa for full flow at standard conditions, is a necessary user input and is highly relevant to define the fan energy consumption. Ideally, fan pressure rises are sized to be just enough for design conditions but minimized to achieve lower energy consumption. Normally, manufacturers will typically provide External Static Pressure (ESP) values, which only account for losses in ducts and fittings but rarely Total Static Pressure (TSP), which is equal to the summation of the ESP and the Internal Static Pressure (ISP) and is the type of pressure needed to be input in *Energyplus*. The latter is related to the pressure losses in air filters, energy recovery heat exchangers and coils and has also been taken into account. EACE [29] did not do the duct sizing, therefore, fan pressure rises have had to be estimated. As such, after taking into account the number of fans per TZ and their nature, rule-of-thumb values for what is considered good design that were obtained from table 5 of Schild and Mysen [37] were used to estimate the diverse fans pressure rise of the DOAS's and the AHU's. For example, for the heating and cooling coils set, a 100 Pa pressure rise was added, for the rotary heat exchanger a 100 Pa pressure was used and for the inlet air filter 50 Pa, with all of these accounting for the ISP in both the AHU's and the DOAS's. For the AHU's supply fans, an ESP of 200 Pa was used. The DOAS's units were sized similarly to the AHU's, but using a higher ESP for the expected larger ducts, as they will serve more zones with larger air flow rates. For the FCU's supply fan, a lower ESP was considered of 50 or 70 Pa depending on the unit and a 100 Pa ISP to account for both water coils. Lower pressure rise for the return fans were selected because of less sources of pressure loss in a typical return air duct. Regarding the total efficiency of the fans, for the DOAS's and AHU's supply and return fans, 70% efficiency was selected with 93% motor efficiency, which is a relatively efficient ventilation system. For the smaller fans in the VRF's terminal zones and the FCU's, a lower total fan efficiency of 60% was used with equal motor efficiency. The VRF's indoor units used the *Fan:OnOff*

object which is constant speed due to limitations within *Energyplus's* VRF models, as explained below in section 3.6.3.1. The performance at part-load speeds for the variable speed fans was specified by using a 4th degree polynomial equation to supply the simulation with power input data at the expected air flow fractions. Figure G.1 in Appendix G shows the correlation used to simulate the VFD fans power, obtained from adapting from a generic VFD fan performance curve data from [43]. The good performance at part-load is noticeable. For example, 50% flow fraction corresponds to 20% of the rated power input.

For the ventilation rate within each thermal zone, the air flow rates presented in table 2.4 were input using the *DesignSpecification:OutdoorAir* object, in which the ventilation rate was defined in $\frac{m^3}{s.person}$ for all occupied spaces. For the non-occupied spaces with ventilation, the flow per zone in $\frac{m^3}{s}$ was input. This object was, in turn, referenced by the *AirTerminal:SingleDuct:VAV:NoReheat* and the *AirTerminal:SingleDuct:Mixer* objects, that are used as the connection between the air equipment and the terminal units in the latter case, or, in the case of the DOAS's air that is supplied directly to the spaces, as the terminal unit itself, in the former case.

The object *ZoneVentilation:DesignFlowRate* was also kept for simulating the exhaust fans from non-conditioned spaces, such as the corridors or the bathrooms, and their consumption. The air flow rates for each zone were kept from the original model. Similarly, the air infiltration from OA was also simulated through the *ZoneInfiltration:DesignFlowRate*. This object was slightly changed because it was verified that there was no distinction in the flow rates between perimeter and indoor zones. As such, the flow rates for indoor zones were vastly reduced to account for some indoor air that has similar OA temperature, especially in the zones with contact to the open space lobby. The values were assumed as plausible. This was a compromise as this area was not the principal focus of the implementation.

Air-side Control

The control of the air-side HVAC system is accomplished through a diverse use of setpoint managers, OA controllers and working schedules.

The air-side HVAC components were decided to be available from 07:30 to 20:00 for most of the spaces to allow for a warm up period before occupancy in order to ensure that the space is comfortable when people arrive. This time depends on a number of factors such as the heat capacity of the building, the outdoor conditions and the system capacity [35]. For the spaces served by VRF's, different schedules were selected. For instance, the Espaço 24h rooms and CGD room were scheduled to have the VRF system available 24/7 to match the occupancy profile of the spaces. In an attempt to save energy, the setpoint in these spaces during the night was slightly changed to ease the load on the VRF's. For the heating season, the setpoint from 02:00 to 07:00 was reduced to 18 $^{\circ}C$ while for the cooling season, the setpoint was increased to 26 $^{\circ}C$, a 2 $^{\circ}C$ increase. Moreover, the scheduling of the setpoint temperatures in the offices of the 2nd and 3rd floors were also changed, to control to the intended comfortable temperatures from 08:30 to 18:00 during the week, as that is the scheduled occupation of these spaces, in an attempt to save energy during non-occupied times.

The supply air temperature was controlled to maintain a constant setpoint throughout all the equipment. For the energy recovery equipped DOAS's, the control of the HX outlet air temperature was

achieved with a setpoint with outdoor air reset, the *SetpointManager:OutdoorAirReset* object, which modulates the setpoint according to the HX effectiveness and the OA dry bulb temperature with the season reset taken into account, as the return air temperature will change twice during the year. The DOAS's supply temperature was set with a *SetpointManager:Scheduled* object. The control of the supply air temperature for the AHU's was found to be challenging as initial attempts mixed heating and cooling at the same time and intermediate temperatures of 22 $^\circ C$ were being calculated. That was not acceptable and the problem was improved by using *SetpointManager:Coldest* and *Warmest* objects for, respectively, the heating and cooling setpoints with the aforementioned 14/29 $^\circ C$ setpoints, however, during condenser heat recovery operation, the supply air temperature is not controlled well, as will be seen in section 4.1.3. Additionally, for all mixed air nodes after the mixing boxes, *SetpointManager:MixedAir* objects were introduced to establish a temperature setpoint at the mixed air nodes taking into account the supply air temperature defined.

3.6.2.1 Air Side Approximations

The DX UTAN's E1 and E2 that will serve the rooms in Espaço 24h of TZ's 41, 83, 84, 85 and 92 were combined in a single unit for the simulation, by adding up the rated heating and cooling capacities, because both units will serve spaces in a single thermal zone and this was not possible to model without rearranging them. This is not deemed a big approximation because both UTAN's E1 and E2 will be equal units with the same capacity and very similar projected air flow rates (within 15% of each other). The same happened with UTAN - E which served zones that were also served by UTAN - ES and UTAN - EN. Therefore, the capacity of UTAN - E was combined accordingly in both UTAN - ES and EN.

Another drawback of maintaining these thermal zoning configuration is the impossibility of separating different purpose rooms within the same zone, such as V1.13 within TZ109. This room is a computer room while the other three rooms that belong to that TZ are normal classrooms, therefore, additional heat gains will arise in the space of V1.13. This was not modeled, however, it is an isolated case and, as such, its impact is negligible to the overall results.

Economizer providing free-cooling in the DOAS units will also be available in the real project and it will contribute to savings of chiller/HP and pump energy as the OA, when in beneficial thermodynamic conditions, will serve as the ventilation source bypassing the water coils. This was not implemented as difficulties were found in combining the DOAS with heat recovery with the economizer control. This leads to a small overestimation of the pump and chiller energy when compared to using air economizers.

The DX Coils for the DX DOAS units used were the variable-speed model with 10 speeds whose performance curves for part-load conditions were employed from an example file in *Energyplus*. The actual system is expected to possess a higher degree of adjustability to the load, owing to state-of-the-art compressor control technology and variable refrigerant flow capacity.

The implementation of the water coils used the simplified model in which the number of tubes per row, the number of rows and the thermal properties of the coils were not defined, and this would be possible with the *Coil:Cooling:Water:DetailedGeometry*. Moreover, the coils used are simplified models which use the effectiveness-NTU relationship to predict heat transfer. These components, therefore, are

not as detailed as they could be. Its impact, however, is not considerable as this coil model is the norm for large buildings where detailed coil data is not known.

The majority of the AHU's (with exception of UTA - 8 and UTA - 9) will have neutral DOAS air as an input, as mentioned in section 2.4.3. This, however, was not found to be possible to model within *Energyplus* to a satisfactory degree; therefore, it was decided to implement the AHU's with direct OA intake to the mixing box, without the heat recovery that the DOAS would provide. This will alter the sizing of the heating and cooling coils and of the supply fans in both components. The DOAS's that serve the AHU's intake will have a lower capacity and smaller air and water flow rate, with the inverse happening on AHU's equipment in order to achieve the desired supply air conditions. However, the ventilation rate per person will still be achieved as the air flow rate will be controlled and computed with the number of occupants at a given simulation timestep.

The sizing of the majority of the air systems was done with recourse to the *Sizing:System* and *Sizing:Zone* objects, in which the nominal air flow rates and capacities are sized taking into account the design days defined with the OA requirements and the design weather of the project. This was done because it was impossible to directly input the values projected by EACE [29] as it led to errors in the simulation. In general, autosizing the objects allows for a more stable simulation as *Energyplus* has some strict limits related to, for example, ratios of air flow rates per rated total capacity.

3.6.3 Modeling of the VRF Systems

The VRF systems were implemented using a number of *Energyplus* objects that simulate the indoor and outdoor units separately.

The outdoor units were simulated using the *AirConditioner:VariableRefrigerantFlow* that models an air-to-air HP condensing unit, which includes the compressor and the outdoor fan, through empirical equation fit based on manufacturer's performance data. Five terminal zones were introduced through the *ZoneTerminalUnitList* object that encompass each terminal unit. The zones were the LTI spaces (TZ's 103, 104, 105 and 172), the Espaço 24h (E24) spaces (TZ's 41, 83, 84, 85, 92), the bar (TZ 78), the restaurant (TZ 91) and the CGD room (TZ 82). The models chosen to be employed for each space can be seen in table 3.7.

Table 3.7: Models for the VRF systems within each space, all from *Mitsubishi Electric*[TM].

Space	Outdoor Unit Model	Outdoor Unit Cooling/Heating Capacity [kW]	EER/COP[1]	Most Common Indoor Unit Model
LTI	PUHY-P550YKSB-A1	63/69	3.78/3.99	PEFY P63 VMA-E
E24	PUHY P500YSKB-A1 + P600YSKB-A1 [2]	55/63 + 69/76.5	3.55/3.95	PEFY P50 VMA-E
Restaurant	PUHY P400YKB-A1	45/50	3.32/4	PEFY P71 VMA-E
Bar	PUHY P200YKB-A1	22.4/25	4.32/4.3	PEFY P40 VMA-E
CGD Room	PUHY P250YKB-A1	28/31.5	4.06/4.29	PEFY P63 VMA-E

[1] EER refers to cooling, COP to heating.

[2] Data for the P550 was used for the performance curves, at they are similar to P500's and P600's data and also used in LTI.

For each zone, a *ZoneHVAC:TerminalUnit:VariableRefrigerantFlow* object was created alongside the supply fan of the type *Fan:OnOff*, and the heating and cooling VRF coils. The objects used to model the coils were the *Coil:Heating:DX:VariableRefrigerantFlow* and *Coil:Cooling:DX:VariableRefrigerantFlow*. The *ZoneHVAC:EquipmentConnections* object was used to define the zone inlet and exhaust nodes. These connections can be seen in the scheme of figure 3.11. The *AirTerminal:SingleDuct:Mixer* was also used again to connect the DOAS's air to the inlet of all indoor units, with the exception of the CGD room system which is not served by a DOAS's.
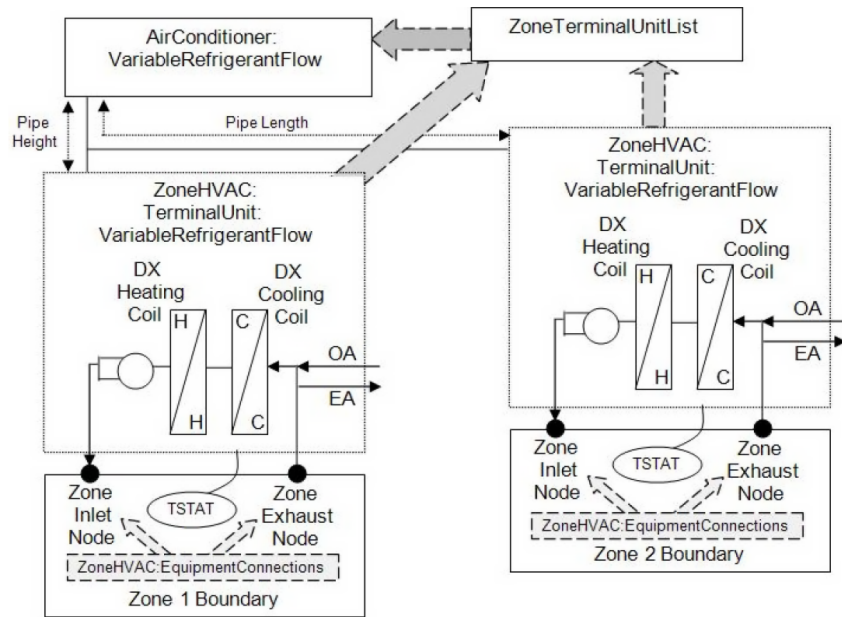
Figure 3.11: Scheme of the VRF system in *Energyplus*, obtained from [41]

The performance of the outdoor and indoor units for each model were introduced according to catalog data [45], from *Mitshubishi Electric*[TM] and using the guidelines from Raustad [46]. As such, the type of curves shown in table 3.8 were built and introduced. These were computed based on catalog data with the use of regression tools for each model, both for cooling and heating operation. In Appendix D one can see the graphical data for a single model that was used to create such performance curves. Additional data that was input in the *ZoneHVAC:TerminalUnit:VariableRefrigerantFlow* for each indoor terminal unit was, among others, the OA flow rate hard-sized to 0 due to the DOAS air that is input in the inlet, the fan configuration set as draw-through (after the coils), the on and off parasitic electric energy use of the indoor units is introduced, which is information contained in the datasheets, as well as the rated heating capacity sizing ratio that sets the indoor units heating coil size in relation to the indoor units cooling coil size.

In the *AirConditioner:VariableRefrigerant* object, in addition to the first 11 curves listed in table 3.8, parameters such as the minimum and maximum outdoor temperatures for heating and cooling, the EER/COP's, the availability schedules, the minimum part-load ratio (0.11), the thermostat control type and location of the master thermostat location are entered, alongside some other parameters. The master thermostat's location sets the working mode (cooling or heating) in accordance to the master's thermostat mode.

Table 3.8: Curves input in the modeling of the VRF systems in *Energyplus*

Type of Curve	Comment
Cooling/heating CAPFT for low temperatures	Full load cooling/heating capacity function of ODB and IWB temperatures at lower temperatures
CAPFT boundary	Used for separation of the low and high temperatures CAPFT curves
Cooling/heating CAPFT for high temperatures	Full load cooling/heating capacity function of ODB and IWB temperatures at higher temperatures
Cooling/heating EIRFT for low temperatures	Energy input ratio function of ODB and IWB for lower temperatures
Cooling/heating EIRFT boundary	Used for separation of the low and high temperatures EIRFT curves
Cooling/heating EIRFT for high temperatures	Energy input ratio function of ODB and IWB for higher temperatures
Cooling/heating EIRFPLR for low PLR	Energy input ratio function of part load ratio for PLR $\leq$ 1
Cooling/heating EIRFPLR for high PLR	Energy input ratio function of part load ratio for PLR $>$ 1
Cooling/heating combination ratio correction factor	Capacity multiplier when combination ratio $\geq$ 1
Piping length correction for cooling and heating	Correction for the capacity with the piping length
Defrost EIRFT curve	Energy input ratio function of ODB and IWB during defrosting periods
Indoor unit cooling/heating CAPFT	Cooling/heating capacity function of IWB for the indoor units
Cooling/heating CAPFFF	Cooling/heating capacity function of air flow rate fraction for the indoor units

Notes: ODB - Outdoor Dry-Bulb; IWB - Indoor Wet-Bulb; Combination Ratio $= \frac{\text{Total Indoor Unit Capacity}}{\text{Outdoor Unit Total Rated Capacity}}$,

EIR = Energy Input Ratio = 1/COP = 1/EER

3.6.3.1 VRF Approximations

Energyplus has 2 different models for VRF systems, an older empirical equation-based curve model and a new physics based model, which is able to consider the dynamics of more operational parameters. Although the new model is more accurate in predicting energy usage in VRF's, as seen in [47], the performance data that it requires is not easily available yet from the manufacturers, such as part-load performance for the compressor with inverter technology. However, the old model uses performance data that is widely available in manufacturer's databooks. Being unable to find satisfactory performance data, the older model was used to simulate the VRF units. Hong *et al.* [47] also showed the old model's tendency to under estimate the daily energy usage with an over 10% error in both cooling and heating mode. It also does not allow the use of variable speed fans for the indoor units, therefore, it requires the use of the *Fan:OnOff* object to model in indoor unit supply fan. This object, which models a constant speed fan, will overestimate the fan energy usage in the VRF when compared to the projected variable speed indoor fans due to lower part load capability. A certain balance is expected to be achieved with the underestimating of the energy use by the model and the higher energy intensive constant speed fans.

The curves were introduced with great detail for each model. Despite that, for heating mode, the CAPFT and EIRFT curves were used without a boundary curve because of the nature of the data for different indoor dry-bulb temperatures and because of the typical wet-bulb temperatures during the year, which rarely dips below 0 $^\circ C$. Therefore, only data for 20 and 25 $^\circ C$ indoor dry bulb temperature and outdoor wet-bulb temperature higher than 4 $^\circ C$, which is the transition temperature (seen in figure D.3), was input for the curves.

Chapter 4

Results and Discussion

In this section, the main results of the simulation for the new system are presented together with an analysis of several TZ's that are served by different HVAC systems and alongside a direct comparison between the old and new HVAC systems. Furthermore, an energy consumption comparison is performed between real consumption data and the simulation model of the new projected system and its limitations are summarized. The thermal zoning can be consulted on Appendix A.

4.1 Main Results

An annual simulation was performed with the computational parameters as specified in section 3.4 and the main results are presented below.

4.1.1 Hydraulic Plant Operation

The hydraulic plant design was the most challenging part of the implementation and the one that required more research and trial and error. Therefore, it is important to observe some details of its operation in the model. Moreover, as the chiller/HP's were sized in the simulation as projected by EACE [29], it is also quite important to provide an insight on the sizing of the plant.

Starting with the heating only operation, figure 4.1 shows the part-load ratio of the two circuits in a single HP and the supply and return hot water temperature for a week in January and aims to showcase two points. The first is that only one circuit of a single HP is activated during the entire year, which accounts for a heating capacity of 325 kW (half of the rated 650 kW for the entire unit for the water and OA temperatures considered). This activation is controlled by the simulation through the calculated demand of hot water in the hot water coils. This leads to the conclusion that the system is oversized for heating only operation. Note that the heating capacity projected is only 512 kW per unit, which is about 21% less than the actual capacity in the model. This oversizing, while still existing, is not decisive as the majority of the demands are for cooling (as will be seen further down) and therefore, chilled water. It is, therefore, inevitable taking into account the nature of the reversible chillers. The second point is that, unlike the rest of the year, the control of the supply water temperature is done at

63

the supply side with a constant 45 °C setpoint. This was deemed a necessity due to the control of the *WaterHeater:PumpedCondenser* object not allowing for the modulation of the supply temperature.
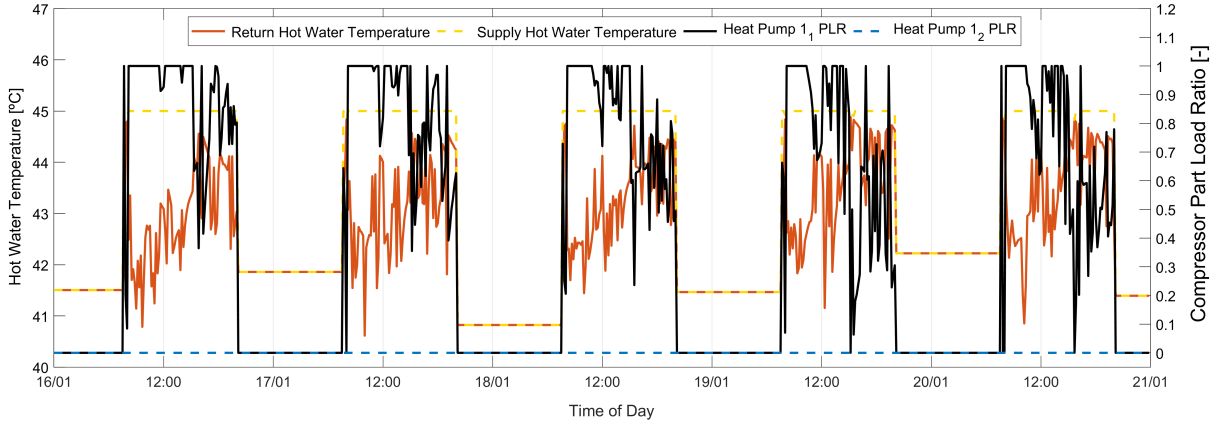
Figure 4.1: Simulation data for the plant operation of the heating only mode during a week in January. Only one heat pump part-load ratio is presented as the others are off for the entire year.

Regarding the operation with heat recovery during which the model, is, in fact, a 4-pipe system, figure 4.2 is presented that shows data for the recovery operation during three week days in September, for both the cooling side and the heat recovery side.
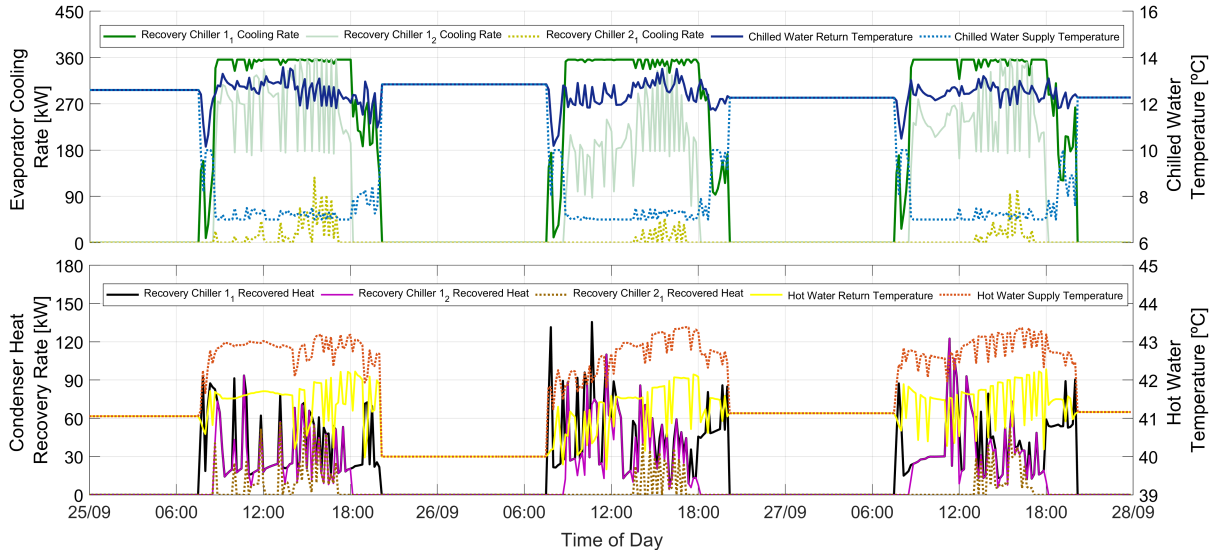
Figure 4.2: Simulation data for the plant recovery operation during 3 week days in September. In the graphic above, the chiller side is displayed with the evaporator cooling rate and the supply and return water temperatures. Below, the recovery side is shown with the correspondent recovery variables.

The figure intends to demonstrate the control of the hot and chilled return water temperature at a constant setpoint with modulation of the supply temperature according to the demand. This is achieved moderately well, despite not being able to precisely control the 12 or 40 °C temperature setpoint, likely due to the simulation timestep set being too big. For the chilled water case, the return tends to hover slightly above 12 °C. The supply setpoint is, for the majority of the time, hovering near the minimum 7 °C due to the load demands. However, the temperature modulation is especially visible in the morning and afternoon period, when the loads are reduced, during which the supply temperature modulates between

7 and 10 $^\circ C$. For the hot water, a similar process takes place with an oscillating return temperature hovering sightly above 40 $^\circ C$. The supply water temperature never exceeds 43.5 $^\circ C$ despite being able to modulate between 42 and 45 $^\circ C$. This happens due to the lower heating demands not requiring maximum water temperature. Moreover, the evaporator cooling rate and condenser heat recovered can be seen. Only three refrigeration circuits are shown which account for a fully activated and a half-activated unit, since these are the only ones being called by the simulation. In fact, the remainder 3 circuits available are never called during the entire time they are available. The evaporator cooling rates are always larger than the recovered heat as the cooling needs are larger at this time, but the control of the unit with regards to how much heat is recovered is visible. Comparing the first and second day shown, it is visible that in the first there is a larger cooling need throughout the day, with the first circuit practically always fully loaded, the second modulating its capacity during some time of the day and the third circuit very lightly loaded. Despite that, during that day, the recovered heat across the three circuits is quite similar. For the second day, there is a lower overall cooling load but the recovered heat from the first unit has the highest peak in all of the three days, with a recovery of about 135 kW. This showcases the condenser heat control algorithm, in which the fraction of refrigeration fluid heat that is transferred to the cooling tower circuit and to the hot water circuit is dynamically adjusted according to the heating demand in that timestep. Additionally, it is also noticeable the drastically lowered output of the chiller after about 18:00 owing to the reduced occupation in the classrooms and to the shut down of the setpoint in the offices of the 2nd and 3rd floor.

Furthermore, figure 4.3 showcases three important chiller parameters during 2 days in April: the EER, the TER[1] and the PLR.
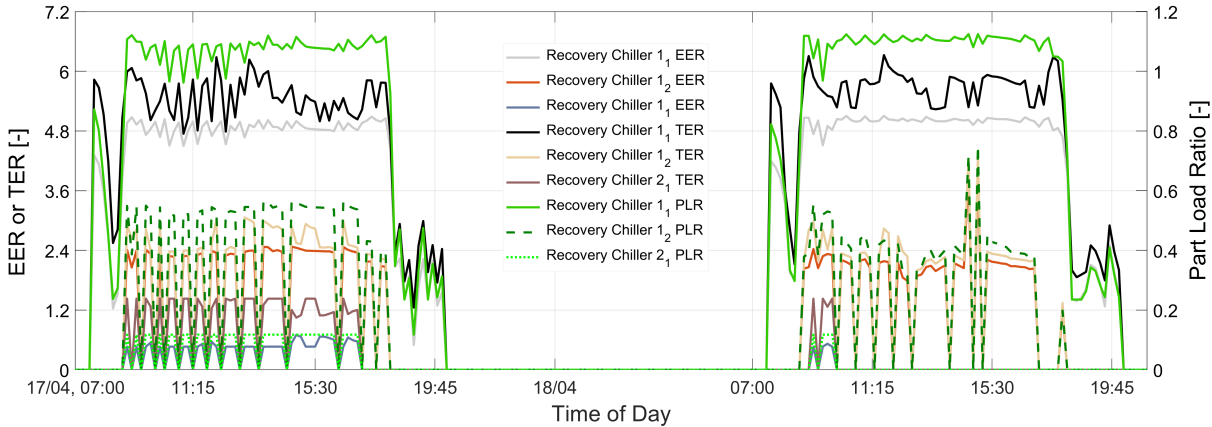
Figure 4.3: Data during 2 days in April of the recovery chiller's EER and PLR.

One can see a direct correlation between them as they are calculated using the curves constructed from the technical bulletin and shown in section 3.6.1. A problem with the implementation was discovered by watching these variables: at lower PLR's, these units should have a higher efficiency than at full load (PLR = 1), as visible in the data from the technical bulletin shown in Appendix C. However, as visible in the figure, for lower PLR's, the EER's output is also lower, hovering near 2.4. This is not realistic and

---

[1]The Total Energy Ratio (TER) is a measure of the total efficiency of a heat recovery capable chiller, see figure 2.6

is a source of error leading to higher electric consumption of the chiller than in reality. However, this happens only for the minority of the loads; the majority of the load is handled by the first circuit which work at realistic efficiency values of approximately 4.8. Nevertheless, the performance curves introduced were checked and no error was found in them, however, the source of this incongruity was not found. It is likely a bug in *Energyplus*. The TER was calculated manually and, for the first unit, hovers at the 5 to 6 range that is within the expected value for this chiller for partial heat recovery. The TER of the other circuits are unrealistically lower due to the error mentioned above. The PLR exceeds 1 for the 1st unit but that is expected as it is 1 for the rated atmospheric conditions and the unit is working at lower outdoor temperature.

Regarding the operation for cooling only, which is active for approximately 3.5 months, figure 4.4 showcases the HVAC plant operation for a day in July.
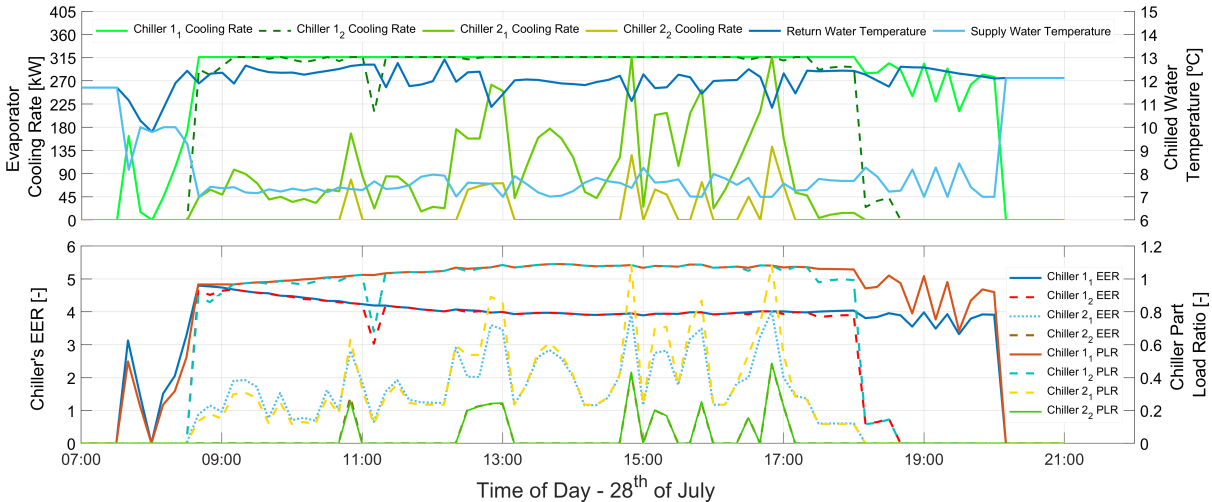
Figure 4.4: Cooling only HVAC plant data for the 28th of July. Above, the evaporator cooling rate of the 4 active chiller circuits and the temperatures of the supply and return chilled water are shown. Below, the performance of the 4 chiller circuits is presented with EER and PLR data.

The day chosen, the 28th of July, possesses the highest cooling loads of the year as the fourth circuit (chiller 2_2) is activated at times. As such, one can conclude that the 3rd chiller is never used and the second circuit of the the second unit is only partially activated at times. In fact, the highest cooling rate in the simulation is at 16:50, when a total of approximately 1090.6 kW is output by the chillers where the total available cooling rate for those outdoor conditions and leaving water temperature across the 6 circuits is approximately 1896.6 kW. This equates to a maximum chiller plant load of 57.7% and a safety factor of 73.9%. As such, the simulation model, which has its limitations, indicates an oversizing of the HVAC plant. Nevertheless, there is a need for a safety factor and for a backup unit in case of operation problems. However, the results of the simulation show that it is likely that this safety factor is higher than required. The recommendation would, therefore, be to revise the sizing of the chillers, more specifically, to maintain the number of units but to size them with less capacity each. Assuming a 35% safety factor, instead of the calculated 73.9%, the total available capacity for the 3 units in these circumstances would be 1472.3 kW, which equates to 490.8 kW each. At rated *Eurovent* conditions and considering that, at these conditions, each unit can output 16% above its rated conditions, each unit would have 423 kW of

cooling capacity. However, note that the weather file used has lower peak summer temperatures than the design temperatures chosen by EACE[2], as such, the oversizing demonstrated by the simulation is exacerbated by this fact.

Furthermore, one can see the control of the return water temperature and the modulation of the supply water temperature, in a similar manner of the recovery units, with quite good control of the return water temperature setpoint.

The error related to inferior efficiency at lower than nominal part load ratios, as mentioned above, is also visible in table 4.1.

Table 4.1: Operation data for the chillers during the 28th of July. Assuming a realistic combined EER of 4.1 considering the units selected and the ambient conditions, a percentage of error was calculated to account for the unrealistic EER values for part load ratios. Also shown is the average EER during the time the cooling only operation is available and during times of chiller usage.

	Average EER [-]	% Cooling Handled	Daily Chiller Input Energy [MWh]	Daily Energy with EER = 4.1 [MWh]	% Error
Chiller 1_1	3.90	47.00			
Chiller 1_2	4.09	38.40			
Chiller 2_1	1.90	12.60		-	
Chiller 2_2	0.76	2.00			
All combined	3.66	100	12.67	11.31	12.00
Combined average from 01/06 to 15/09	3.53	-		-	13.90

During this day, the percentage of load handled by each circuit is visible above, alongside average EER's for the day and a combined average EER taking into account the percentage of load of each chiller. Assuming an expected average value of 4.1, the overall chiller energy expenditure for that day is overestimated in 12% with an added daily consumption of 1.36 MWh. This is for the highest load day. However, an average EER of 3.53 was calculated for all the days in which cooling only is active, which equates to a percentage of error in relation to EER at 4.1 of 13.9%. This value is a gross estimation as the efficiency of the chillers is highly dependent on the outdoor air temperature, on the part load ratio and on the leaving water temperature. As such, this 13.9% of overestimation is highly dependent on the reference and is only given to provide an idea on how much more energy do the chillers consume in this model, when compared to what would be expected.

Overall, the hydraulic plant works as expected despite the limitations in the implementation of the chillers. The major source of error is assumed to be the efficiency of these units at partial loads that leads to an overestimation of their energy expenditure.

4.1.2 Analysis on Zones With FCU's as Terminal Units

The most common type of terminal unit will be 4-pipe fan coil units, as such, their performance will massively influence the overall comfort conditions in the building. Given that the HVAC plant is designed

---

[2]The weather file for the 28th of July has a peak temperature of 30.2 at 15:00, which is about 9.3% lower than the peak summer temperature of the design conditions.

with a safety factor, which was shown to likely be higher than intended, satisfactory temperature control should be expected inside each TZ, at least with simultaneous availability of heating and cooling. It is not, however, that simple as there are numerous other variables to take into account in the simulation such as the models used and its implementation in *Energyplus*, the sizing being done by the simulation or hard-sized, or other computational matters such as the timestep used, the numerical algorithms chosen, among others, as seen in section 3.4.

In this section, the indoor air temperatures for 9 FCU-served TZ's are shown in two representative weeks, weekend included that are the last pair of days represented in each graph, to provide a global insight of the thermal behavior and control of these zones, in 2 graphs of figure 4.5.
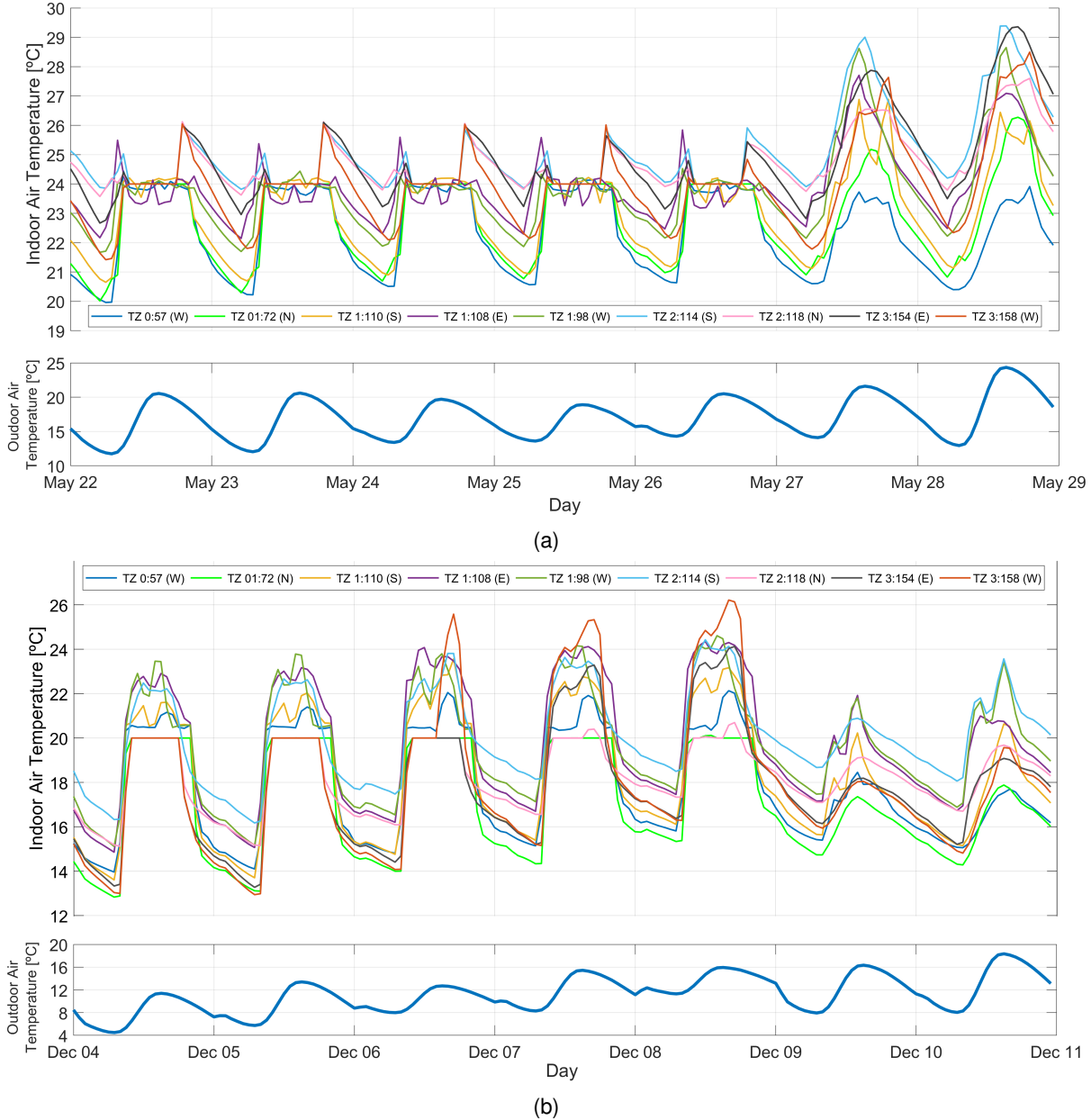
Figure 4.5: Zone temperature data for 9 FCU-served zones during a week in May where the chillers are operating with heat recovery and during a week in December where only heating is available. The outdoor air temperature is also presented during both weeks. All the zones chosen are on the building perimeter. Each zone has its floor level and facade orientation shown in the legend.

A week in May is shown, figure 4.5a, during which the setpoint control is extremely precise with the temperatures, in the worst zone, always within 1 $^{\circ}C$ of the setpoint. Most zones have its setpoint controlled accurately during recovery chiller availability, such as TZ 57, TZ 98, TZ 118, TZ 154 and TZ 158. Some zones do show more difficulties in maintaining the setpoint, such as TZ 108 and TZ 110, due to occasional oscillations that arise because of difficulties in achieving zone convergence. However, it is uncommon and did not affect the global results. The early peaks in late-afternoon from the spaces in the 2nd and 3rd floors are due to the reduced schedule for the setpoint in these spaces, as mentioned in the air-side control part of subsection 3.6.2. The weekend period, which corresponds to the last pair of days presented, show the thermal behavior trend without HVAC control and without space occupation, with daily peak temperatures in some spaces of up to 29 $^{\circ}C$. As expected, the simultaneous availability of heating and cooling provide the model with a tighter temperature control.

Contrarily, in figure 4.5b, a week in December is shown during which only heating is available. This introduces a likelihood of having overheated TZ's. About half of the TZ's highlighted show this behavior, and the zones with solar exposure during the day are, obviously, more affected, and therefore, require cooling. Naturally, TZ 72 and TZ 118 show a satisfactory control of the temperature and both possess a northerly orientation with no direct sun radiation, as such, their heating loads are higher. On the worst behaved zones, such as TZ 108 and TZ 98, peak temperatures of about 24 to 25 $^{\circ}C$ can be seen. TZ 154 and TZ 158 have an unrealistic behavior with accurate control for the first two days presented but erratic control for the remaining three days of the week. The FCU's should be able to modulate the water and air flow rate to adapt to the thermal needs. However, this was not achieved fully. Therefore, a shortcoming of the model was the tendency to overheat at times when only heating was available.

During cooling only times, the thermal behavior was more satisfactory given the fact that the vast majority of the loads during that time, are, indeed, cooling loads.

Note that for the real project, taking into account the sizing of the plant, these terminal units will be able to better control the indoor temperatures than what is represented here owing to the simultaneous availability of heating and cooling. These peaks are, almost certainly, related to computational errors originating from the complex water heater heat pump implementation in *Energyplus*.

This figure 4.5, therefore, proves, once again, that the 4-pipe system is needed to provide Pavilhão de Civil with simultaneous heating and cooling and, consequently, adequate indoor temperature control.

4.1.3   Analysis on Zones With AHU's as Terminal Units

This section focus on the thermal performance of the zones that are directly served by an AHU, which are the ones referenced in table 2.6. As mentioned in the air-side control part of section 3.6.2, there were difficulties in controlling the supply air temperature of these 4-pipe AHU's that will effectively work as 2-pipe in the simulation during about 6 months. This led to an unrealistic supply air temperature during the time when the recovery chillers are active, as intermediate supply air temperature values of 22-23 $^{\circ}C$ are being output. That, in turn, led to unsatisfying thermal conditions inside these spaces during those 6 months, which can be seen in figure 4.6. A possible solution for this problem was not

found in useful time. However, the supply air temperature control during the cooling and heating only phase works well with values closely controlled to the setpoint. To showcase these questions, figure 4.6 is presented, which aims to showcase indoor air temperatures in 3 different representative months.
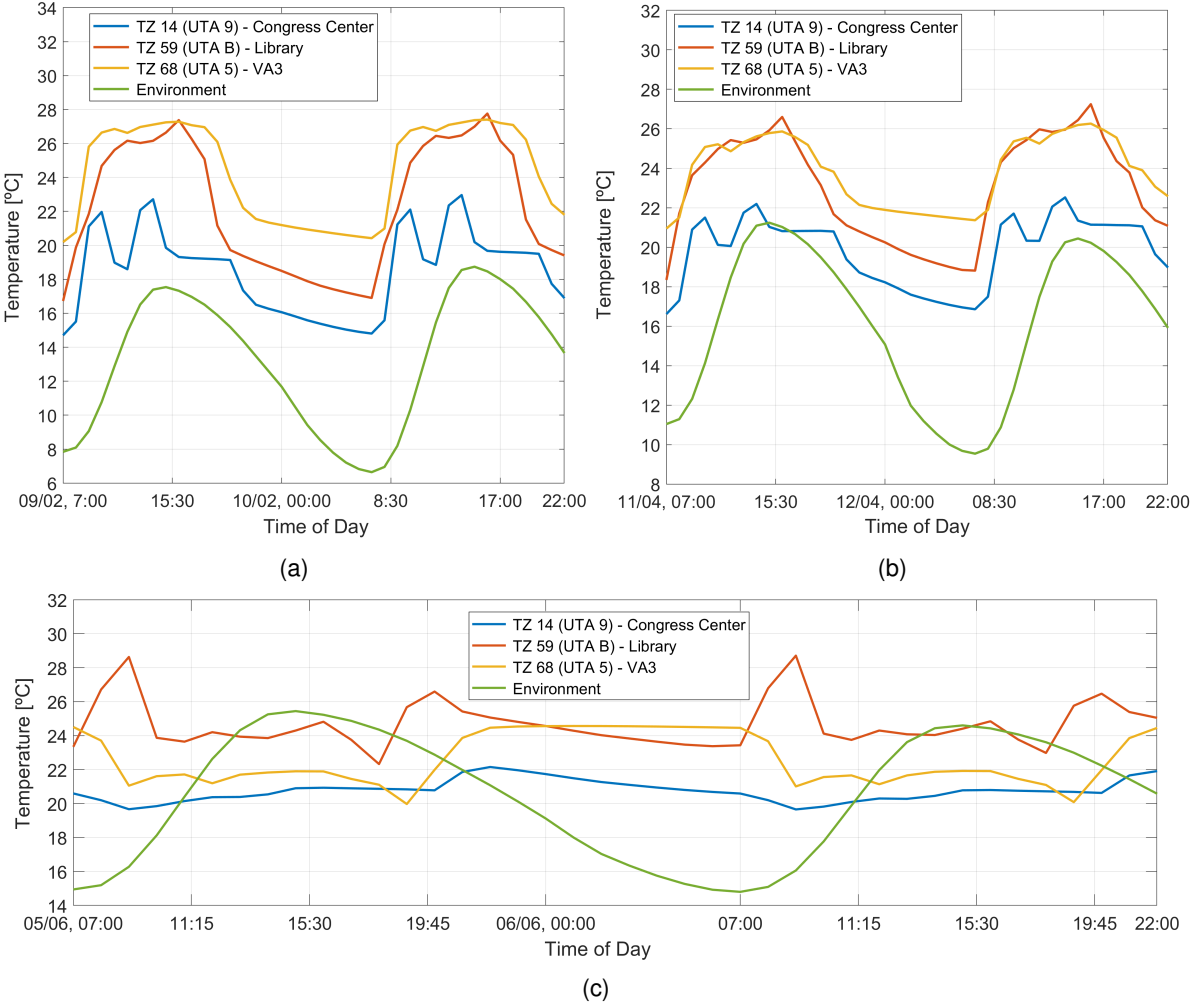
Figure 4.6: Indoor air temperature data for some zones served by AHU's at 3 different representative months: (a) - During two days in February with indoor air temperature setpoint at $20\,^{\circ}C$; (b) - During two days in April with indoor air temperature setpoint at $20\,^{\circ}C$; (c) - During two days in June with indoor air temperature setpoint at $24\,^{\circ}C$.

The first figure, 4.6a, represents two days where only heating is available, leading to a close control of the supply temperature according to the setpoint. This, in general, causes overheating of most TZ's during occupied hours with temperatures close to $26\,^{\circ}C$ throughout the day. That is caused by two factors: the first and main factor is that it is likely that there is a close balance between the heating and cooling loads in most spaces, such as all VA's amphitheaters, library and congress center rooms, and since there is no cooling available, it introduces a disequilibrium. Secondly, the flow rate is not being adjusted as expected by the variable flow fans for most spaces which is unrealistic to the project, probably because of incorrect control mechanisms with the setpoint managers and outdoor air control. The UTA 9, 10, 11, 12 and 13 are an exception to this behavior because in the TZ's of these spaces, there are hours with null occupancy in the daily schedule, therefore, the outdoor air flow rate is lowered

during these null occupancy times[3].

The second figure, 4.6b, is representative of the main problem with the AHU's implementation, which is when both heating and cooling is available, the supply air temperature is not set at the desired setpoint. This is an area in which the model requires improving. As such, the daily temperatures are always in the 26-27 $^{\circ}C$ range, independently of the setpoint being at 20 or 24 $^{\circ}C$. Again, an exception to this was the spaces served by the UTA 9, 10, 11, 12 and 13, where the temperatures are much closer to the intended setpoint.

The third figure, 4.6c, illustrates the thermal performance during cooling only availability, with steady 14 $^{\circ}C$ supply air. Despite that, it seems that the sizing of the capacity of the water coils and the air flow rate is not adequate as the indoor temperatures are not satisfying. The UTA - B serving the library shows a tighter setpoint control during most part of the day, exception being early morning and late afternoon. The other zones are not capable of controlling the temperature to the desired setpoint with temperatures in the 21 to 22 $^{\circ}C$ range, while the setpoint is at 24. This behavior also happens on most of the other AHU-served zones that are not shown in the figure.

In a nutshell, the thermal behavior of the spaces served by the AHU's are the weakest part of the implementation and it is an area that should be improved in future works, perhaps with the usage of a higher level control method, namely, Energy Management System[4] (EMS). In reality, this behavior will not take place as, assuming a correct control of the air flow rate and its supply temperature, these spaces will be able to achieve a tighter temperature control and, therefore, comfortable conditions.

4.1.4   Analysis on Zones With VRF Units

Regarding the zones which will be served by VRF terminal units, two graphs were constructed that aim to showcase the thermal performance of 5 TZ's for two different heating and cooling weeks. They can be observed in figure 4.7.

The two weeks chosen were: 1) the 3rd week of June while there still is normal occupation prior to the summer brake with relatively high outdoor temperatures and 2), the 1st week of December, with relatively low outdoor air temperatures.

For the vast majority of occupied hours, the VRF system is capable of meeting the cooling/heating loads as the indoor air temperature calculated matches the setpoint. Both the restaurant (TZ 91) and the main room of the LTI (TZ 103) follow the setpoint perfectly during occupied hours. The same happens in the Espaço 24h zones (TZ 84 and 82) that have 24/7 HVAC availability. In TZ 84, a night setpoint of 18 and 26 $^{\circ}C$ was introduced from 03:00 to 07:00, in which the occupation is almost null, in an attempt to save energy during these hours. Turning the VRF system off in these spaces during the night might also be a viable solution when the real system is in place. Some oscillations were verified in the thermal zone of the bar (TZ 78), in which the indoor temperatures tend to float 1 to 2 degrees higher during a part of the day, as visible in the figure. Also visible was the thermal performance of some TZ's during

---

[3]Note that the outdoor air flow rate is controlled by the outdoor air requirements per person, as defined in the *DesignSpecifications:OutdoorAir* object.
[4]Energy Management System (EMS) is an *Energyplus* module that is programmable within the software and allows for a higher level of control, increasing the flexibility of the equipment control when compared to the standard *SetpointManager* objects.

the weekend, which are the last 2 days presented in the graph, such as the LTI, the restaurant and the bar. During that time, seeing that the VRF system is off, the temperature oscillates freely according to the daily temperature and reaches daily peaks of 32 $^\circ C$ in the LTI and 29 $^\circ C$ in the bar. The control of the temperature in the LTI (TZ 103) during saturday morning is also visible in both graphs. For the week in December, the TZ 103 of the LTI showed a odd trend where, on Sunday, the uncontrolled temperature increases during the day and reaches a 23 $^\circ C$ peak despite the daily OA temperature not surpassing 18 $^\circ C$ and despite its orientation being northerly. The same takes place in the bar, however, that is more expected given its southerly orientation. This temperature increase in the LTI is explained by the electric equipment heat gains that are on during Sunday.

(a)

(b)
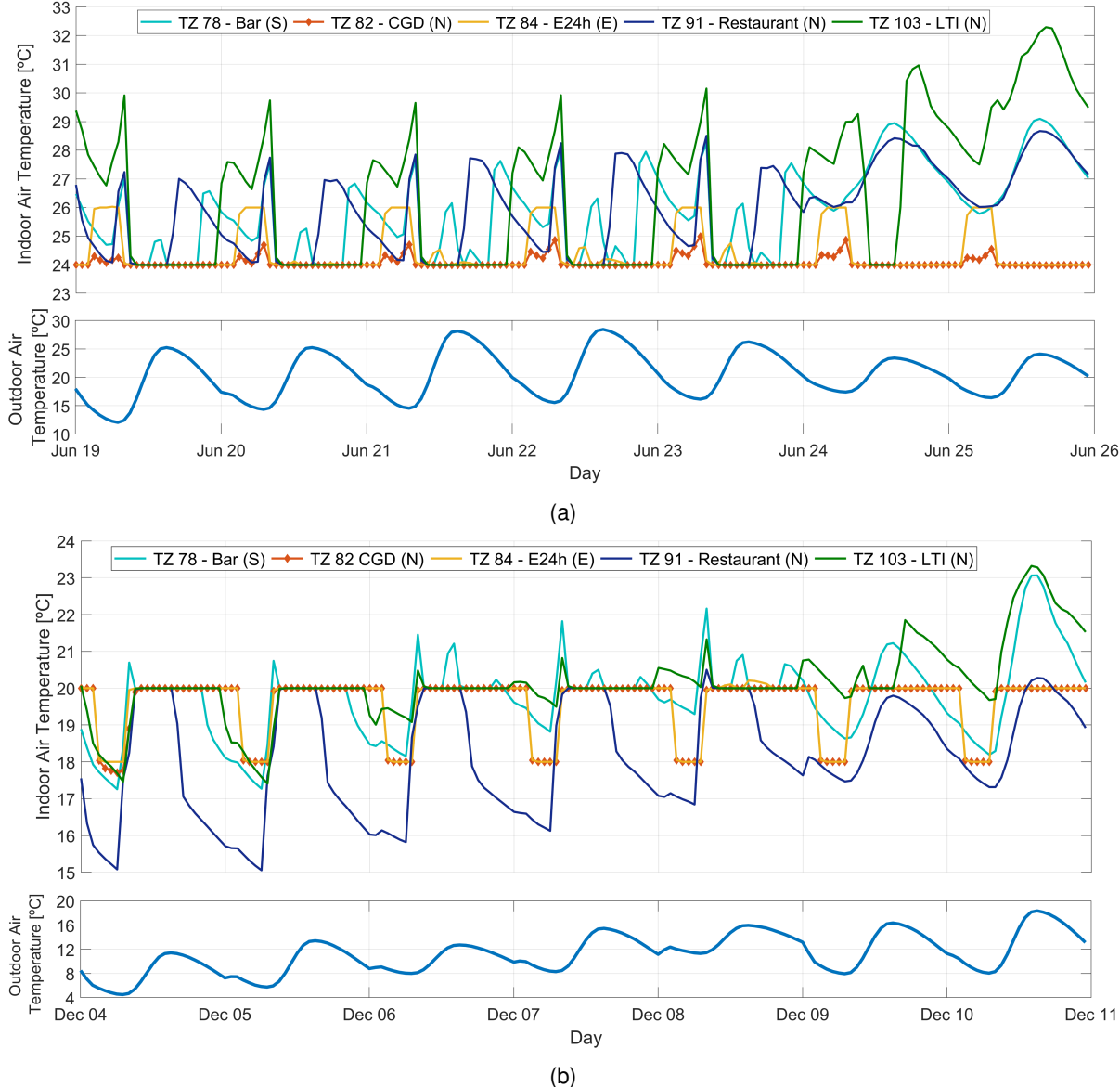
Figure 4.7: Zone temperature data for a week in June and in December. All the zones chosen are served by VRF units which are active at different times depending on the occupation schedule. Each zone has its floor level and facade orientation shown in the legend.

It was also noted that even during the cooler months, most VRF spaces call for cooling in order to

meet the temperature setpoint. Such is visible in figure 4.8 that shows VRF heating and cooling rate data for 3 week days in December. It aims to showcases the domination of the cooling rates in the restaurant (TZ 91), in the CGD room (TZ 82) and in a set of 4 classrooms in Espaço 24h (TZ 84), even during December. Heating is only needed in the early morning to bring the temperature to the setpoint after natural cooling during the night and in the restaurant, during the afternoon although in far lesser rates than the cooling ones.
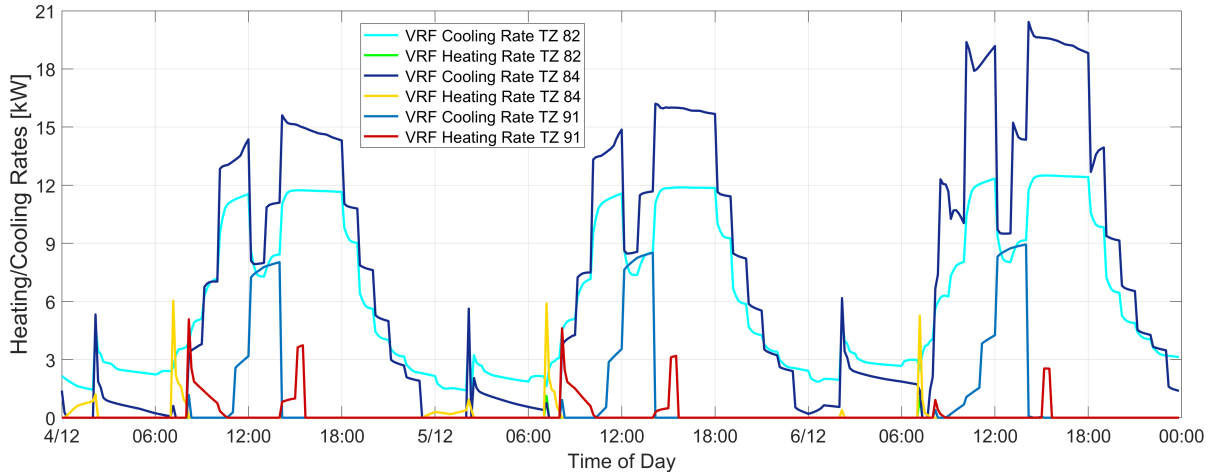
Figure 4.8: VRF terminal unit heating and cooling rates for the 4th, 5th and 6th of December in 3 TZ's.

In general, the VRF systems in the simulation model work the best of all HVAC systems as the setpoint is almost always matched during occupied times. They allow for good control of the temperature and are in dire need to be installed, especially in the Bar and in the classrooms of Espaço 24h, with the exception of Aquário - CGD Room, as the conditions in these spaces are often really uncomfortable and, to a certain extent, unhealthy.

4.2 Comparison With the Old Energyplus Model

In order to directly compare the performance of the new projected HVAC system with the older thermal model with the actual HVAC system, initially done by Marçal [17] and improved upon by the *Campus Sustentável* team, the old model was re-run, still in V8.3, with some slight changes to introduce the improvements generated in the non-HVAC portion of the model, such as in the internal gains description[5] and in the shading. Additionally, for sizing reasons, the *SizingPeriod:DesignDay* object was altered to match both cooling and heating design days conditions to the new project. Finally, modifications also include the cooling interior temperature setpoint, which was lowered by a single degree to $24° C$, and the computational parameters slightly changed to the same as in the new model. Shown below in figure 4.9 is a direct comparison between the old model and the new model, for the end-use energy consumption, as calculated by *Energyplus*.

---

[5]In the old model, electric heaters were implemented in the offices of the 2nd and 3rd floors using the *ElectricEquipment* object, as they are used regularly as a way to combat the lack of capacity of the current HVAC system. They were kept in the old model but removed in the new model as they will no longer be necessary, hence the added interior equipment annual consumption in the old model's case.
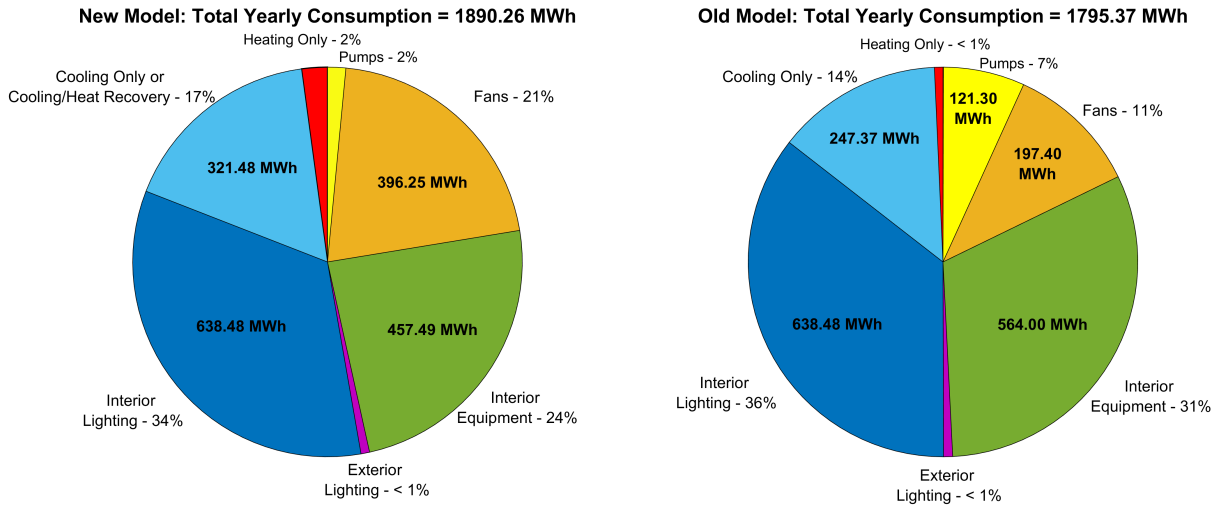
Figure 4.9: Direct comparison of the yearly energy consumption between the old system and the new system, as calculated by *Energyplus*.

A vast increase in fan and cooling consumption is noticeable, which was expected due to the vast increase in the number of fans, as the new model employed 184% more fan objects than the old one. The majority of those are related to the vast number of FCU's in the new HVAC project and also to the new VRF's indoor units. A decrease in pump consumption was calculated as there will be less pumps in operation and the new pumps will be much more efficient and, more importantly, will have variable speed capability on the secondary circuit.

Heating corresponds for heating only operation, which accounts for approximately only 23% of the year, and the VRF systems in heat pump mode. Cooling accounts for the chiller input power, both in cooling only and heat recovery operation, active 77% of the year, which partly explains the increase in consumption alongside the increase in installed power, and also the VRF systems in cooling mode. Overall, a 5% increase in yearly energy consumption was calculated. This was expected taking into account that a lot more zones will have access to air conditioning equipment and the installed capacity of the system will also increase. Additionally, the need to assure ventilation rates with the diverse DOAS's also accounts for a portion of the increase.

Looking into the overall comfort conditions, a vast improvement was verified, as expected. In order to calculate the occupants thermal comfort, besides the indoor air temperatures values, the PMV's were also calculated and the clothing insulation of the occupants was defined in a per month basis with values that were deemed plausible taking into account typical weather. In Appendix E, these values are presented in figure E.1. In order to evaluate in a thermal zone basis, table 4.2 is presented that displays average monthly values of temperature and PMV's for 4 representative months - January (Winter), April[6] (Spring), July (Summer) and November (Autumn). Care was taken to only account for occupied time during HVAC control[7]. In it, 10 representative TZ's are directly compared, and they were chosen based on their terminal air conditioning and representing different facades of the building.

---

[6]During April, the new model considers the average monthly setpoint to be $21\,^\circ C$ as the changeover from 20 to 24 occurs in the 21st while the old model already has the setpoint at $24\,^\circ C$.

[7]The average for most zones were calculated on week days from 08:00 to 20:00. For the offices in the 2nd and 3rd floors, it is week days from 09:00 to 18:00. For the VRF-served zones, each zone schedule was taken into consideration.

Table 4.2: Direct monthly comparison between the projected new and the current HVAC system. Values of average monthly PMV's and average indoor air temperatures are presented in 10 thermal zones for week days during occupied times, alongside the average % of deviation between the setpoint and the calculated average temperatures.

Floor:TZ (Orientation) Type of HVAC System	Month	Average PMV [-]		Average Temperature [°C]		| % Deviation vs Setpoint |	
		New	Old	New	Old	New	Old
01:60 (Underground)	Jan	0.39	-1.28	25.33	15.93	26.63	20.35
	Apr	0.12	-0.90	24.98	19.70	18.96	17.93
UTA 2	Jul	-0.10	0.85	22.57	26.68	5.96	11.16
	Nov	0.19	-0.75	24.46	19.33	23.19	3.33
0:78 (S)	Jan	0.33	0.57	20.21	22.72	1.07	13.60
	Apr	0.34	0.71	21.62	24.31	2.95	1.27
VRF	Jul	1.05	1.98	25.27	30.13	5.29	25.55
	Nov	0.41	0.90	21.06	24.54	5.32	22.72
0:84 (E)	Jan	-0.26	1.05	19.98	26.69	0.10	33.46
	Apr	-0.26	1.54	21.24	29.03	1.17	20.95
VRF	Jul	0.48	3.53	24.25	34.60	1.05	44.16
	Nov	-0.38	1.92	20.19	30.26	0.93	51.29
1:94 (W)	Jan	-0.13	-0.13	22.28	21.25	6.27	11.40
	Apr	-0.45	0.13	21.24	24.13	1.01	0.56
FCU	Jul	0.40	2.02	24.16	30.72	0.68	28.01
	Nov	-0.50	0.22	20.18	23.76	0.88	18.80
1:103 (N)	Jan	-0.44	0.08	19.95	22.89	0.25	14.46
	Apr	-0.37	0.01	21.27	23.97	1.35	3.30
VRF	Jul	0.59	2.13	24.62	30.64	2.59	27.68
	Nov	-0.50	0.31	20.22	24.32	1.10	21.62
1:109 (E)	Jan	0.02	0.17	22.79	22.31	13.94	11.56
	Apr	-0.31	0.85	21.44	26.07	2.10	8.63
FCU	Jul	0.60	2.77	24.59	32.07	2.45	33.62
	Nov	-0.43	0.91	20.23	25.86	1.10	29.32
2:114 (S)	Jan	0.21	-0.35	21.88	21.20	9.41	5.99
	Apr	-0.37	0.01	21.54	23.73	2.57	1.13
FCU	Jul	0.86	1.51	25.78	28.14	7.42	17.24
	Nov	-0.47	0.05	20.47	23.43	2.36	17.13
2:128 (W)	Jan	-0.59	-0.45	20.30	21.15	1.49	5.76
	Apr	-0.62	-0.22	20.93	23.20	0.31	3.33
FCU	Jul	0.40	2.05	24.31	31.53	1.30	31.37
	Nov	-0.70	0.08	19.96	24.29	0.22	21.45
3:150 (N)	Jan	-0.74	-0.23	19.74	22.55	1.29	12.73
	Apr	-0.65	-0.40	20.90	22.25	0.50	7.31
FCU	Jul	0.39	1.19	24.18	27.48	0.75	14.50
	Nov	-0.80	-0.09	19.87	23.42	0.64	17.09
3:152 (E)	Jan	-0.39	-0.60	21.50	19.99	7.49	0.03
	Apr	-0.35	0.10	21.38	23.81	1.82	0.78
FCU	Jul	1.00	1.67	25.55	28.15	6.47	17.31
	Nov	-0.65	-0.10	20.06	23.01	0.30	15.04

Overall, the setpoint is more closely followed in the new projected system, which is expected taking into account that the current system is undersized in relation to the building needs. The zones served by the VRF units follow the setpoint impeccably while the zones served by FCU's also follow the setpoint quite well but with some oscillations, as seen above. Additionally, the slight overheating during January, during which only heating is available, can be seen for some zones, such as TZ 94, 109 and 114, where average monthly temperatures are in the 21-22 $^{\circ}C$ range. The case of TZ 84 is the most extreme in which the old DOAS's are not enough to assure a comfortable condition where PMV's are always on the hot side, with the situation in July being really dire with an average temperature of 34.6 $^{\circ}C$. The same happens in the other rooms from Espaço 24h, such as the rooms from TZ 41, 83 and 85. In TZ 60, served by the UTA 2, the control is not adequate in the new model, as explained above, despite calculating comfortable conditions as the PMV indicates. In TZ 114 and 152, the new model has some difficulties in keeping the setpoint at the 24 $^{\circ}C$ level during July, as average temperatures of over 25.5 $^{\circ}C$ were calculated. With average PMV's of 0.86 and 1 respectively, it is considered to be in the slightly warm sensation. As such, according to the PPD-PMV graph of figure 2.2a, about 25% of the occupants would be dissatisfied. In parallel, TZ 78, also is also unable to keep the setpoint during July, with an average temperature of 25.27 $^{\circ}C$ and an average PMV of 1.05. The TZ's chosen are, in general, representative of the overall thermal conditions in the building with the new HVAC system. For the remaining months not represented, the thermal behavior and trends is similar to what was presented.

Regarding the PMV values, it was noted that, in the months where the setpoint is at 20 $^{\circ}C$, despite an excellent control of it, the calculated PMV's tend to the slightly cool side with some values lower than -0.5. This is due to the amount of clothing insulation that was used for each month. Those are, however, still comfortable conditions for about 90% of the occupants, according to the PPD-PMV relationship. Also, the current system during cooler months is also falsely aided by electric heaters present, which aid in producing comfortable PMV values, despite not being able to keep the indoor temperature setpoint.

It was also confirmed that the current HVAC system has a lot more difficulties in achieving comfortable conditions during the summer, as seen from the temperatures and PMV values for July. This situation had already been concluded and proved in previous thesis, mentioned in section 2.2.

4.3   Comparison With Real Consumption Data

The real data available for comparison was the total electricity consumption for 2018 and access to it was kindly granted by *Campus Sustentável* through the EnergIST platform, which is briefly explained in section 1.3. It was decided to compare the monthly values for the entire 2018 year with the simulation results of the new model. It is important to note that the weather file used for the simulation was the generic one used for all simulations which renders this an indirect comparison but allows, nonetheless, for an idea of the performance expected for a typical year when compared to the current working conditions. Furthermore, the HVAC consumption data monitored in EnergIST only accounts for about 50%

of the total HVAC consumption in the building due to the arrangement of the electric panels[8]. Data from the audit from 2015 showed that the HVAC portion of the building represents 40% of the total energy consumption [12] - see figure 1.4. As such, the total electricity consumption data from EnergIST was used to estimate the HVAC consumption[9], using this assumption.

In figure 4.10, one can compare monthly energy consumption and gain an insight on how much more HVAC-related energy is expected to be consumed.
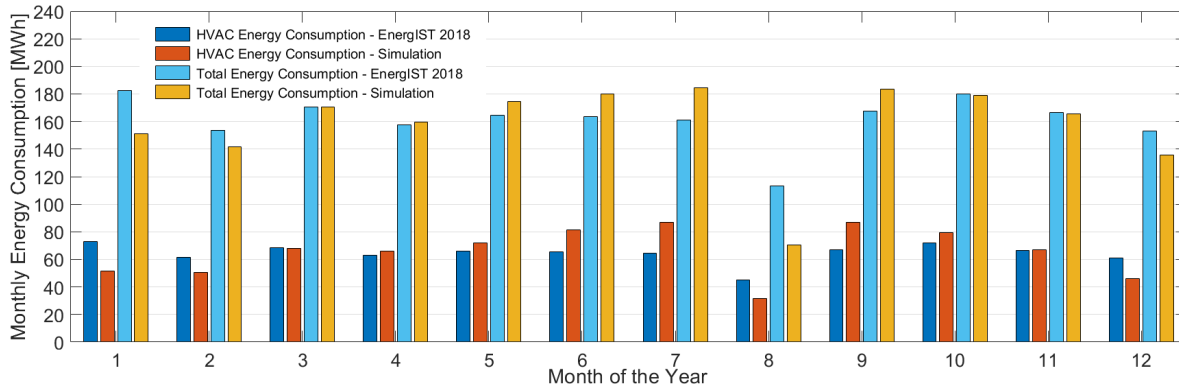
Figure 4.10: Monthly comparison of the HVAC and total energy consumption in Pavilhão de Civil between real data from 2018 and the results from the simulation, using the default weather file.

The new simulation model showed a 2% decrease on the overall yearly electricity consumption, compared to the data from EnergIST in 2018 - approximately 1933 MWh was the real consumption in EnergIST while *Energyplus* output a yearly consumption of about 1890 MWh. This is a positive outcome, as while an increase in electricity expenditure is not expected, a vast increase in the thermal comfort of the occupants will be possible. Regarding the total electricity consumption per month, overall, both data were quite similar. In general, for the Winter months, the new model is expected to consume less energy due to the elimination of the need to employ electric heaters in the spaces, which are a significant contributors to the heating energy consumption. For the hotter Summer months, a larger HVAC consumption was calculated (about 25% higher in June, 34% in July and 10% in September) that is justified by the increase in equipment capacity, on the number of spaces served and on the larger ventilation rates. For the mid-season time, during Spring and Autumn months, the benefit of having heat recovery is visible; while the HVAC consumption is not lower, it is extremely similar and a vast increase in the thermal comfort of the whole building is achieved. This fact is another positive outcome and is possible by using more efficient equipment with variable flow capacity and heat recovery, both in the water-side and on the air-side. Overall, the yearly HVAC energy consumption increased only about 2%.

The trends of increase and decrease of energy consumption matched quite well for the overall energy consumption and for the HVAC energy expenditure with the exception of months were only heating was available (December, January and February). During March, April and May, a quite flat HVAC energy consumption was verified in both cases, with the increase in expenditure during June and July. August

---

[8]The data from EnergIST had some interruptions due to technical issues, nonetheless, the data shown was, for all months, representative of over 90% of the monthly time.

[9]Note that the data from the EnergIST is from 2018 while the audit was done in 2015. However, no major changes were introduced in the building in this time period, as such, the assumption is considered acceptable.

showed a 30% lower HVAC consumption and a 38% lower total energy consumption, which leads to the conclusion that the description of the model of the building activity during this month is possibly under estimated[10]. From September until December, the HVAC consumption figure matches the trends shown in reality quite well with a gradual decrease of energy expenditure.

The comparison done in this section, despite not being a direct one, due to the weather file used and to the estimation of the real HVAC consumption in EnergIST, allows for an understanding of the benefits of the new projected HVAC system, in which, a similar total consumption was calculated (likely inferior while in operation), but with a significant increase on the thermal comfort of the occupants.

4.4   Summary of the Limitations of the Model

Despite the best efforts for producing an extremely precise description of the HVAC plant, such was not totally possible owing mainly to limitations within the *Energyplus* models. This section is dedicated to the explanation of the limitations of the model and steps required to output realistic energy consumption data, in conjunction with the approximations introduced, as explained in sections 3.6.1.1 and 3.6.2.1.

First of all, as mentioned above repeatedly, there is a problem related to lower than expected chillers efficiency at part load ratios inferior to 1. This happens when the *Chiller:Electric:EIR* object is used, which is during cooling with heat recovery and during cooling only. This is considered a limitation of the model and a source of energy consumption overestimation. It should not, however, effect the thermal behavior of the diverse TZ's.

Furthermore, a secondary heating plant had to be created to connect the condenser of the chiller to a water tank, as visible in figure 3.10. As such, a secondary constant speed set of pumps were introduced that will not exist in the project. Therefore, their consumption was removed in post-processing and accounted for an yearly consumption of approximately 21.45 MWh.

Moreover, as explained before, using the *Chiller:Electric:EIR* object with an air-cooled condenser and heat recovery is not possible, therefore, it required the construction of a fictitious condenser water circuit with a cooling tower. In it, a set of variable speed pumps were introduced, alongside the cooling tower that has a fan which consumes electricity. Respectively, these accounted for approximately 4.8 MWh and 6 MWh of yearly consumption that was removed in post-processing.

Finally, an incoherence that can quite possibly be a bug in the software, was found in the heat pumps evaporator fans that were implemented in the *WaterHeater:HeatPump* compound object through the *Fan:SystemModel* object. In it, an availability schedule was introduced to limit the availability to the time when the heating only heat pump system is active. However, these kept consuming energy in the remainder months at a constant pace. Furthermore, during the time when they were active, despite only 1 circuit being activated, the remaining 5 fans were consuming at a constant pace even when the HP's compressor was off. As such, in post-processing, the energy consumption of these during both these times was removed which accounted for approximately 7.5 MWh of yearly consumption.

---

[10]During August, the model simulated a reduced activity period of 20 days, which is possibly exaggerated when compared to last year habits.

Chapter 5

Conclusions

The new HVAC system of Pavilhão de Civil will allow for a significant improvement of the indoor thermal comfort. That was concluded from the analysis of the indoor air temperatures predicted. Additionally, healthier ventilation rates that comply with the legislation will also, to an extent, improve the IAQ.

The simulation, despite having a great number of uncertainty sources which could not be avoided, allowed for a good prediction of the energy that will be spent in the HVAC system. A 5% increase of annual energy consumption was calculated when compared to the old *Energyplus* model with updated conditions and a 2% decrease in yearly consumption was calculated when compared to the real 2018 yearly energy consumption. The HVAC energy consumption is expected to be similar. In fact, an only 2% increase in HVAC energy consumption was calculated when compared to EnergIST data. In the new HVAC system, 3 units will be used, each with over 550 kW of projected cooling capacity, with added VRF-served zones and a higher number DOAS's to assure ventilation rates, with water heat recovery and exhaust air heat recovery.

It is expected that the actual energy expenditure will be, in reality, lower than predicted as the simulation employed full load conditions on the building, that is, the occupation, lighting, and electric equipment is always at full design load. This is not accurate as there are diverse periods where the occupation is remarkably lower. Also, the project was conceived to be specially efficient at part-load conditions, allowing for great adjustability with in-room control. Moreover, the chillers consumption in recovery and in cooling only mode was overestimated due to an unknown bug, in values of over 12% but surely lower than 15%. Moreover, the sizing of the fans in the simulation is not final and subject to an estimation and the VRF's terminal units were implemented with constant speed fans, which is untruthful to the project. Moreover, the lack of air-side economizers in the DOAS's units of the implementation can also be invoked as a contributing reason for the energy overestimation expected.

The number of chillers selected to be used never surpassed 2 units for the 3 operating modes, with the second unit frequently not being needed and only being called during peak season. The results of the simulation model created show, therefore, that the HVAC plant is oversized, even with a backup unit which concedes a great degree of redundancy for maintenance and possible malfunctions. Despite the necessity for a safety factor, and for a backup unit, it should be not higher than 40%, which was

not verified in the simulation. The proposed action is to revise the sizing of the reversible chillers by selecting lower capacity units. The results of the simulation model, for a safety factor of 1.35, allow for a recommendation to size each unit with approximately 423 kW of rated cooling capacity. These were, however, results from the simulation model that has its limitations and that should be taken into account, as explained before.

Above all, this new HVAC system will, unlike the current system, allow for a great adjustability of temperatures and schedules due to the new terminal units which will possess in-room thermostats and control. This will vastly improve the comfort of the future occupants. The air will also be much more healthy and breathable, owing to the ventilation rates being assured by the diverse DOAS's. At the same time, the overall energy consumption is expected to be quite similar, if not inferior to the actual system in normal operating conditions.

5.1 Guidelines for Future Work

Regarding the future work, there are a number of issues that could be improved in the model, other types of analysis could be performed to better estimate energy consumption, and other energy saving measures could be envisaged in the building. As such, some guidelines are given in this section to future students or engineers that will deal this model and the new HVAC system in Pavilhão de Civil.

Despite the best effort to produce an accurate model, there are always improvements that can be introduced in it. Firstly, to improve the control of the 4-pipe AHU's which gave unsatisfactory results, using EMS, which could also be employed to better control the HVAC plant supply air setpoints at different points in time and of the air loop. Secondly, the introduction of the air-side economizer on the diverse DOAS's, which was not implemented due to the complex control needed. Thirdly, a continued improvement of the HVAC hydraulic plant, experimenting with more complex control using EMS and trying to solve the problem with the chiller performance at lower than nominal part load ratios.

As mentioned by Almeida [20] in his thesis, the interior lights are controlled by a schedule and not on the illuminance levels inside the spaces, which is not what realistic for the most part. As such, the lightning system on *Energyplus* should be subjected to improvements.

To perform a thermal and economical analysis with the use of different HVAC equipment, such as a boiler to provide the heating source and its consequences on emissions and primary energy consumption. Also to experiment with a more efficient strategy to dynamically control the OA flow rate to each space, such as demand controlled ventilation (DCV) and to access its benefits.

As an analysis on the computational parameters was not performed and based upon older works and references such as Marçal, Hong *et al.* [17, 42], the computational parameters of the model could be studied with a sensitivity analysis to decide on the optimal combination.

Finally, as an added and more advanced way to assess changes in buildings, one could employ optimization models with tools such as artificial neural networks or genetic algorithms to assess future changes in either retrofitting or on the construction of new buildings. These technologies can, for instance, be used to quantitatively assess technology choices in a retrofit project [48].

Bibliography

[1] European Union. Energy efficiency in buildings in the EU. `https://ec.europa.eu/energy/en/topics/energy-efficiency/buildings`, 2019. Online, accessed 18 February 2019.

[2] International Energy Agency. The future of cooling - opportunities for energy-efficiency air conditioning, 2018.

[3] I. Soares. As políticas e prioridades para a eficiência energética e para as energias renováveis em Portugal, 15 July 2016. Lisbon, Presentation from Ordem dos Engenheiros.

[4] PorData. Total de consumo de energia eléctrica por tipo de consumo. `https://www.pordata.pt/Portugal/Consumo+de+energia+el%C3%A9ctrica+total+e+por+tipo+de+consumo-1124`, 2019. Online, accessed 18 February 2019.

[5] PorData. Produção de energia eléctrica a partir de fontes renováveis (%). `https://www.pordata.pt/DB/Portugal/Ambiente+de+Consulta/Gr%C3%A1fico`, 2019. Online, accessed 18 February 2019.

[6] ODYSSEE-MURE. Energy efficiency trends and policies in the household and tertiary sectors - an analysis based on the odyssee and mure databases. `http://www.odyssee-mure.eu/publications/br/energy-efficiency-in-buildings.html`, 2015. Online, accessed 25 March 2019.

[7] P. Moseley and A. Bruhin. High energy performing buildings: Support for innovation and market uptake under horizon 2020 energy efficiency. Technical report, Publications of the European Union, 2018.

[8] A. Kaklauskas, E. K. Zavadskas, and S. Raslanas. Multivariant design and multiple criteria analysis of building refurbishments. *Energy and Buildings*, 37(4):361 − 372, 2005.

[9] P. O. Costa Campos, R. P. B. Neto, and R. Figueira. IST, green campus? Technical report, IST, 2008.

[10] I. S. Técnico. Pesquisa de espaços: Pavilhão de civil. `https://fenix.tecnico.ulisboa.pt/publico/findSpaces.do?spaceID=2448131361042&method=viewSpace&_request_checksum_=a822e2c9d8abb9a4080bad56aafac2fc9b1620fe`, 2018. Online; accessed 04 July 2018.

[11] M. Correia Guedes, I. Anselmo, G. Lopes, and M. Águas. Um projecto para a reabilitação energética do edifício do departamento de engenharia civil do I.S.T. Technical report, IST and ADENE, 2002.

[12] J. a. Martinez, M. de Matos, J. a. Patrício, and R. Pereira. Relatório de auditoria energética (elétrica) e medidas de racionalização energética - edifício - pavilhão de civil, 2015.

[13] J. Toste de Azevedo, P. Ferrão, and M. de Matos. O projeto campus sustentável e a redução da fatura energética do Instituto Superior Técnico. In *PCEEE 2014: EFICIÊNCIA ENERGÉTICA COMO FATOR DE COMPETITIVIDADE*. Fundação Calouste Gulbenkian, 2014.

[14] P. Ferrão and M. de Matos. Sustainable energy campus: A challenge on smart facilities and operations. In *Handbook of Theory and Practice of Sustainable Development in Higher Education: Volume 3*, pages 241–255. Springer International Publishing, 2017.

[15] T. Vilhena. Simulação dinâmica e estudo de medidas de racionalização energética do pavilhão de engenharia civil do IST. Tese de Mestrado, Instituto Superior Técnico, 2013.

[16] J. Patrício. Modelação dos consumos energéticos no pavilhão de civil do IST e definição de medidas de racionalização dos consumos energéticos. Tese de Mestrado, Instituto Superior Técnico, 2013.

[17] G. Marçal. Simulação dinâmica do sistema de climatização do pavilhão de civil do IST em EnergyPlus. Tese de Mestrado, Instituto Superior Técnico, 2015.

[18] F. Santos. Diagnóstico do desempenho do sistema de climatização do pavilhão de civil através do uso do EnergyPlus. Tese de Mestrado, Instituto Superior Técnico, 2016.

[19] C. Faustino. Influência dos vãos envidraçados no desempenho energético de edifícios. Tese de Mestrado, Instituto Superior Técnico, 2012.

[20] L. Almeida. Assessement of the new shading system installed on pavilhão de civil through EnergyPlus. Tese de Mestrado, Instituto Superior Técnico, 2017.

[21] T. Garção. Improvement of the civil engineering building envelope at IST using EnergyPlus. Tese de Mestrado, Instituto Superior Técnico, 2017.

[22] P. O. Fanger. Fundamentals of thermal confort. *Advances In Solar Energy Technology*, 4, Field 8: 3056–3061, 1988. Proceedings of the Biennial Congress of the International Solar Energy Society, Hamburg, 13-18 September 1987.

[23] P. O. Fanger. *Thermal Confort: Analysis and applications in environmental engineering.* Danish Technical Press, 1970.

[24] ASHRAE Technical Committees. *2017 ASHRAE Handbook - Fundamentals.* ASHRAE, 2017.

[25] I. Oom. Gestão colaborativa da iluminação e climatização. Tese de Mestrado, Instituto Superior Técnico, 2017.

[26] J. Esteves. Gestão inteligente aplicando o conceito "internet of things". Tese de Mestrado, Instituto Superior Técnico, 2018.

[27] Engineering ToolBox. Carbon dioxide concentration - comfort levels. `https://www.engineeringtoolbox.com/co2-comfort-level-d_1024.html`, 2008. Online, accessed 22 November 2018.

[28] J. G. Allen, P. MacNaughton, U. Satish, S. Santanam, J. Vallarino, and J. D. Spengler. Associations of cognitive function scores with carbon dioxide, ventilation, and volatile organic compound exposures in office workers: A controlled exposure study of green and conventional office environments. *Environmental Health Perspectives*, 124:805–812, 2016.

[29] EACE. Projecto de reabilitação dos sistemas de AVAC do pavilhão de civil do IST. Private document with access granted by IST, 2018.

[30] S. Taylor, R. McFarlan, R. Tozer, and G. Avery. Degrading chilled water plant delta-t: Causes and mitigation. *ASHRAE Transactions*, 108:641–653, 01 2002.

[31] Carrier. Heat recovery from air-colled chillers - applications for heat reclaim chillers, 2009. White Paper.

[32] Clivet. SPINchiller multifunction - WSAN-XSC3 MF 90.4-240.4 range, 2018. Technical Bulletin.

[33] Mitshubishi Electric, Hydronics and IT Cooling Systems S.p.A. Units for 4-pipe systems, air and water source, with scroll, screw and inverter screw compressors, from 33 to 1125 kw, 2018. Product Brochure.

[34] ASHRAE Technical Committees. *2016 ASHRAE Handbook — HVAC Systems and Equipment*. ASHRAE, 2016.

[35] X. Pang, M. A. Piette, and N. Zhou. Characterizing variations in variable air volume system controls. *Energy and Buildings*, 135:166 – 175, 2017.

[36] Carrier. Fans in VAV systems, 2005. Technical Development Paper.

[37] P. G. Schild and M. Mysen. Reccomendations on specific fan power and fan system efficiency. Technical report, International Energy Agency - Energy Conservation in Buildings and Community Systems Programme, 2009. Technical Note AIVC 65.

[38] Mitsubishi Electric - Cooling and Heating. DOAS and VRF: Applying systems for high-performance buildings, 2018. White Paper.

[39] D. Crawley, L. Lawrie, F. C. Winkelmann, W. Buhl, Y. Huang, C. O. Pedersen, R. Strand, R. Liesen, D. Fisher, M. Witte, and J. Glazer. Energyplus: Creating a new-generation building energy simulation program. *Energy and Buildings*, 33:319–331, 2001.

[40] ASHRAE. Lisbon Portela (WMO: 085360) Weather Data from 2017 ASHRAE Handbook - Foundamentals (SI). `http://ashrae-meteo.info/index.php?lat=38.77&lng=-9.13&place=%27%27&wmo=085360`, 2017. Online, accessed 18 December 2018.

[41] U.S. Department of Energy. *Input Output Reference*, EnergyPlus™ version 8.8.0 documentation edition, 2016.

[42] T. Hong, F. buhl, and P. Haves. EnergyPlus run time analysis, 2008. Document prepared in the Lawrence Berkeley National Laboratory.

[43] J. B. Maxwell. How to avoid overestimating variable speed drive savings. Technical report, Energy Systems Laboratory - Texas AM University, 2005. Twenty-Seventh IETC - Industrial Energy Technology Conference.

[44] U.S. Department of Energy. *Engineering Refererence*, energyplus™ version 8.8.0 documentation edition, 2016.

[45] Mitshubishi Electric. Data Book YKB/YLM 2nd Edition - R410A series, 2015. Air Conditioning Systems - City Multi.

[46] R. Raustad. Creating performance curves for variable refrigerant flow heat pumps in EnergyPlus. Technical report, Florida Solar Energy Centre, 2016.

[47] T. Hong, K. Sun, R. Zhang, R. Hinokuma, S. Kasahara, and Y. Yura. Development and validation of a new variable refrigerant flow system model in EnergyPlus. *Energy and Buildings*, 117, 12 2015.

[48] E. Asadi, M. G. da Silva, C. H. Antunes, L. Dias, and L. Glicksman. Multi-objective optimization for building retrofit: A model using genetic algorithm and artificial neural network and an application. *Energy and Buildings*, 81:444 – 456, 2014.

Appendix A

Thermal Zones

The thermal zones used in the *Energyplus* simulation are presented here.

Figure A.1: Thermal zones of the 03 floor.

Figure A.2: Thermal zones of the 02 floor.

Figure A.3: Thermal zones of the 01 floor.

Figure A.4: Thermal zones of the ground floor.

Figure A.5: Thermal zones of the 1st floor.

Figure A.6: Thermal zones of the 2nd floor.
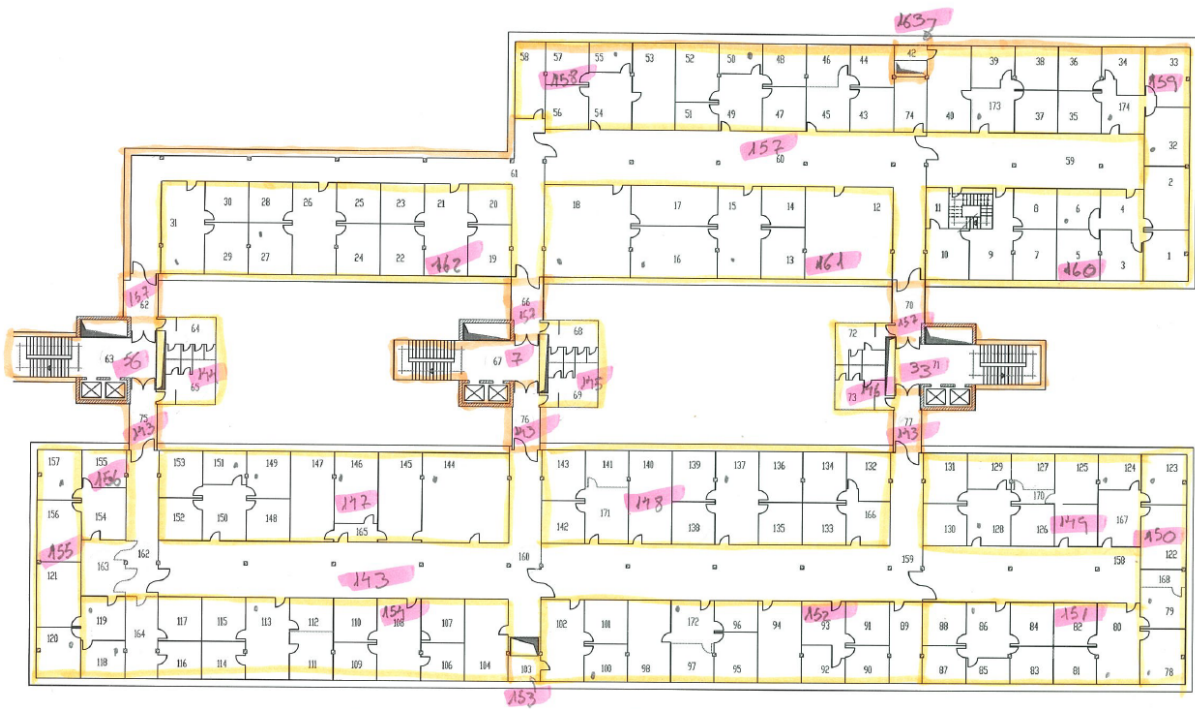
Figure A.7: Thermal zones of the 3rd floor.

Appendix B

HVAC Plant Control Mechanism

The optimization of the equipment of the plant is fundamental for its efficiency. As such, a number of strategies will be employed to achieve this. Those are explained in this section

Control of the chiller through the return temperature (supply water reset)

Typically, a hydronic chiller plant would produce chilled or hot water at a constant temperature independently of the loads. A ΔT between the return and supply would be defined, typically of 5 $^\circ C$. During part-load, what would happen is that the return water drops below the design ΔT and the unit always cools/heats the water to the leaving water temperature setpoint. This leads to low ΔT syndrome, as defined in [30]. This can potentially be a sub optimal efficiency solution because, depending on the unit, it may have to work harder and expend a higher amount of compressor energy to maintain the relatively low leaving water temperature setpoint. This depends on the unit's performance at part-load conditions. For instance, a typical centrifugal chiller would achieve its peak efficiency at 80% while a VFD compressor based chiller will typically achieve peak efficiency at 30-50 %, which is consistent with the performance of the unit projected at part-load. Instead, EACE designed the plant so that the control of the chillers/HP's will be done through the return water temperature. A constant return temperature will be aimed for and the unit will modulate the leaving temperature depending on the current load. This way, the evaporation temperature increases during part-load which reduces energy usage and, therefore, increasing seasonal energy efficiency and the same happens in the condenser when in heat pump mode, with the exception that the condensing temperature is reduced. The following example in figure B.1 illustrates this perfectly in a cooling scenario.
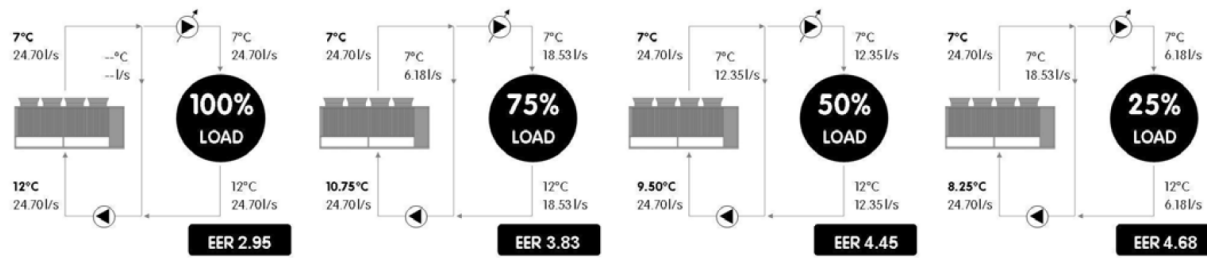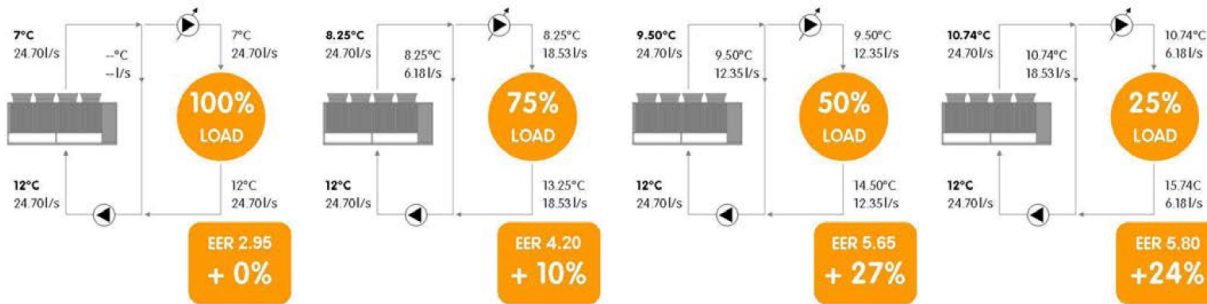
Figure B.1: Comparison between constant supply and return water temperature at 4 differing loads, with added efficiency benefits showcased. Obtained from [32].

Chillers/HP's in parallel

As seen in figure 2.5, they will be sequenced according to the load. Adding to the highly adaptability of each unit to the load, as explained above, sequencing of the chillers according to the load will allow for an even greater part-load performance. In a very low load situation, only one of the units will be on, while in a situation of high load, all units will be on.

Primary and secondary circuit pumps in parallel

As can be seen in figure 2.5, the primary and secondary pumps will be sequenced according to the load. In the case of the primary circuit, each pump is coupled to a chiller. An activation of a chiller will translate in an activation of the corresponding pump. Regarding the secondary circuit, the pumps will activate according to the load in a stepped manner. This will only be possible with a well designed and efficient communication between the plant's sensors and actuators for the diverse valves and pumps.

The inertial tanks

Two units that are visible in figure 2.5, each with 7500L volume capacity, will be recycled from the current HVAC system and will serve as a buffer for the chillers/HP's with the intent of minimizing the number of compressor start-ups. Minimizing the start-ups allows not only for a higher efficiency due to starting energy required, but also for a prolonged component life while assuring a smoother plant operation.

Appendix C

4-Pipe Chiller/Heat Pump Catalog Data

The data used to model the Chiller/HP units is shown in this appendix, from the official technical bulletin [32]. The chiller selected was the *Clivet*[TM] SPINChiller[3] WSAN-XSC3 MF 200.4 4T SC.

Size			200.4	Size			200.4
Cooling				**Compressor**			
Cooling capacity	1	[kW]	545	Type of compressors		-	Scroll
Compressor power input	1	[kW]	172	Refrigerant			R-410A
Total power input	2	[kW]	188	No. of compressors		No	4
EER	1	-	2,91	Rated power (C1)		[HP]	100
Water flow-rate	1	[l/s]	26,0	Rated power (C2)		[HP]	100
Cold user side exchanger pressure drops	1	[kPa]	46,7	Std Capacity control steps		No	6
Cooling capacity (EN14511:2013)	3	[kW]	543	Oil charge (C1)		[l]	13
Total power input (EN14511:2013)	3	[kW]	189	Oil charge (C2)		[l]	13
EER (EN 14511:2013)	3	-	2,87	Refrigerant charge (C1)		[kg]	79
ESEER (EN 14511:2013)	3	-	4,45	Refrigerant charge (C2)		[kg]	79
Cooling capacity (AHRI 550/590)	7	[kW]	543	Refrigeration circuits		No	2
Compressor power input (AHRI 550/590)	7	[kW]	171	**Internal exchanger**			
Total power input (AHRI 550/590)	7	[kW]	187	Type of cold user side exchanger		-	PHE
COPr	7	-	2,90	Type of hot user side exchanger		-	PHE
Heating				Cold user side exchanger water content		[l]	49
Heating capacity	4	[kW]	627	Hot user side exchanger water content		[l]	43,2
Compressor power input	4	[kW]	155	Cold user side minimum system water content		[l]	3234
Total power input	2	[kW]	171	Hot user side minimum system water content		[l]	4097
COP	4	-	3,67	**External Section Fans**			
Water flow-rate	4	[l/s]	30,0	Type of fans		-	AX
Hot user side exchanger pressure drops	4	[kPa]	38,8	Number of fans		No	10
Heating capacity (EN14511:2013)	5	[kW]	629	Type of motor		-	AC/P
Total power input (EN14511:2013)	5	[kW]	173	Standard airflow		[l/s]	49776
COP (EN 14511:2013)	5	[kW]	3,64	**Connections**			
Cooling 100% - Heating 100%				Cold user side water fittings		-	5"
Cooling capacity	6	[kW]	556	Hot user side water fittings		-	5"
Heating capacity	6	[kW]	720	**Power supply**			
Total power input	6	[kW]	164	Standard power supply		V	400/3~/50
Global efficiency	8	[kW]	7,76	**Electrical data**			
				FLA Total		A	396,6
				FLI Total		kW	252,4
				M.I.C. - Value		A	946,1
				M.I.C. - with soft start accessory		A	786,1

1. Data referred to the following conditions: internal exchanger water = 12/7 °C. Entering external exchanger air temperature 35°C. Internal exchanger fouling factor = 0.44 x 10^(-4) m² K/W. Considering cooling only operation.
2. The Total Power Input value does not take into account the part related to the pumps and required to overcome the pressure drops for the circulation of the solution inside the exchangers
3. Data compliant to Standard EN 14511:2013 referred to the following conditions: - Internal exchanger water temperature = 12/7°C - Entering external exchanger air temperature = 35°C. Considering cooling only operation.
4. Data referred to the following conditions: internal exchanger water = 40/45 °C. Entering external exchanger air temperature = 7°C D.B./6°C W.B. Internal exchanger fouling factor = 0.44 x 10^(-4) m² K/W. Considering heating only operation.
5. Data compliant to Standard EN 14511:2013 referred to the following conditions: - Internal exchanger water temperature = 40/45 °C. Entering external exchanger air temperature = 7°C D.B./6°C W.B. Considering heating only operation.
6. Data referred to the following conditions: exchanger water cooling side = 12/7 °C. exchanger water heating side = 40/45°C. Exchanger fouling factor = 0.44 x 10^(-4) m² K/W
7. Data compliant to Standard AHRI 550/590 referred to the following conditions: internal exchanger water temperature = 6,7 °C. Water flow-rate 0,043 l/s per kW. Entering external exchanger air temperature 35°C. Internal exchanger fouling factor = 0.18 x 10^(-4) m2 K/W. Considering cooling only operation.
8. Global Efficiency = (Cooling capacity + Heating capacity) / Total power input

Figure C.1: Main datasheet for the chiller/HP unit selected, obtained from [32].

Cooling performance

Size	To (°C)	ENTERING EXTERNAL EXCHANGER AIR TEMPERATURE (°C)											
		25		30		35		39		42		48	
		kWf	kWe	kWf	kWe	kWf	kWe	kWf	kWe	kWf	kWe	kWf	kWe
200.4	5	576	148	539	161	500	176	472	189	469	192	287	119
	6	590	150	551	163	512	177	485	191	482	193	295	119
	7	600	151	563	165	524	179	495	192	493	194	302	120
	10	631	155	589	168	548	183	518	195	517	198	317	122
	15	695	163	653	177	614	192	589	206	399	112	-	-
	18	754	168	705	182	667	198	636	210	441	114	-	-

kWf = Cooling capacity in kW. The data do not consider the part related to the pumps, required to overcome the pressure drop for the solution circulation inside the exchangers

kWe = Compressor power input in kW

To (°C) = leaving internal exchanger water temperature (°C) - Performances in function of the inlet/outlet water temperature differential = 5°C

Heating performance

Size	Ta (°C) D.B./W.B.	LEAVING INTERNAL EXCHANGER WATER TEMPERATURE (°C)									
		35		40		45		50		55	
		kWt	kWe	kWt	kWe	kWt	kWe	kWt	kWe	kWt	kWe
200.4	-7 / -8	460	119	457	132	448	147	-	-	-	-
	-5 / -6	482	120	479	133	471	148	-	-	-	-
	0 / -1	548	123	542	136	530	151	521	168	-	-
	2 / 1	578	124	570	137	559	152	547	169	-	-
	7 / 6	650	126	641	140	627	155	609	172	594	195
	12 / 11	752	130	735	143	718	157	694	175	677	198

kWt = Internal exchanger heating capacity (kW). The data do not consider the part related to the pumps, required to overcome the pressure drop for the solution circulation inside the exchangers.

The kWt heating capacity does not consider any defrosting cycles. For the real heating capacity calculation, including defrosting cycles, please refer to "Integrated heating capacities" table.

kWe = Compressor power input in kW

Ta = Entering external exchanger air temperature

D.B. = Dry bulb

W.B. = Wet bulb

Figure C.2: Cooling and heating performance and input power at different ambient and water temperatures, obtained from [32].

Integrated heating capacities

Entering external exchanger air temperature °C (D.B. / W.B.)	-7 / -8	-5 / -6	0 / -1	2 / 1	Other
Heating capacity multiplication coefficient	0,86	0,89	0,88	0,90	1,00

The integrated heating capacity represents the real heating capacity considering the defrost cycles too.

To obtain the integrated heating capacity multiply the heating performance value in kWt (shown in the heating performance tables) by the coefficients indicated in the table.

DB = dry bulb

WB = wet bulb

Figure C.3: Heating capacity multipliers for defrost cycles at low outdoor air temperatures, obtained from [32].

Cooling 100% - Heating 100% performance

Size.	Tw (°C)	Leaving water temperature hot user side																											
		20/25				30/35				35/40				40/45				45/50				50/55			
		kWf	kWe	kWt	GLE	kWf	kWe	kWt	GLE	kWf	kWe	kWt	GLE	kWf	kWe	kWt	GLE	kWf	kWe	kWt	GLE	kWf	kWe	kWt	GLE
200.4	5	635	110,2	746	12,54	592	132,8	725	9,92	562	146,7	709	8,67	522	162,8	685	7,42	478	181,6	659	6,26	438	203,5	640	5,30
	6	656	110,8	767	12,84	611	133,4	744	10,16	580	147,3	728	8,88	539	163,3	702	7,60	493	182,2	675	6,41	452	203,9	655	5,43
	7	676	111,4	788	13,14	629	134,1	764	10,39	598	147,9	747	9,10	556	163,8	720	7,79	505	182,5	687	6,53	463	204,3	666	5,53
	10	724	112,8	837	13,84	669	135,4	805	10,88	634	149,0	784	9,52	587	164,8	752	8,13	534	183,5	718	6,82	489	205,0	693	5,76
	15	803	115,4	919	14,92	746	138,0	885	11,82	707	151,4	859	10,35	662	167,5	829	8,90	615	186,4	802	7,60	-	-	-	-
	18	871	117,6	989	15,81	813	140,3	954	12,60	773	153,6	927	11,07	717	169,4	887	9,46	661	188,2	850	8,03	-	-	-	-

kWf = Cold user side cooling capacity (kW). The data do not consider the part related to the pumps, required to overcome the pressure drop for the solution circulation inside the exchangers

kWt = Hot user side exchanger heating capacity (kW). The data do not consider the part related to the pumps, required to overcome the pressure drop for the solution circulation inside the exchangers.

kWe = Compressor power input in kW

Tw = Leaving water temperature cold user side

GLE = Global Efficiency = (Cooling capacity + Heating capacity) / Total power input

D.B. = Dry bulb

W.B. = Wet bulb

Figure C.4: 100% recovery performance data at different chilled and hot water, obtained from [32]. The outside air temperature for this operation is not specified in this table.

Cooling performance at part load

Size	STEP	External exchanger entering air temperature (°C)											
		35			30			25			20		
		kWf	kWe_tot	EER	kWf	kWe_tot	EER	kWf	kWe_tot	EER	kWf	kWe_tot	EER
200.4	6	524	191	2,75	563	176	3,04	600	162	3,52	627	149	4,01
	5	442	148	2,86	476	137	3,32	507	126	3,84	529	115	4,37
	4	361	105	3,27	388	97	3,80	414	90	4,40	432	82	5,00
	3	309	87	3,37	332	81	3,92	354	74	4,53	370	68	5,15
	2	258	69	3,54	277	64	4,11	295	59	4,76	308	54	5,41
	1	128	35	3,51	138	32	4,08	147	30	4,72	154	27	5,36

kWf = Cooling capacity in kW   kWe_tot = Unit total power input in kW
STEP = Active capacity steps (the maximum number indicates full capacity / the minimum number indicates the smallest partialization step)
Internal exchanger water = output temperature 7°C/ input * (variable) / constant flow equal to the nominal value.

Figure C.5: Cooling part load performance and input power for 6 different steps at 7 $°C$ leaving chilled water temperature and different ambient temperatures, obtained from [32].

Heating performance at part load

Size	STEP	Entering external exchanger air temperature (°C)																	
		-7/-8			-5/-6			-0/-1			2/1			7/6			12/11		
		kWt	kWe_tot	COP	kWt	kWe_tot	COP	kWt	kWe_tot	COP	kWt	kWe_tot	COP	kWt	kWe_tot	COP	kWt	kWe_tot	COP
200.4	6	460	135	3,41	482	136	3,55	548	139	3,95	578	140	4,13	650	142	4,58	752	146	5,15
	5	394	111	3,55	414	112	3,71	469	114	4,13	496	114	4,34	560	116	4,82	639	118	5,40
	4	328	87	3,77	344	88	3,93	392	89	4,40	414	90	4,61	469	91	5,15	534	93	5,75
	3	252	67	3,74	265	68	3,92	304	69	4,42	322	69	4,65	367	70	5,22	420	72	5,86
	2	176	48	3,69	187	48	3,90	217	49	4,47	230	49	4,70	265	50	5,34	306	51	6,05
	1	88	24	3,61	93	24	3,82	108	25	4,37	115	25	4,60	132	25	5,23	153	26	5,92

kWt = Heating capacity in kW   kWe_tot = Unit total power input in kW
STEP = Active capacity steps (the maximum number indicates full capacity / the minimum number indicates the smallest partialization step)
Internal exchanger water = output temperature 35°C/ input * (variable) / constant flow equal to the nominal value.

Figure C.6: Heating part load performance and input power for 6 different steps at 35 $°C$ leaving hot water temperature and different ambient temperatures, obtained from [32].

Table C.1: Calculated recovery performance for the CAPFT and EIRFT curves with interpolation from the cooling only data. Data in bold is from the 100% recovery operation with 35 $°C$ assumed OA temperature, 7 $°C$ LChW temperature and 45 $°C$ LHW temperature.

Leaving Chilled Water Temperature [$°C$]	Entering Condenser OA Temperature [$°C$]	Cooling Only Capacity [kW]	Cooling Only Compressor Power Input [kW]	Adjusted Recovery Cooling Capacity [kW]	Adjusted Recovery Compressor Power Input [kW]
5	25	596	141	599,45	135,83
	30	559	154	562,23	148,35
	35	519	169	**522,00**	**162,80**
	40	480	185	482,77	178,21
6	25	611	143	614,42	137,36
	30	574	156	577,21	149,85
	35	536	170	**539,00**	**163,30**
	40	496	187	498,78	179,63
7	25	628	145	640,68	138,09
	30	588	157	599,87	149,52
	35	545	172	**556,00**	**163,80**
	40	506	188	516,21	179,04
10	25	656	148	676,75	139,37
	30	616	160	635,49	150,67
	35	569	175	**587,00**	**164,80**
	40	529	190	545,73	178,93
15	25	722	155	749,16	141,87
	30	684	169	709,73	154,69
	35	638	183	**662,00**	**167,50**
	40	600	199	622,57	182,14

Appendix D

VRF Units Catalog Data

The data used for the VRF units is summarized here for the LTI's VRF system, which is the *Mitsubishi Electric*[TM] PUHY-P550YSKB-A1 + PEFY-P63VMA-E from a product catalog [45]. These data was employed for each VRF system to input the performance curves in *Energyplus*.

Outdoor Unit - PUHY-P550YKSB-A1

Model			PUHY-P550YSKB-A1 (-BS)	
Power source			3-phase 4-wire 380-400-415 V 50/60 Hz	
Cooling capacity	*1	kW	63.0	
(Nominal)		kcal/h	54,200	
	*1	BTU/h	215,000	
	Power input	kW	16.66	
	Current input	A	28.1-26.7-25.7	
	EER	kW/kW	3.78	
Temp. range of	Indoor	W.B.	15.0~24.0°C (59~75°F)	
cooling	Outdoor	D.B.	-5.0~52.0°C (23~126°F)	
Heating capacity	*2	kW	69.0	
(Nominal)		kcal/h	59,300	
	*2	BTU/h	235,400	
	Power input	kW	17.29	
	Current input	A	29.1-27.7-26.7	
	COP	kW/kW	3.99	
Temp. range of	Indoor	D.B.	15.0~27.0°C (59~81°F)	
heating	Outdoor	W.B.	-20.0~15.5°C (-4~60°F)	
Indoor unit	Total capacity		50~130% of outdoor unit capacity	
connectable	Model/Quantity		P15~P250/2~47	
Sound pressure level (measured in anechoic room)	dB <A>		63.5	
Sound power level (measured in anechoic room)	dB <A>		84.5	
Refrigerant	Liquid pipe	mm (in.)	15.88 (5/8) Brazed	
piping diameter	Gas pipe	mm (in.)	28.58 (1-1/8) Brazed	

Set Model				
Model			PUHY-P250YKB-A1 (-BS)	PUHY-P300YKB-A1 (-BS)
FAN	Type x Quantity		Propeller fan x 1	Propeller fan x 1
	Air flow rate	m³/min	175	210
		L/s	2,917	3,500
		cfm	6,179	7,415
	Control, Driving mechanism		Inverter-control, Direct-driven by motor	Inverter-control, Direct-driven by motor
	Motor output	kW	0.92 x 1	0.92 x 1
*3	External static press.		0 Pa (0 mmH$_2$O)	0 Pa (0 mmH$_2$O)
Compressor	Type x Quantity		Inverter scroll hermetic compressor	Inverter scroll hermetic compressor
	Manufacture		AC&R Works, MITSUBISHI ELECTRIC CORPORATION	AC&R Works, MITSUBISHI ELECTRIC CORPORATION
	Starting method		Inverter	Inverter
	Motor output	kW	6.9	8.1
	Case heater	kW	-	-
	Lubricant		MEL32	MEL32

Notes:
1. Nominal cooling conditions (subject to JIS B8615-2)
   Indoor: 27°CD.B./19°CW.B. (81°FD.B./66°FW.B.), Outdoor: 35°CD.B. /24°CW.B. (95°FD.B./75°FW.B.)
   Pipe length: 7.5 m (24-9/16 ft.), Level difference: 0 m (0 ft.)
2. Nominal heating conditions (subject to JIS B8615-2)
   Indoor: 20°CD.B. (68°FD.B.), Outdoor: 7°CD.B./6°CW.B. (45°FD.B./43°FW.B.)
   Pipe length: 7.5 m (24-9/16 ft.), Level difference: 0 m (0 ft.)
3. External static pressure option is available (30Pa, 60Pa/3.1mmH$_2$O, 6.1mmH$_2$O).

Figure D.1: Main datasheet, obtained from [45].

PUHY-		P400YSKB-A1	P450YSKB-A1	P500YSKB-A1
Nominal Cooling Capacity	kW	45.0	50.0	56.0
	BTU/h	153,500	170,600	191,100
Input	kW	11.0	12.59	14.54

PUHY-		P550YSKB-A1	P600YSKB-A1	P650YSKB-A1
Nominal Cooling Capacity	kW	63.0	69.0	73.0
	BTU/h	215,000	235,400	249,100
Input	kW	16.66	19.43	20.97

Indoor unit temperature correction
To be used to correct indoor unit capacity only
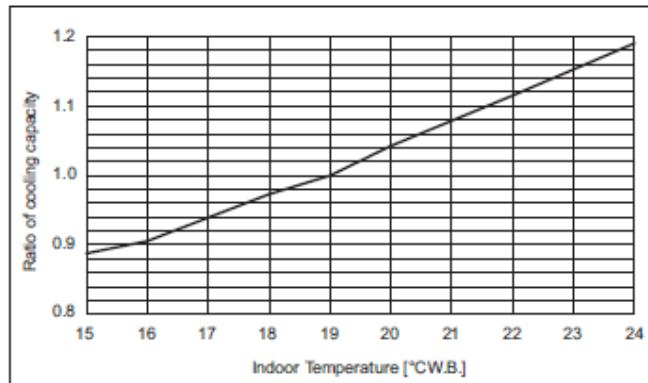
Outdoor unit temperature correction
To be used to correct outdoor unit only
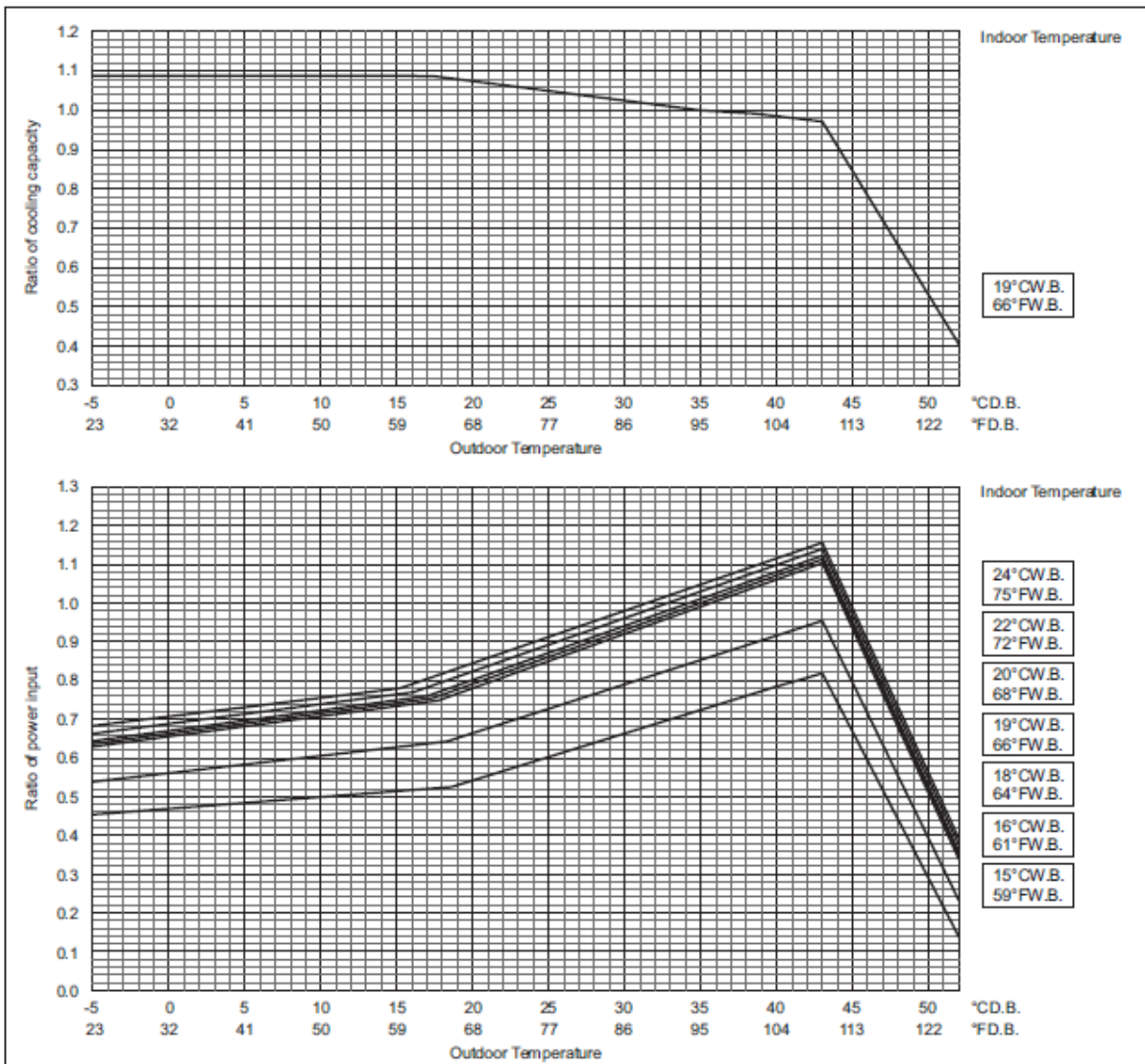
Figure D.2: Temperature correction for cooling operation, obtained from [45].

PUHY-		P400YSKB-A1	P450YSKB-A1	P500YSKB-A1
Nominal Heating Capacity	kW	50.0	56.0	63.0
	BTU/h	170,600	191,100	215,000
Input	kW	12.24	13.72	15.46

PUHY-		P550YSKB-A1	P600YSKB-A1	P650YSKB-A1
Nominal Cooling Capacity	kW	69.0	76.5	81.5
	BTU/h	235,400	261,000	278,100
Input	kW	17.29	19.36	21.00

Indoor unit temperature correction
To be used to correct indoor unit capacity only
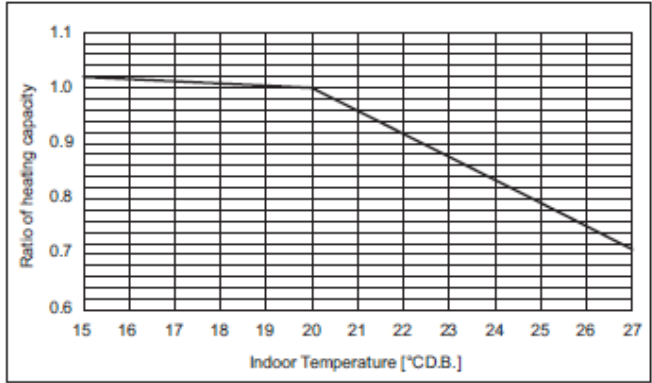
Outdoor unit temperature correction
To be used to correct outdoor unit only
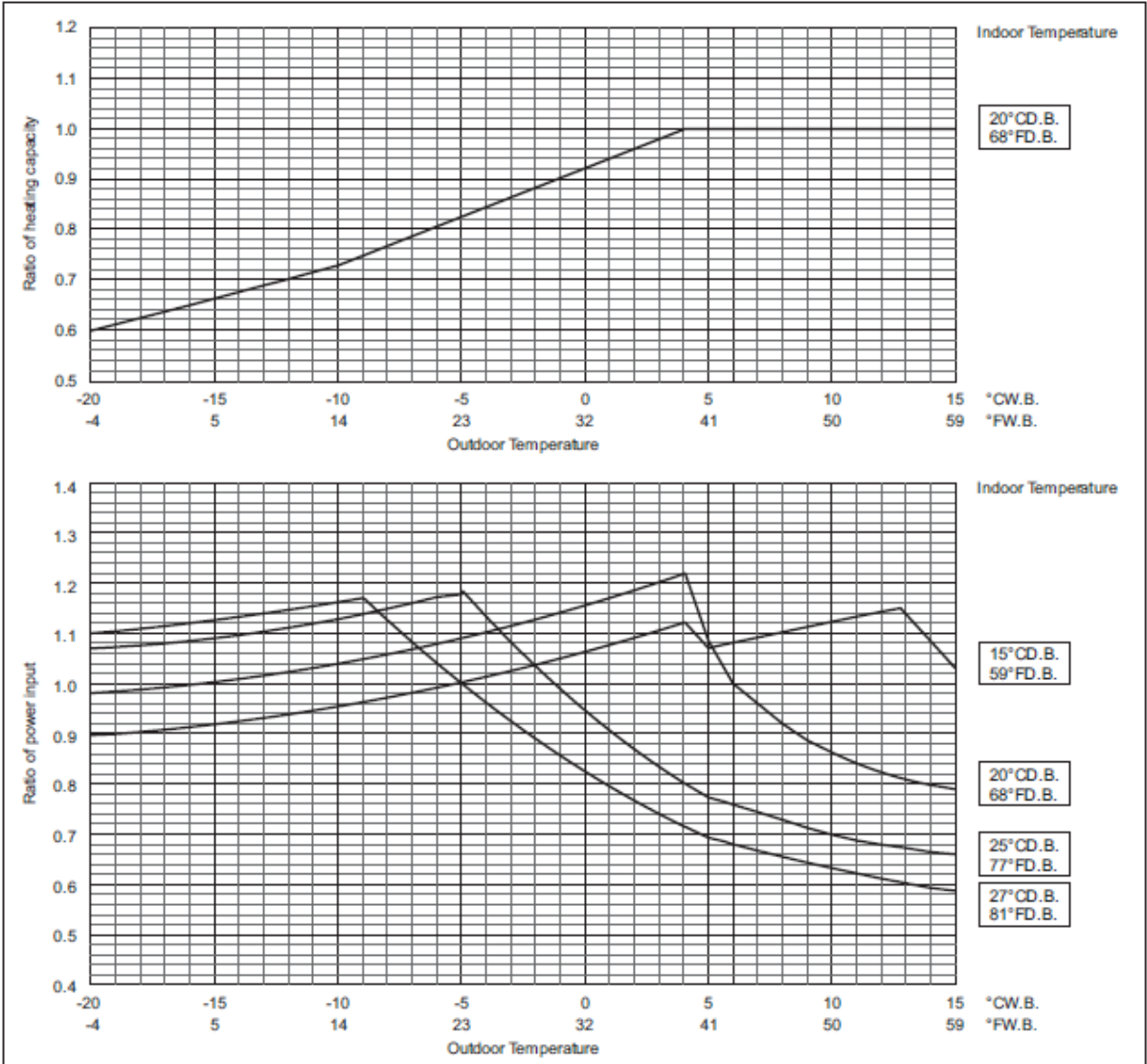
Figure D.3: Temperature correction for heating operation, obtained from [45].

Figure D.4: Indoor units sizing correction for both cooling and heating operation, obtained from [45].
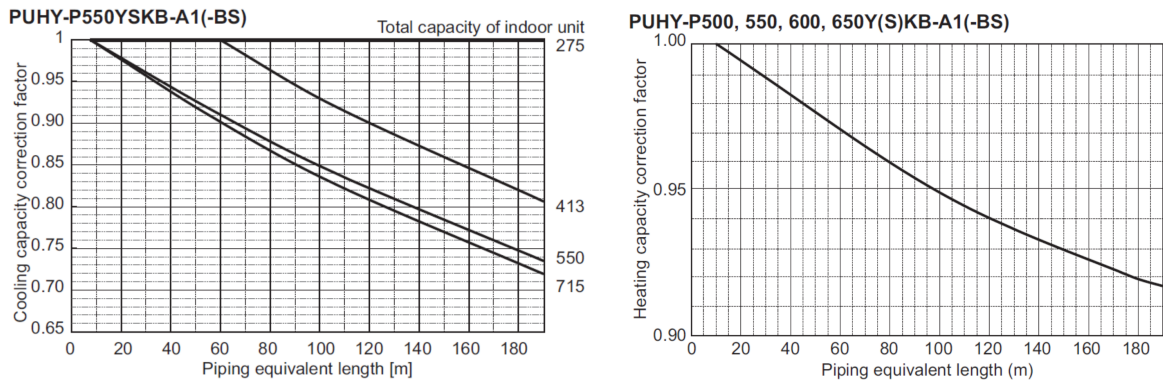
Equivalent length = (Actual piping length to the farthest indoor unit) + (0.50 × number of bends in the piping) m

Figure D.5: Piping length correction, including equivalent piping length formula for both cooling and heating operation, obtained from [45].

Due to frost at the outdoor heat exchanger and the automatic defrost operation, the heating capacity of the outdoor unit can be calculated by multiplying the correction factor shown in the table below.

Table of correction factor at frost and defrost

Outdoor inlet air temp. °C	6	4	2	1	0	-2	-4	-6	-8	-10	-20
PUHY-P550YSKB-A1(-BS)	1.00	0.94	0.87	0.86	0.87	0.88	0.90	0.90	0.93	0.93	0.93

Figure D.6: Frost operation correction for different outdoor air dry-bulb temperatures, obtained from [45].

Indoor Unit - PEFY-P63VMA-E

This indoor unit is the most common type to be used within LTI's spaces, therefore, the datasheet data is presented here.

Model			PEFY-P63VMA-E
Power source			1-phase 220-230-240V 50/60Hz
Cooling capacity	*1	kW	7.1
(Nominal)	*1	kcal / h	6,100
	*1	BTU / h	24,200
	*2 Power input	kW	0.12
	*2 Current input	A	1.01
Heating capacity	*3	kW	8.0
(Nominal)	*3	kcal / h	6,900
	*3	BTU / h	27,300
	*2 Power input	kW	0.10
	*2 Current input	A	0.90
External finish			Galvanized steel plate
External dimension HxWxD		mm	250 x 1,100 x 732
		inch	9-7/8 x 43-5/16 x 28-7/8
Net weight		kg(lbs)	32(71)
Heat exchanger			Cross fin(Aluminum fin and copper tube)
FAN	Type x Quantity		Sirocco fan x 2
	*4 External static press.	Pa	<35> - 50 - <70> - <100> - <150>
		mmH$_2$O	<3.6> - 5.1 - <7.1> - <10.2> - <15.3>
	Motor Type		DC motor
	Motor output	kW	0.121
	Driving mechanism		Direct-driven by motor
	Air flow rate		(Low-Mid-High)
		m^3 / min	13.5 - 16.0 - 19.0
		L/s	225 - 267 - 317
		cfm	477 - 565 - 671

Notes:
1. Nominal cooling conditions
   Indoor:27°CDB/19°CWB(81°FDB/66°FWB), Outdoor:35°CDB(95°FDB)
   Pipe length:7.5m(24-9/16ft.), Level difference:0m(0ft.)
2. The values are measured at the factory setting of external static pressure.
3. Nominal heating conditions
   Indoor:20°CDB(68°FDB), Outdoor:7°CDB/6°CWB(45°FDB/43°FWB)
   Pipe length:7.5m(24-9/16ft.), Level difference:0m(0ft.)
4. The factory setting of external static pressure is shown without < >.
   Refer to "Fan characteristics curves", according to the external static pressure, in DATA BOOK for the usable range of air flow rate.

Figure D.7: Main datasheet, obtained from [45].

Cooling capacity with PUHY-P400-650YSKB-A1, EP550-650YSLM-A1

PEFY-P-VMA(L)-E CA: Capacity (kW), SHC: Sensible Heat Capacity (kW)

Model size (Rated kW)	21.5°C D.B. 15°C W.B.		23°C D.B. 16°C W.B.		25°C D.B. 18°C W.B.		27°C D.B. 19°C W.B.		28°C D.B. 20°C W.B.		30°C D.B. 22°C W.B.		32°C D.B. 24°C W.B.	
	CA	SHC	CA	SHC	CA	SHC	CA	SHC	CA	SHC	CA	SHC	CA	SHC
20 (2.2)	2.0	1.8	2.0	1.9	2.2	1.9	2.2	2.0	2.3	2.0	2.5	2.0	2.6	2.0
25 (2.8)	2.5	2.0	2.6	2.1	2.7	2.1	2.8	2.2	2.9	2.2	3.1	2.2	3.3	2.2
32 (3.6)	3.2	2.4	3.3	2.5	3.5	2.5	3.6	2.6	3.8	2.6	4.0	2.6	4.3	2.6
40 (4.5)	4.0	3.3	4.1	3.4	4.4	3.4	4.5	3.6	4.7	3.6	5.0	3.6	5.4	3.5
50 (5.6)	5.0	4.1	5.1	4.2	5.5	4.2	5.6	4.4	5.9	4.4	6.3	4.4	6.7	4.4
63 (7.1)	6.3	5.0	6.5	5.2	6.9	5.1	7.1	5.5	7.4	5.5	7.9	5.4	8.5	5.4
71 (8.0)	7.1	5.5	7.3	5.6	7.8	5.6	8.0	5.9	8.4	5.9	8.9	5.9	9.5	5.8
80 (9.0)	8.0	5.9	8.2	6.0	8.8	6.0	9.0	6.3	9.4	6.3	10.1	6.3	10.7	6.2
100 (11.2)	10.0	8.1	10.2	8.3	11.0	8.3	11.2	8.8	11.7	8.8	12.5	8.8	13.4	8.7
125 (14.0)	12.5	9.9	12.8	10.1	13.7	10.1	14.0	10.7	14.7	10.7	15.7	10.6	16.7	10.5
140 (16.0)	14.3	11.1	14.6	11.4	15.7	11.4	16.0	12.0	16.8	12.1	17.9	12.0	19.1	11.8

* The capacity does not depend on the outdoor temperature. kcal/h = kW x 860, BTU/h = kW x 3,412

Heating capacity with PUHY-P450-500YKB-A1, P400-650YSKB-A1

All indoor units SHC: Sensible Heat Capacity (kW)

Model size (Rated kW)	15°C D.B. SHC	20°C D.B. SHC	25°C D.B. SHC	27°C D.B. SHC
15 (1.9)	1.9	1.9	1.5	1.3
20 (2.5)	2.5	2.5	2.0	1.8
25 (3.2)	3.3	3.2	2.5	2.3
32 (4.0)	4.1	4.0	3.2	2.8
40 (5.0)	5.1	5.0	4.0	3.5
50 (6.3)	6.4	6.3	5.0	4.5
63 (8.0)	8.2	8.0	6.3	5.7
71 (9.0)	9.2	9.0	7.1	6.4
80 (10.0)	10.2	10.0	7.9	7.1
100 (12.5)	12.7	12.5	9.9	8.9
125 (16.0)	16.3	16.0	12.7	11.3
140 (18.0)	18.4	18.0	14.3	12.8
200 (25.0)	25.5	25.0	19.8	17.7
250 (31.5)	32.1	31.5	25.0	22.3

* The capacity does not depend on the outdoor temperature. kcal/h = kW x 860, BTU/h = kW x 3,412

Figure D.8: Capacity table for cooling and heating at different indoor air temperatures, obtained from [45].

Appendix E

Thermal Comfort

Table E.1: ASHRAE's thermal sensation scale [24]

PMV Range	Sensation
-3 to -2	Cold
-2 to -1	Cool
-1 to -0.5	Slightly Cool
-0.5 to 0.5	Neutral
0.5 to 1	Slightly Warm
1 to 2	Warm
2 to 3	Hot

These clothing insulation values were input in the model for it to calculate the thermal comfort of the occupants through the PMV-PPD thermal comfort model. The values were deemed plausible taking into account the typical weather in Lisbon and were based on the 2017 ASHRAE Handbook - Fundamental [24].
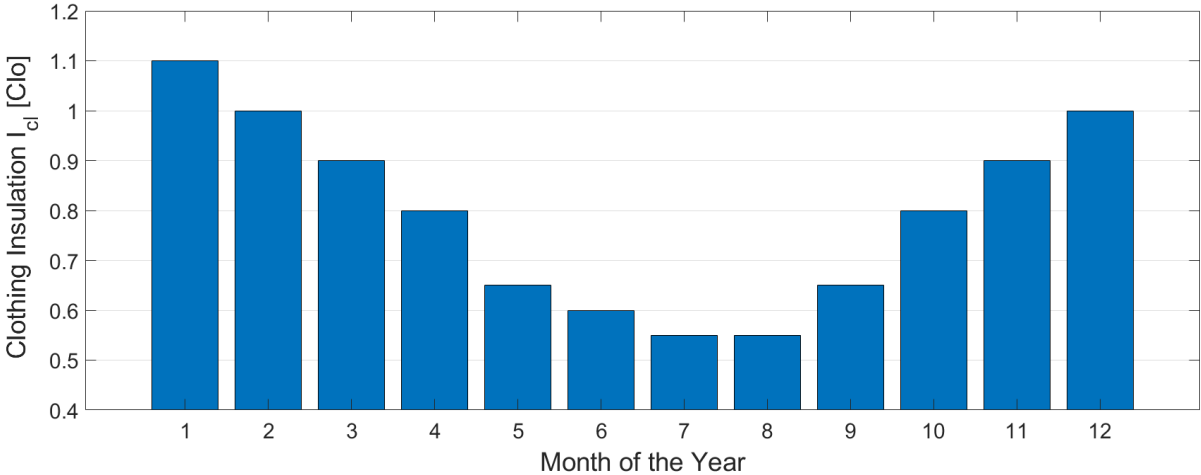
Figure E.1: Monthly clothing insulation values considered for the calculation of the thermal comfort through the PMV values.

Appendix F

Technical Details of the In-Room V1.10 Sensor

Table F.1: Technical details of the temperature and humidity sensor and carbon dioxide sensor.

Type of sensor	Model	Parameter	Value
Temperature and Humidity	Sensirion SHT31-DIS	Temperature Accuracy [$^\circ C$]	$\pm$ 0.3
		Temperature Resolution [$^\circ C$]	0.015
		Humidity Accuracy [% RH]	$\pm$ 2
		Humidity Resolution [% RH]	0.01
CO_2	Telaire 6613 CO_2	Accuracy	$400 <$ PPM < 1250, $\pm$ 30 ppm
			$1250 <$ PPM < 2000, $\pm$ 5% + 30 ppm
		Measurement Range	0 to 2000 PPM

Appendix G

Fan/Pump Part-Load Performance Curve
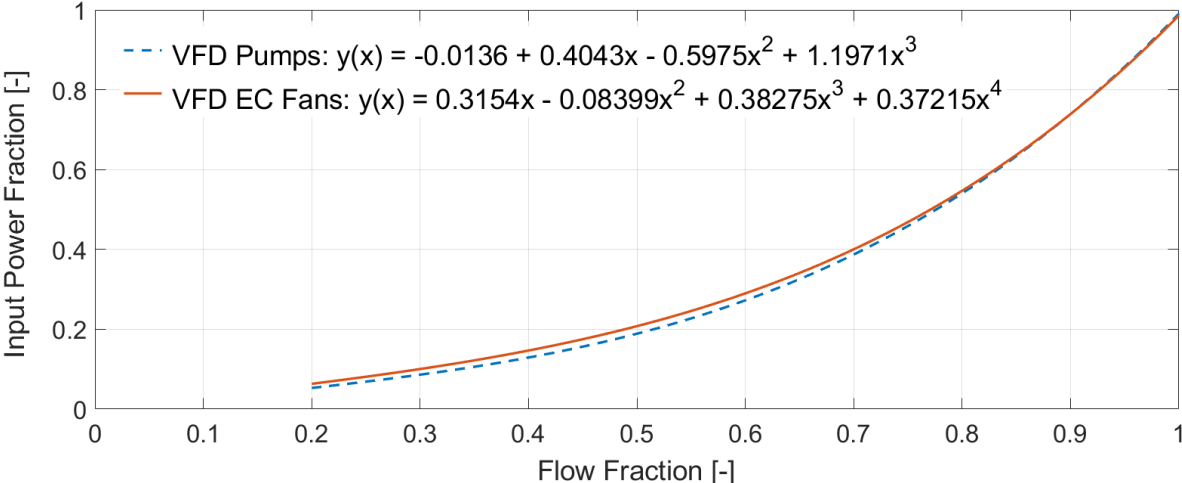
Figure G.1: Curves for the part-load performance of the variable speed pumps and fans as introduced in the model.